Doctoral Dissertation

Development of relocation model of molten metallic fuel in core disruptive accident of sodium-cooled fast reactor

Sungbo Moon

Department of Nuclear Engineering

Graduate School of UNIST

2019

Development of relocation model of molten metallic fuel in core disruptive accident of sodium-cooled fast reactor

A dissertation
submitted to the Graduate School of UNIST
in partial fulfillment of the
requirements for the degree of
Doctor of Philosophy

Sungbo Moon

11/12/2018
Approved by

_____

Advisor
In Cheol Bang

Development of relocation model of molten metallic fuel in core disruptive accident of sodium-cooled fast reactor

Sungbo Moon

This certifies that the dissertation of Sungbo Moon is approved.

11/12/2018

signature

_____

Advisor: In Cheol Bang

signature

_____

typed name: Seung Jun Lee

signature

_____

typed name: Eisung Yoon

signature

_____

typed name: Dong Wook Jerng

signature

_____

typed name: Yun-Jae Kim

Abstract

After Fukushima accident (All of the core cooling systems and emergency power generator are deactivated because of the tsunami) in 2011, researchers started to focus the nuclear power plant accident research on the core disruptive accident (CDA) phenomena. Core disruptive accident phenomena are highly hazardous accident phenomena among the accident events because of disruption of first boundary of radioactive materials. If enough core cooling is not guaranteed or if core thermal power increase dramatically, fuel pin can be damaged by higher temperature than its safety limit (e.g. melting temperature). Not only melting temperature, if fuel is made by metal, eutectic reaction between fuel and cladding can damage the cladding. The temperature of this reaction is much lower than that of melting temperature of cladding. After this cladding breach, Molten fuel can be released into coolant channel and radioactive material can be spread into the primary cooling system. If second boundary (reactor vessel, in the case of light water reactor) is ruptured, contamination of containment building would be happened. If confimentment building is damaged by pressurization inside, explosion from inside/outside factor or impact from outside, radioactive source term can be released into environment .

Nuclear power plant safety issue becomes the primary concern to obtain a permission of construction and operation. The safety criteria of this permission are getting harder to satisfy after Fukushima accident. This circumstance is expanding from design-ongoing reactor to already constructed reactor. Not only light water reactor which is already operating widely, other next generation reactor systems like fast reactor perform safety assessment. The fast reactor is one of generation IV design reactor. In this research, Sodium-cooled Fast Reactor (SFR) severe accident phenomena (especially core disruptive accident; CDA, initiating phase) are considered. This initiating phase covers from fuel cavity generation to molten fuel ejection and molten fuel relocation inside coolant channel.

In Korea, Prototype Gen-IV Sodium-cooled Fast Reactor (PGSFR) is considered as next promising GEN-IV reactor. And this reactor will use metal fuel as their core element which is different from well-known oxide fuel of SFR. If metal fuel is melted, density and flow of this molten metal fuel make the reactivity negative. Because of its inherent safety of metal fuel, SFR using metal fuel is known as its safety in the case of severe accident, especially CDA. But its detailed phenomenon is not fully understood. To simulate CDAs in SFR, severe accident analysis code is being developed and it has not been developed for metal fuel (Recently, SAS4A for metal fuel is developed). And most codes are systematic codes which are not able to look at detail phenomena of the CDA. In this research, MESFRAC (MEtal fuel Sodium-cooled Fast Reactor accident Analysis Code) is developed to determine the safety of CDA accident. This code can simulate the phenomena of metal fuel SFR initiating phase event which is molten fuel relocation in a simple way. This code uses temperature of fuel cladding, temperature of molten fuel, amount of molten fuel and pressure inside cavity as initial condition. The

fully voided channel is assumed. This assumption comes from the study of most severe accident analysis of metal-fueled SFR. MESFRAC is FORTRAN based 1-D coolant channel fluid dynamics code. To calculate whole process easily and fast, Eulerian finite difference semi-explicit formulation is used. The strength of this code is the ability of flexibility of simulation and simple model. This kind of code can be modified easily when better model is chosen. And, it is easy to simulate various cases fast which is not able to do for big systematic codes. MESFRAC considers behavior of molten metal fuel only. The heat transfer between molten fuel and other structures (Duct and cladding) is calculated using energy conservation equation. And solidified metal fuel in each mesh is considered. It is assumed that solidified molten fuel is attached to each mesh. The amount of molten fuel which is going to upper plenum and lower plenum is considered. This amount of fuel that is out of active core is considered as negative reactivity and criteria of safety of accident analysis. Also, the methodology and results of safety map is introduced. To validate the code, some unprotected accident scenario is used as initial condition of MESFRAC. The effect of pressurization inside cavity is associated with the amount of molten fuel that is discharged from active core. Pressure of molten fuel cavity inside cladding increase due to fission gas as burn-up is increasing. MESFRAC considers the bond sodium pressurization effect inside cavity. Metal fuel use sodium to increase heat conductivity of boundary between fuel and cladding. This filling of metal fuel is not ignorable in the cavity pressure. Mass discharged from active core is considered as the guideline of safety of accident.

Contents

List of Figures

List of Table

Nomenclature (TBU)

A	Area	[m^2]
a	Acceleration	[m/s^2]
C	Coefficients	
CFNACL	SAS4A PLUTO2 input	
C1~C3	SAS4A PLUTO2 input	
CIA	SAS4A PLUTO2 input	
D	Diameter, hydraulic diameter	[m]
e	Internal energy	[J/kg]
F	Friction factor	[-]
f	Fraction	[-]
g	Gravitational acceleration	[m/s^2]
H	Heat transfer coefficient times area	[J/s·K]
h	Heat transfer coefficient	[J/m^2·s·K]
k	Heat conductivity	[J/m·s·K]
m	Atomic mass	
N	Number	[-]
P	Pressure	[Pa]
Q	Fission heat source	[W/kg]
r, R	Radius	[m]
S'	Mass sink or source per unit of generalized smear volume	[kg/(s·m^3)]
T	Temperature	[K]
t	time	[s]
u	Velocity	[m/s]
V	Volume	[m^3]
z	Axial coordinates	[m]

Greek symbols

ρ	Density	[kg/m^3]
$\theta_{k,i}$	Volume fraction of component k in the axial cell i	[-]
ν	Viscosity	[kg/ms]
ω	Friction coefficient (bearing)	[-]
λ	Darcy friction factor	[-]
σ	Surface tension	[J/m^2]
η	Dynamic viscosity	[m^2/s]

Subscripts

ca	*Cavity*
ch	*Coolant channel*
cl	*Cladding*
ch,op	*Open channel*
fu	*Molten fuel*
ff	*Frozen fuel*
fv	*Fuel vapor*
vg	*Vapor and gas mixture*
Mi	*Mixture of sodium vapor, fission gas, fuel vapor, steel vapor and liquid sodium*
Na	*Sodium*

Chapter 1. Introduction

1.1 Research background and motivation

Although sodium-cooled fast reactor[1.1] is one of 4th generation of nuclear power plant, Sodium which can be higher temperature is used as coolant for primary heat removal system rather than water as light water reactor (LWR) does. This SFR use fast neutron spectrum for fission reaction. Lower neutron energy spectrum (this is called thermal neutron) is used for general light water reactor that is operated for past times. Using this fast neutron, technology of turning long-lived radionuclides into short-lived radionuclide material can solve the problem of handling of radioactive waste material. And, this can enhance the usage of uranium in an efficient way. Because of those positive benefits, Sodium-cooled fast reactor has been developed in Korea, Japan, US, Russia, France and so on. But to deal with its construction, the safety of this reactor in the case of accident is most important.

Not only IV-gen reactor[1.2], all of reactor needs to be proven that they are safe even severe accident is happened by accident. But problem is, general public doesn't support the safety of nuclear power reactor because of some accidents. The probability of nuclear power plant severe accident is much smaller than most of car accident and crash of airplane. But it is true that just one or three well known accidents experience makes general public have doubt or question for the safety of nuclear power reactor. Those "well known severe accidents" are Chernobyl accident, Three Mile Island (TMI) accident and Fukushima accident. Nuclear power plant can have small accidents, but the common factor that can make public believe that nuclear plant can be dangerous is all of three accident shows core melt of damage of nuclear fuel. Basically, nuclear power plant safety methodology is defense-in-depth. This methodology focus on the barrier of nuclear fuel. This barrier will keep radioactive material not to release to environment. First wall is fuel cladding. And others are reactor vessel and primary containment building[1.3]. At least one barrier (cladding) is collapsed in above accidents and radioactive material inside cladding is leaked to the environment. This radioactive material leakage needs evacuation of personnel and local residents if the radioactivity is not much effective. Results of some accident shows genetical modification of plants near plants. These phenomena of accident damage near environment grows public's fear. But most of information which raise public's fear are exaggerated.

Although those public's fear, the public agreement opinion of construction of nuclear power plant are also growing. The reason is that the advantage of using nuclear power plant is much bigger than the probability of severe accident. One advantage of nuclear power plant is national energy security. Energy security means non-interruption supply of energy and this can affect the development of technology hugely. In the case of uranium cost, the portion of uranium in the power generation cost is about 10 %

which is much lower than the cost of fossil fuel. The main reason of this difference between two electricity generation cost is from the potential energy density difference between uranium and fossil fuel. Uranium 1 g can produce energy which is equivalent to 3 tons of coal fuel. This makes the effect of oil price of electricity power generation price small from fuel cost because this fuel cost is very small. Second advantage is reducing green-house gasses using nuclear power plant. Typical green-house gas is carbon dioxide. The amount of carbon dioxide emission of nuclear power plant is 1/1000 of coal power generation and 1/5 of solar energy generation. Some amount of carbon dioxide is generated in the process of uranium mining/concentrate/conversion/fuel production not in the process of electricity generation. After Paris climate agreement, the reduction of green-house gas is more important. Third advantage of using nuclear power plant is economic feasibility. As compared to other power sources, the unit cost for nuclear power plant is 55 won/kWh that is 85 % of bituminous coal and 23 % of solar energy generation. Not only those 3 advantages, there are lots of other benefits for nuclear power plant.

To solve conflict between for and against, persuade the safety of nuclear power plant to public is important. The probability of accident and influence on environment when accident happens should get recognition of their safety (The probability is very low, and risk is also ignorable if accident occurs). Especially, after Fukushima accident, interest about unexpected natural disaster effect on nuclear power plant grew. To deal with this, study of very low probability accident (severe accident) which can release radioactive material (source term) is conducted. Those are reason of severe accident analysis.

Now, back on the sodium-cooled fast reactor[1.4], problem of accident analysis is one important gateway of permission for nuclear power plant construction. So, safety assessment is needed for plant which is already built, and which is will be built. To do this, the thermo-hydraulic simulation codes has been developed. In the case of SFR, system above proto type nuclear reactor is not constructed in the world. In the case of Korea, study of prototype reactor step is on-going which is Prototype Gen-IV Sodium cooled Fast Reactor. Korean SFR will use pool type reactor vessel with metal fuel as their nuclear fuel which is different from other systems using the oxide fuel. Because of this new type of nuclear fuel, severe accident code for this kind of system is not fully developed. Up to now, SAS4A[1.5] and SIMMER[1.6] code is developed for this SFR severe accidents. Those two codes cover different phenomena. In chapter 1.3. will explain this difference. Those severe accident analysis code can calculate from core thermal hydraulics to reaction of primary and secondary cooling system. But, in this research, code development focusing on the hydraulics of coolant channel which is very simple to modify model inside code is objective of this research. This code will calculate the ejection of molten fuel to coolant channel and relocation of molten metal fuel inside coolant channel. Not only this, bond sodium effect on cavity pressurization will be considered which is not modelled in SAS4A (After development of SAS4A-metal fuel, this model is added). This code will calculate the relocated molten metal fuel mass inside channel, mass of fuel out of core (in upper plenum and lower plenum) and mass

of solidified fuel inside channel. From this calculation results, the safety of SFR and early termination of severe accident are debated.

1.2 Safety issues of SFR with metal fuel/oxide fuel

In this research, SFR pool primary cooling system is studied. One big difference between SFR and LWR is that different neutron energy spectrum is used respectively. Moderated neutron is used for LWR and almost none-moderated neutron is used for SFR. This fast neutron (high energy neutron) makes higher conversion ratio between fission neutron and captured neutron. And because increasing number of useable neutrons from fission reaction has high energy spectrum, neutron economy is enhanced. This is one of strength of fast reactor. This high energy fast neutron has another merit; breeding and transmutation. To use this fast neutron, high enrichment of nuclear fuel is needed. As thermohydraulic characteristic, high exit coolant temperature which has advantage of high efficiency of energy conversion is one merit. Another is unnecessariness of motor because electromagnetic pump will be used for liquid metal coolant system. High power density compared to LWR and breed-and-burn system for long life core are also advantage of SFR.

Unlike the light-water reactors previously developed for the safety of the Sodium-cooled fast reactors, differences in these new systems make a big difference to the existing systems in safety-related issues. In the case of a pull-type system, there is no additional piping system, so the accident of coolant leakage considered in light-water reactors is not taken into account and no additional coolant injection system is required by the coolant leakage. Unlike water, the safety margin for sodium is higher and the pressurization is not required due to the higher boiling point. In fact, the pull-type Sodium-cooled fast reactor will have 1 atm operating pressure.

In addition to the change in cooling system, the Korean SFR has a big difference in that it uses metal fuel unlike its LWR using conventional oxide fuel[1.7]. Metal fuel has a greater advantage than oxide fuel in terms of neutrons. In the case of metal fuel that does not contain oxygen atom, a higher energy neutron spectrum can be created, which can produce more neutrons than the neutrons absorbed inside the fuel pins. In the case of metal fuel, the temperature difference in the axial/radius direction is not significantly different due to the reduction of the contact heat transfer resistance which is significantly better than the oxidie fuel and the contact resistance by the bond sodium. This type of metal fuel has a heat transfer coefficient of 10 times more than that of an oxide fuel. The low temperature difference at different locations in the axial/radius direction of these fuel creates a small zero- to full-power diver reactivity swing. This has the advantage of reactivity control. The maximum temperature during normal operation of the metal fuel is lower than 1000 K. In the event of an accident, as the temperature of the fuel rises in the overheating state, the fuel may form a eutectic mixture in the interface between the

metal fuel and the cladding, which may cause fuel damage at a lower temperature than the melting point of the fuel and cladding. Such eutectic reaction reduces the thickness of the solid cladding and can, in turn, have the greatest impact on fuel damage.

As metal fuel is irradiated during operation, the temperature of the fuel and cladding increases, along with thermal expansion and internal component transfer. In addition, fission gases are generated and move, creating a porous media inside the fuel. The cladding is also in contact with metal fuel, which causes the components of the cladding to move into the metal fuel. The transfer of components of these metal fuel and surrounding structures will result in changes in material properties in some areas. For this reason, there is a ring-shaped melt inside the elevated metal fuel. Using high-energy neutrons at high speeds using metal fuel, unlike light-water reactors that use thermal energy and nuclear oxidizing fuel, has two kinds of feedback. First, the negative Doppler reactivity is reduced, which increases the coolant void reactivity. If the temperature of the core increases due to low coolant flow or increased fuel power during an accident, the positive reactivity shall be inserted by the sodium boiling and the negative reactivity corresponding to this positive reactivity should be considered (or the geometry of the core can be modified to induce neutron release to produce a negative reactivity). Factors that can cause negative reactions at high speeds using metal fuel are the expansion of the axial/radius direction, the Doppler feedback, and the emission of molten fuel and density changes by the generation of molten fuel. Experiments have been conducted to determine the behavior of these metal fuel at normal times or during normal departure. A basic phenomenon on the safety of metal fuel was studied by the In-pile test.

1.3 SFR severe accident code: SAS4A and SIMMER

The study of the first generation of reactors (Magnox), the current third generation commercial reactors, CANDU, RBMK, PWR, etc. is actively moving on the fourth generation of nuclear power plants with the characteristics of the future's high economic, sustainability, safety, and nuclear proliferation resistance. Those are advantage of 4^{th} generation of nuclear power plant compared to the existing reactor types, including the currently operated nuclear fission reactor worldwide. Sodium-cooled Fast Reactor (SFR), lead-cooled fast reactor (LFR), gas-cooled fast reactor (GFR), and supercritical cooling water reactor (SCWR) are fast reactor candidate of this 4th generation reactor. Among them, the SFR is being studied domestically. However, due to increased interest in safety after the Fukushima accident, the study of accident phenomena is being considered primarily by interest in the safety of the SFR. A study of the severe accident analysis was conducted on the reactor core in general, and the severe accident analysis codes were developed to simulate the severe accident. The difference between these severe accident analysis codes and the general accident analysis codes is that the ability of the core damage accident (CDA) calculation capabilities are present. The general accident analysis code simulates a comprehensive core and heat transfer and a thermodynamic response to an accident in the system. In the case of general accident codes, most of the accident analysis are stopped if the flow of coolant stops or the power of the core rises rapidly, causing damage to the core or a boiling of coolant. Most accident safety analysis codes belong to this category. Typically, there is MARS-LMR. Unlike these general accident analysis codes, the severe accident analysis codes simulate the CDA, further calculation of the phenomena and the movements of radioactive materials. Examples of light water reactors are MARS, MELCOR, MAPP, and ASTEC in Europe.

Unlike light-water reactors, the Sodium-cooled fast reactor is still a research reactor that has not yet been built that produces a conversion to high-power electrical energy, and studies have been conducted on many phenomena in the event of a severe accident. Studies have been conducted focusing on the serious accident of the SFR, which uses metal fuel. In Korea, research is active on the accident phenomenon of PGSFR (Prototype Gen-IV sodium-cooled Fast Reactor), that will use the metal fuel. There are two major analytical codes for severe accidents on the SFR worldwide. One is SAS4A and the other is SIMMER. The analysis range of the two codes varies depending on the accident analysis stage. In a study related to the accident of SFR in Japan, a study was conducted on the phenomenon following the critical accident stage of the SFR. Starting with nuclear fuel damage, the conditions for each stage and the conditions for the next stage are presented by classifying the phenomena that may occur in the core as an initating phase, transition phase, etc. When these accident steps are applied, the SAS4A interprets the initializing phase and then the accident until after the early-discharge phase and the material-relocation phase. The SAS4A has so far developed a version for the analysis of oxide fuel

and currently development of metal fuel has been carried out. To date, SAS4A has been updated to a version that can simulate metal fuel from a previous code that interprets oxide fuel. The SAS4A, which has been updated to date, has the following analytical skills:

1. Detailed sub-channel model improvement of the overall core size analysis to solve temperature and flow distribution

2. Possible 3D visualization of sub-channel calculation results

3. Support for external CFD simulation coupling to solve flow distribution

4. Support for calculating axial expansion feedback from duct walls of the assembly

5. Define Custom Coolant Physical Properties

6. Material relocation of metal fuel.

The SIMMER[1.9] code is currently capable of 2D analysis (SIMMER-III) and 3D analysis (SIMMER-IV). The SIMMER code is a code developed by the JNC (Japan Nuclear Cycle Development Institute, O-arai Engineering Center). The three speed field calculations, multi-face, multi-component and fluid dynamics codes in the Eulerian methodology. In addition to the behavior of the fuel, the surrounding structure is interpreted. These structures correspond to fuel pins, nuclear scans, etc. SIMMER calculates the thermal/mechanical loading of the vessels and the re-position to melt and blast cell of the core.

1.4 Model description of SAS4A and scope of simulation

SAS4A computer code is developed in Argonne National Laboratory (ANL) for the Integral Fast Reactor (IFR) programs for many different systems of Liquid-metal-cooled nuclear reactor (LMR). As explained above, SAS4A code is developed to analyze the severe accident of nuclear power plant, especially for very initial phase of core disruptive accident. SAS4A is combined with SASSYS-1 computer code, which is developed to deal with loss of decay heat removal accidents. The initial phase covers from start of transition to the end of ejection of molten fuel

Before the molten fuel and fission gas mixture is released from pin capacity, the coolant channel includes sodium and metal structure melt. However, there will be very complex situations where fuel and fission gases begin to interact with the original components. The thermal hydrothermal phenomena within these channels involve a number of components that must be tracked separately. The moving components of a channel are solid and liquid fuel, solid and liquid metal, with fission gases and vapors of fuel, steel and sodium. The movement of the material is interpreted by LEVITATE as a multi-component, multi-phase, and non-equilibrium fluid dynamics model. Behavior analysis is defined by the range of liquid sodium axial, and generally built by the by the slug is called "interaction region". This area can be increased or decreased. Dynamic model of liquid slug, described as simple non-compression; dependent variables in the interaction area are density, speed and enthalpy. The separate mass and energy equations are released for each component, but the three connected moment-tum equations for the three speed fields are released. The substances handled together in the speed field are as follows:

(a) Liquid fuel, liquid steel (from structure)

(b) Fission gas, fuel vapor, steel vapor and 2 phases sodium

(c) Solid fuel and slid steel

Mass, energy and momentum transfer between different components present in the channel are mainly determined by the local material composition, and in turn by the flow regime used. The particulate fuel flow system can cause unrealistically fast fuel distribution. The basic assumption of this model is that the pin cells released from the collapsed fuel pin are split into liquid materials when they enter the coolant channel. In the axial position where the solid fuel pin is still present, the coolant channel is separated from the pin cavity by cladding and the remaining solid fuel. Therefore, the temperature fields of cladding and fuel are calculated by transient heat transfer. Using this model, the temperature of the

channel and cavity are used as boundary conditions. Continuous melting takes place at the common boundary of the fuel pin and is added as a moving component of the cavity diameter and molten fuel and fission gas.

This situation has more complex phenomena at channel boundaries. It is likely that there is a continuous fuel flow system. Melted fuel / cladding surface temperatures typically cause early coagulation of these substances at freezing temperatures. Melted ceramic fuel and the solid metal melting occur. This assumption is usually made from modelling simultaneous fuel-freezing and melting in SAS4A / SASSYS-1 safety analysis code system. The phenomenon is that the frozen fuel shell is mechanically stable and unbreakable. The flow of molten fuel from the bundle of pins is created by the effect of fluid friction shear or buoyancy. The Fuel Freezing model used in LEVITATE allows for the structural formation of partial fuels. If the fuel temperature of the channel falls below freezing temperature, the temperature of the thrust is reached. This input temperature is always between the liquid and solid lines. If the main component of a channel is metal, it leads to the formation of a metal plug. The fuel skin can continue to grow and begin to melt again. Alternatively, the lower cladding may break when it starts to melt.

1.5 Research objective and its scope

In this research, the severe accident code SAS4A will be studied to look at the phenomena of SFR severe accident phenomena. Even though this code is for oxide fuel (metal fuel version of SAS4A is developed), main Fuel-coolant interaction and major factor that can affect the accident phase will be considered. Because of this system code is heavy to deal with, the objective is developing simple code that can calculate the initiating phase of SFR severe accident which is known as Core Disruptive Accident (CDA). This flexible and light code have advantage that can be easily modified and can be easily upgrade just using another advanced model. Also, this small code can calculate various situation that is not affordable in SAS4A. Also, bond sodium pressurization effect is not considered in older version of SAS4A (up to date, the newest version of SAS4A metal version is considering this phenomena). In this code, bond sodium effect will be considered to determine the effect of this kind of pressurizing.

Chapter 2. Analysis of sodium-cooled fast reactor severe accident code

2.1 SAS4A module analysis for important phenomenon of SFR severe accident

Until now, major accidents at nuclear power plants within the country and abroad have mostly been caused by the use of oxide fuel, a compound of uranium and oxygen. The phenomenon of meltdown in the core in the event of an accident on metal fuel, which was adopted at the domestic SFR, is not studied much, so it is necessary to study accident analysis and phenomena for the necessary of the approval of a nuclear power plant in the future. In particular, the phenomenon of steady operation/transient accident inside the Sodium-cooled fast reactor using Metal fuel are very different from that of Oxide fuel. In the case of metal fuel, the accident is shown to be stopped early due to the inherent safety of the fuel itself in the event of an accident. This is a different characteristic from the SFR that uses nuclear fuel. However, this is only in the early stages of the accident, and the behavior of molten fuel is much more uncertain if it leaves the early stages of such a severe accident. If the entire core is melted and the fuel pool is created, the accident can be transferred to the outside wall if there is not enough cooling. In this study, the In-house code is being developed with the aim of modelling the Fuel Coolant Interaction (FCI) phenomenon, which simulates the fuel behavior inside the channel after the metal fuel is dissolved. This phenomenon simulates the behavior of the molten fuel inside the channel in the Initial phase, which may be transferred to the next level upon the severe accident of the SFR, and ultimately calculates the reactivity to determine additional core meltdown caused by another power explosion.

One of the differentiators of this FCI model is independence. For other severe accident codes, it is difficult to simulate a single phenomenon since several modules are applied and act in a complex way to simulate the entire phenomenon occurring in the nuclear reactor. However, in the case of FCI modelling, the fuel behavior can be independently calculated depending on the conditions of the eruption. Second, the relatively simple calculation can quickly determine the impact of the modified model. It allows us to calculate the behavior of the channel inside the fuel, and finally use reactivity worth to determine whether the accident will proceed to the next level.

Before developing the main calculation code, simple version is first developed. the major FCI phenomenon of the metal fuel, in order to identify the behavior of the nuclear fuel emitted inside the channel, was modelled for its impact on the dispersion phenomenon. It is built on a Fortran basis and computations on mass, momentum and energy are extricated. Calculations have been performed at the top of the fuel and the bottom from disrupted point has not been performed. In the lower part, it is assumed that a pool of sodium exists, and the fuel is dropped to simulate boiling. In addition, the material behavior calculated within the channel is calculated only considering the movement of the fuel.

Nuclear fuel that goes down to the bottom meets liquid sodium and disperses it. These dispersed

nuclear fuels will influence the heat transfer between the lower fuel and sodium. The phenomenon is significant when the oxide fuel is sprayed into the water under light water conditions when the nuclear fuel is released outside the cladding, when the oxide fuel is sprayed with sodium, and when the metal fuel is sprayed with sodium. In addition, these dispersion phenomena are significantly different depending on the conditions of the eruption. In particular, the FCI phenomenon when the oxide fuel is sprayed into the water under the conditions of light water reactors has been studied due to the risk of steam explosion in the event of a light-water accident. Experimental and numerical techniques for injection of molten corium perpendicular to the cooling water were studied. These vertical drop experiments simulate the impact of molten corium in the core during a severe accident on the lower part of the reaction. In such cases, the in-vessel retention phase of the severe accident is considered, and the viability of the dispersal is considered Most of the pouring and dispersion experiments in the water of an oxide fuel showed that a spherical dispersion was produced. However, studies on horizontal dispensing within narrow channels, such as the phenomenon corresponding to the initial phase of the SFR have not been conducted significantly.

Compared to the experiments in which an oxide fuel compound was injected vertically into the cooling water, there was not much experiment in which a metal fuel was injected into the sodium. Rather than injecting metal fuel, studies have been conducted to inject sodium with simulant and to observe dispersants. Most of the drop test was using copper, mercury, and silver not sodium. Experiments simulating metal fuel as a simulant were also conducted, not distributed on a narrow channel, but dropped on a pool-type sodium. The variance of diameter results was found to have a significant impact on the injection speed and the temperature of the melt relative to the coolant. S. Nishimura et al. conducted a study using copper, silver, and aluminum to drop them into the Sodium Pool and focused on thermal dissipation.[2.1] For thermal dissipation, it is applied at low speed (low Weber number). This study showed that if the temperature of the coolant (sodium) is lower than the boiling point, the diameter of the dispersal becomes smaller as the temperature of the initial aluminum melt increases. In this process, molten aluminum was able to remain in a liquid form, which allowed hydraulics to be dispersed. If the temperature of the melt is equal to or higher than the boiling point of the cooling water, it was shown that the dissipation is facilitated by the thermal reaction caused by boiling of sodium. This experiment showed a mass median dynamometer of about 1 mm. In the experiment, weber number did not have much effect, and the larger the temperature of the melt, the smaller the dispersal form. This means that hydrophobic instability does not fit in temperature conditions. In Figure.2.1, when Unprotected Loss of Flow Accidents occur in the SFR, sodium boiling in the core results in loss of fuel cooling, and metal fuel inside is ejected. Figure. 2.2. shows the dispersal of aluminum distributed inside liquid sodium. The study of thermal dissipation was also conducted in Zhi-Gang Zhang.[2.2]

In Zhi-Gang Zhang [2.3, 2.4] a study of hydrophobic as well as thermal dissipation was conducted. The

experiment was carried out using a relatively wide range of weber numbers and the resulting relationship to the distributed size was examined. In this study, the experiment was carried out using stainless steel with a single drop. High speed, high We count, showed a lot of variance. In particular, previous studies have shown that there is no difference in mass distribution when molten metal jets are used. J. Namiech et al.[2.5] performed modelling the distribution between oxides and water.

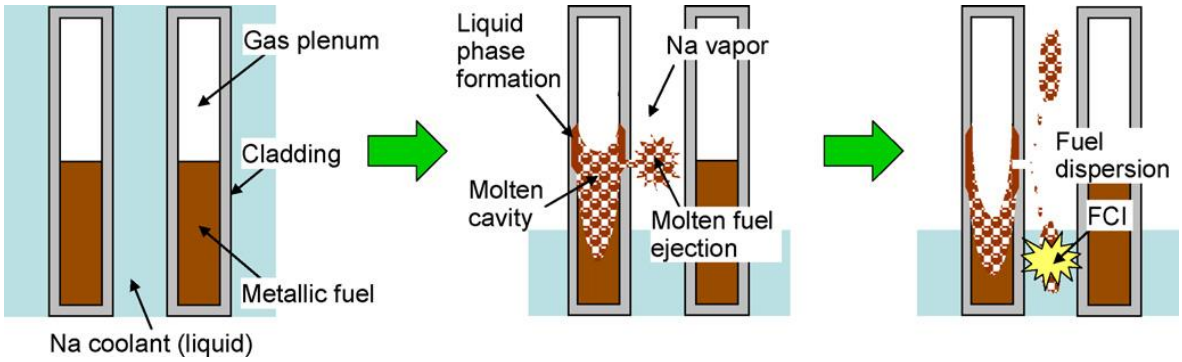

Fig. 2.1 Typical event sequence of ULOF in large size metallic fuel core[2.1]

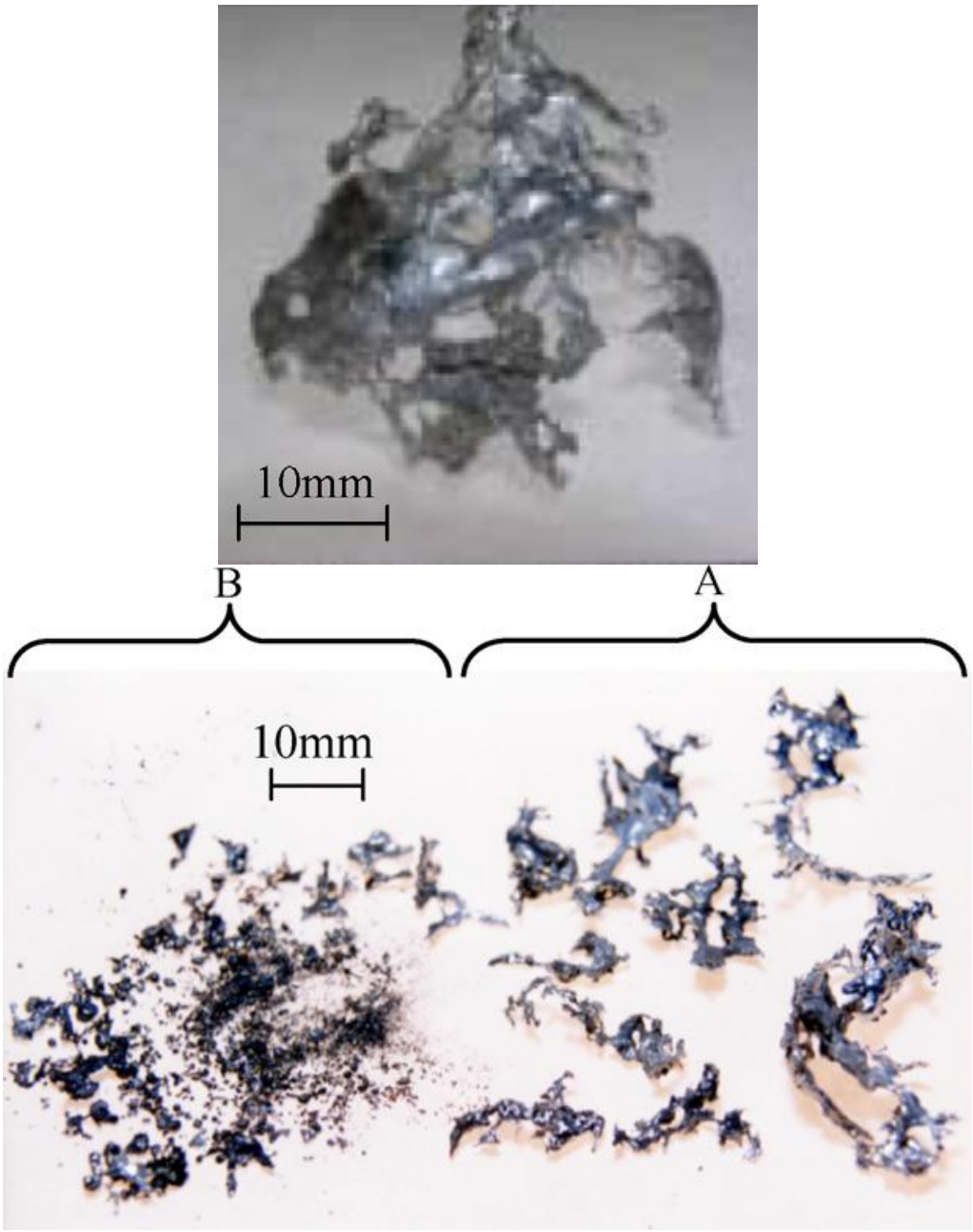

Fig. 2.2. Typical appearance of aluminum fragments[2.1]

2.1.1 SAS4A LEVITATE module analysis

The SAS4A version, developed so far, simulates a phenomenon when only an oxide fuel is used. Generally, oxide fuel means UO_2 and is fundamentally different from metallic fuels such as U-Zr or U-Pu-Zr made of metal alloys. Argonne National Laboratory (ANL) is currently developing a version of SAS4A code for a metal fuel, and related experiments and modeling are underway. To date, SAS5A have developed a module (SSCOMP-A) that calculates the fuel characteristics of a steady state, simulates the mechanical behavior of a transient fuel (DEFORM-5A), and PINACLE-M module that simulates the fuel behavior inside the pin before the fuel cladding is destroyed. However, the development of the LEVITATE-M, which is designed to simulate fuel behavior within the channel, has not yet been completed due to the complicate phenomena of molten fuel behavior.

Table.2.1. and Table 2.2. indicate what properties make a difference between metal and oxide fuel in order to identify differences in behavior of metal fuel compared to the behavior of the oxide fuel. The differences were compared against metal fuel U-5Zr and oxide fuel UO_2. For the first melting point, the oxide nuclear fuel has a melting point equivalent to about 3000 K and the metal fuel has a melting point equivalent to 1500 K. In the case of metal fuel, if a volume expansion occurs due to irradiation or heating, the cladding may come into contact with the cladding, and if the temperature reaches a eutectic temperature upon contact between the two materials, the fusible phenomenon may occur. In the case of metal fuel and cladding, the eutectic point is reached at approximately 1273 K, which can result in the release of molten fuel at a lower temperature than the melting point. The eutectic temperature points of metal fuel is higher than the boiling point of sodium, and hence are ejected from the voiding phenomena of the channel in the event of a severe accident. Indeed, the PLUTO2 module, which simulates the phenomenon of ejection into sodium, was deleted in ANL where the boiling of sodium occurs in the event of a nuclear fuel eruption, resulting in the development of SAS4A.

Thermal conductivity is almost 20 times larger than oxide fuel. This results in a much faster thermal transfer of metal fuel, which results in a distributed phenomenon, which results in coagulation and slow coagulation of oxide fuel with relatively small thermal conductivity. As a result of these properties, a comparison of the dispersion sizes of the two nuclear fuels shows that the fuel is generally small, which can be described as slow solidification during the dispersion caused by the small thermal conductivity described earlier. It can also be seen that it applies to the energy/motor transfer equation of the SAS4A with the oxide fuel described later.

In addition, there is a difference in chemical behavior between oxide and metal fuels. Studies have shown that oxide nuclear fuel may block the cooling channel in response to sodium, and in the case of

metal fuel, studies of the fusible phenomenon should be performed. However, there is an advantage in the case of metal fuel because of its compatibility with sodium. In addition, considering the type of dispersal as a result of the dispersion phenomenon, the oxide nuclear fuel may show the shape of a filament shape or a dispersal, such as a sheet of paper sheet and a fiber, but in the case of metal fuel, it is dispersed into a ball or corner. This suggests that the surface tension of metal fuel in sodium is lower than that of oxide fuel.

E.S. Sowa et al [2.6] conducted experiments in which an oxide fuel was dropped into a pool of sodium and outside of sodium cells. In the experiment, we obtained a maximum of 5 mm from hundreds of micrometers and found a variance (offered) with edges that looked to be dispersed after ageing. As mentioned earlier, oxide fuels could be more active in dispersal activities up to 14 mm prior to solidification. J.D. Gabor[2.7] and J.D. Gabor 2.8 also conducted experiments using metal fuel, showing relatively large variances as well as filaments-type dispersal structures. Sachin Thakre et al [2.9] hydraulically modelled and simulated reactions between these melt and coolant in a 2-D geometry. T. Ginsberg[2.10] also studied Jet Breakup in water-soluble water. Earlier studies did not use nuclear fuel, but A. W. Cronenberg used UO2 and sodium coolant to build a distributed model. This simulates a severe accident on the Sodium-cooled fast reactor that uses oxide fuel. S. Nishimura et al[2.11] studied when metal was injected into the sodium coolant solution. These studies deal with similar phenomena in the core using metal fuel.

To sum up, there are differences in dispersion due to differences in material properties, differences in chemical sodium and cladding, differences in surface tension within sodium, and these differences are not reflected in the calculation model and are currently being modeled for metal fuel. The result of this distribution is to determine the heat transfer area of the fuel material in order to define the behavior of the material in the channel, and depending on the heat transfer area, the flow time of the channel is determined to calculate the distribution of the material in the channel, using the defined reactivity threshold. In order to assess the behavior and re-criticality of molten metal fuel for the upper release of molten metal fuel in the severe accident on metal fuel to be performed in the country (ex-pin), it is necessary to model the dispersion in the channels of molten metal fuel material mentioned above. With the spread of the fuel, modelling the surface area of the fuel is required. In other words, the surface area affects the transfer of energy between the fuel and the coolant, and thus the boiling capacity, releasing a certain amount of nuclear fuel up and down. It is also important to model the phenomena for the zeroing of sodium boiling, since it determines the size of the hardened fuel itself.

Therefore, in SAS4A, an investigation was conducted on the equations that affect heat transfer to nuclear fuels and coolant and surrounding structures. The modules that calculate the behavior of molten

corium in the fuel sodium coolant channel are PLUTO2 and LEVITATE. The difference between the two modules calculates the behavior of PLUTO2 when the melt is ejected in a channel that is filled with sodium and has a void of small sodium vapor. On the other hand, LEVITATE performs a simulation when the melt was ejected when the sodium channel was significantly boiling over a certain standard. As mentioned earlier, SAS4A models the oxide fuel, which is: Figure.2.3[2.12]. shows the molten corium behavior and the mass behavior inside the channel during the TOP situation of PLUTO2, and Figure.2.4[2.12]. shows the mass behavior in the channel at the loss of flow drive over power accident caused by the PLUTO2 LOF and this phenomenon. Figure.2.5[2.12]. shows the flow time for the molten fuel/liquid sodium/sodium vapor lamp generated inside the sodium channels in the fuel using the oxide fuel. Typically, flow time to analyze hydraulics in a channel on the PLUTO2 model of the SAS4A will be interpreted as particulate or droplet flow time, partially or fully annular flow and bubble flow. The variables for determining flow time in these channels are the amount of sodium in the channel and the amount of fuel in the channel. To model the Fuel flow time, SAS4A noted the phenomena shown in the TREAT TOP and CAMEL out-of-pile experiments. In the TRREAT TOP test, the injected fuel into the sodium channel was rapidly dispersed into particles or water droplets and shot up the top. Non-movement fuel is not distributed and during continuous flow from the channel, the fuel is plate-out from the cladding surface. This is in line with the phenomena of oxide fuel specific heat. In the CAMEL out-of-pile experiment, they also observed rapidly fragmented fuel flows and in the case of ejected nuclear fuel, it was located very close to the vent. Based on these experiments, SAS4A simulates a particulate-type dispersion where nuclear fuel is dispersed. If the amount of sodium in the liquid exceeds a certain standard, it is calculated as either annular or bubble flow. During these different flow times, the area of heat transfer between the fuel particles and a mixture of vapors or gases is calculated as follows: For these calculations, however, it is necessary to assume that the fuel is evenly distributed.

$$A'_{fu,vg} = N'_{Pa} 4\pi r_{Pa}^2 \left[1 - \left(\theta_{N1}/\theta_{ch,op}\right)^{Inp}\right] \tag{2.1}$$

$N'_{Pa} = \dfrac{\rho'_{fu}}{\frac{4}{3}\pi r_{Pa}^3 \rho_{fu,sol}}$, number of fuel particles in a generalized smear volume

θ_{N1} = the generalized liquid sodium volume fraction which includes the moving sodium droplets and the static sodium film.

Here the CIA2 is a constant that enters the input. The heat transfer area between liquid nuclear fuel and sodium is defined as follows, not in the form of particles per unit smear volume.

$$A'_{fi.N1} = A'_{Pa} \cdot \left(\theta_{N1} / \theta_{ch,op}\right)^{CIA2} \tag{2.2}$$

$$A'_{Pa} = N'_{Pa} \cdot 4\pi r_{Pa}^2 \tag{2.3}$$

Each constant and variable is equal to the number defined above. In PLUTO2, heat transfer and kinetic exchange are calculated between the components of the channel. If the channel has a low void, as shown above, the heat transfer coefficient between sodium and the cladding is calculated as follows in situations such as liquid fuel and sodium. This situation assumes that the Prandtl number is approximately 0.005.

$$h_{Na,c1,i} = \left[Cl \cdot \left(D_{N1} \cdot \rho_{N1} \cdot \left|u_{Mi,i} + u_{Mi,i+1}\right| \cdot 0.5 \cdot C_{p,N1} / k_{N1}\right)^{C2} + C3 \right. \\ \left. \cdot \frac{k_{N1}}{D_{ch}} \cdot CFNACL \right] \tag{2.4}$$

where C1, C2, C3 is defined from input, k_{N1} is the heat transfer coefficient for sodium, $Cp_{,N1}$ is the heat capacity of liquid sodium, D_{N1} is the hydraulic diameter for the liquid sodium at annular flow regime, and D_{ch} is the hydraulics detector for the channel where the hardened fuel piece exists. If the heat transfer coefficient between sodium and the surrounding structure of the low void fraction is defined as the heat transfer coefficient between the sodium and the cladding defined above.

$$h_{NA,sr,i} = h_{Na,cl,i} \tag{2.5}$$

The heat transfer correlation between the fuel and the coolant at the 'particulate fuel flow regime' using the above heat transfer area is as follows.

$$H_{fu,Na} = h_{fu,N1} \cdot A'_{Pa} \cdot f_{fu,N1} + h_{fu,vg} \cdot A'_{Pa}\left(1 - f_{fu,N1}\right) \tag{2.6}$$

In this equation, $f_{fu,N1}$ is the ratio of fuel to the liquid sodium. The heat transfer coefficient between the above fuel and the liquid sodium is referenced in the Cho-Wright model. In this model, the thermal resistance of the fuel (with respect to the heat transfer coefficient) is defined as follows:

$$h_{fu,N1} = CIA1 \cdot k_{fu} / r_{Pa} \tag{2.7}$$

Here, CIA1 is given in input, and the rpm means the radius of the fuel particles. Thermoelectricity shall be calculated even if the fuel evaporates. The heat transfer from the evaporative fuel to the liquid sodium has different values at the pressure boundary.

$$H_{fv,N1} = \begin{cases} 0 & \text{if } P_{fv} < 10^{-2}\ MPa \\ \left[\mathrm{CFCOFV} \cdot \left(\mathrm{f} \cdot \mathrm{A}'_{\mathrm{cl}} + A'_{sr} \right) \cdot \dfrac{\theta_{vg}}{\theta_{ch,op} - \theta_{Na,fm}} \right] & \text{if } P_{fv} > 10^{-2}\ MPa \end{cases} \tag{2.8}$$

P_{fv} is the pressure of the steam fuel, CFCOFV is the condensation factor of the fuel vapor and f is the specified constant. In this flow condition, the heat transfer area is much smaller than in the particulate flow condition between the fuel and sodium. When the same amount of nuclear fuel is broken down into small pieces, it will have a larger area.

$$H_{fu,Na} = A'_{fu} \cdot \left(\frac{1}{1/h_1 + 1/h_2} \right) \tag{2.9}$$

A'_{fu} is the heat transfer area of the film of molten fuel in a generalized unit smear volume. As mentioned earlier, this heat area is much smaller than the particle-shaped nuclear fuel, so it can be seen as smaller than the heat transfer case. For heat transfer from Fuel Crust to Sodium/Nuclear Gas, the following equation is defined:

$$\frac{1}{h_{ff,Mi}} = \frac{1}{h_1} + \frac{TKFF}{k_{fu} \cdot 2} \tag{2.10}$$

TKFF is the thickness of the coagulated Fuel crust. For h_1, the heat transfer coefficient varies according to the sodium void fraction inside the channel. In this case, the heat transfer rate from the trust to the sodium or fission gas is divided into the heat transfer rate inside the cladding and into the structure.

All the above equations were obtained from the correlation of experimental data. In this way, the SAS4A defines each flow condition as a percentage of the channel of molten fuel and liquid sodium, then calculates the heat transfer between each phase/matter through the appropriate heat transfer equation at each flow time and identifies the mass behavior within the channel.

$$\frac{\partial}{\partial t}\left(\rho_{fu}e_{fu}A_{fu}+\rho_{fu}e_{fu}A_{vg}\right)+\frac{\partial}{\partial z}\left(\rho_{fu}e_{fu}u_{fu}A_{fu}+\rho_{fv}e_{fv}u_{Mi}A_{vg}\right)$$
$$=-\sum_k h_{fu,k}A^{l}_{fu,k}\left(T_{fu}-T_k\right) \qquad (2.11)$$
$$-\sum_k h_{fv,l}A^{l}_{fv,l}\left(T_{fu}-T_l\right)+Q\left(A_{fu}\rho_{fu}+A_{vg}\rho_{fv}\right)$$

Meaning of each term is below:

Afu, Avg = Area of mixture of moving liquid or solid, vapor/gas mixture

Alfu,k = Contact area between moving fuel and some component K per length

Alfv,l = Contact area of component K and fission gas per length

ρfv = Density of saturated vaporized fuel

ρfu = Density of liquid or solid fuel

efu = internal temperature of liquid or solid fuel

General momentum conservation equation of movable solid or liquid fuel and liquid sodium/vaporized sodium is bellow

$$\frac{\partial}{\partial t}\left(\rho'_{Mi}u_{Mi}\right)+\frac{\partial}{\partial z}\left(\rho'_{Mi}u^2_{Mi}\right)$$
$$=-\theta_{Mi}\frac{\partial P_{ch}}{\partial z}-\rho'_{Mi}g$$
$$-\frac{F_{Mi}\rho'_{Mi}}{2D_{Mi}}\cdot u_{Mi}\cdot\left|u_{Mi}\right|-f_{drag}\cdot\left(u_{Mi}-u_{fu}\right)\cdot\left|u_{Mi}-u_{fu}\right|$$
$$-f_{bb}\rho_{fu,liq}\frac{\theta_{Mi}}{2}\cdot\left[\frac{\partial}{\partial t}\left(u_{Mi}-u_{fu}\right)+u_{Mi}\frac{\partial}{\partial z}\left(u_{Mi}-u_{fu}\right)\right]$$
$$-S'_{Na,deet}u_{Mi}-S'_{Na,co}u_{Mi}-S'_{fv,co}u_{Mi} \qquad (2.12)$$

These formulas have been modelled for the dispersion of "oxide fuel" and have not reflected the consequences of dispersion due to the FCI phenomena of metal fuel in sodium coolant. As mentioned previously, the heat transfer area along with the dispersion of the oxide fuel and other metal fuel events will need to be modified to correlate the heat transfer/momentum transfer accordingly.

Table. 2.1. Phenomenological difference between oxide and metal fuel from their physical properties

Property	Oxide	Metal	Phenomenological difference
Melting temperature	3118 K	1517 K	Sodium boiling temperature is much less then that of oxide, the chance of ejection to void is higher in oxide
Specific heat	506 J/kg/K	201 J/kg/K	The specific heat of the oxide fuel is high when the same amount of nuclear fuel is released, and the energy ratio to the melting point is nearly 10 times higher when compared with the overheating and flaming of the melt. This can cause further dispersion in boiling heat transfer between sodium before the fuel is hardened.
Density	8860 kg/m^3	15400 kg/m^3	The ejection at the same pressure (same internal pressure) would indicate a low eject rate for metal fuel. Due to the nature of the metal fuel, the electrics between the fuel and the cladding are thinned to create a lower pressure, which is emitted at a lower rate than the oxide fuel.
Heat conductivity	2.5 W/m/K	52 W/m/K	Metal fuel is much larger. High thermal conductivity requires rapid thermal equilibrium

Table. 2.2 Other factors that can affect the difference between oxide and metal fuel

Factor	Oxide	Metal	Difference in the accident
Chemical difference	Chemical reaction with sodium	Eutectic reaction is possible	Oxide fuel can react with sodium and that can block the channel. In the case of metal fuel, eutectic is needed
Surface tension in sodium	The discharge results show oxide fuel surface tension would be higher than that of metal fuel		Thin filament fragmentation is happened in metal fuel

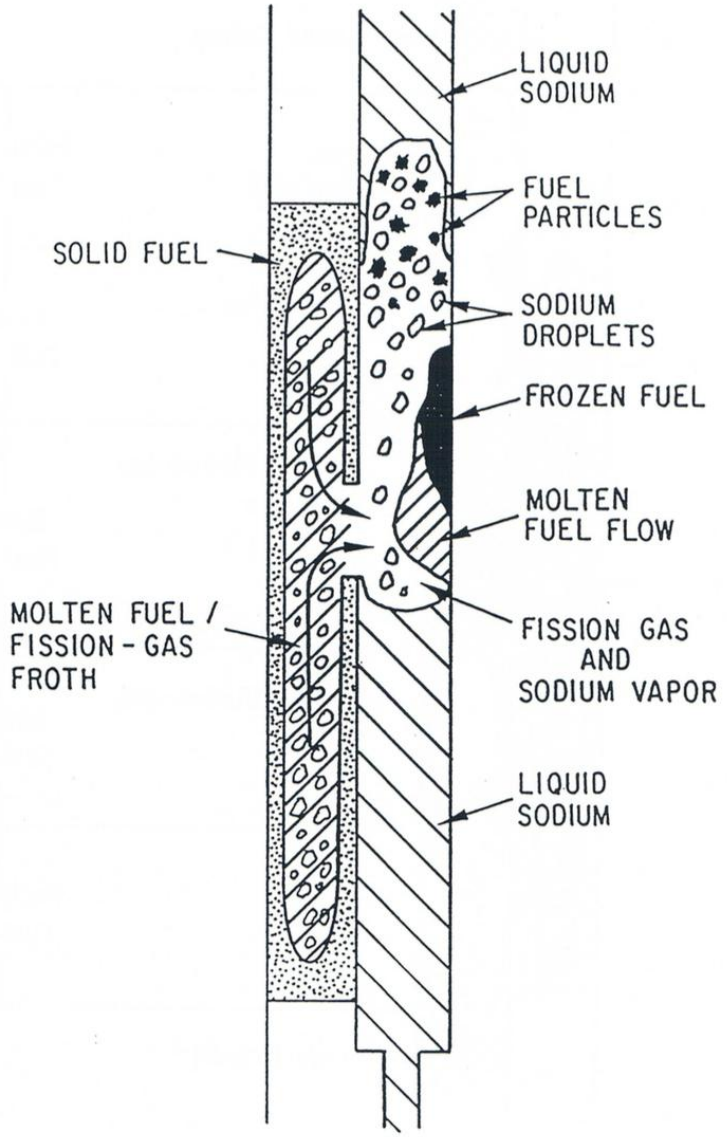

Figure. 2.3. Component behavior schematic of PLUTO2 in TOP accident[2.12]

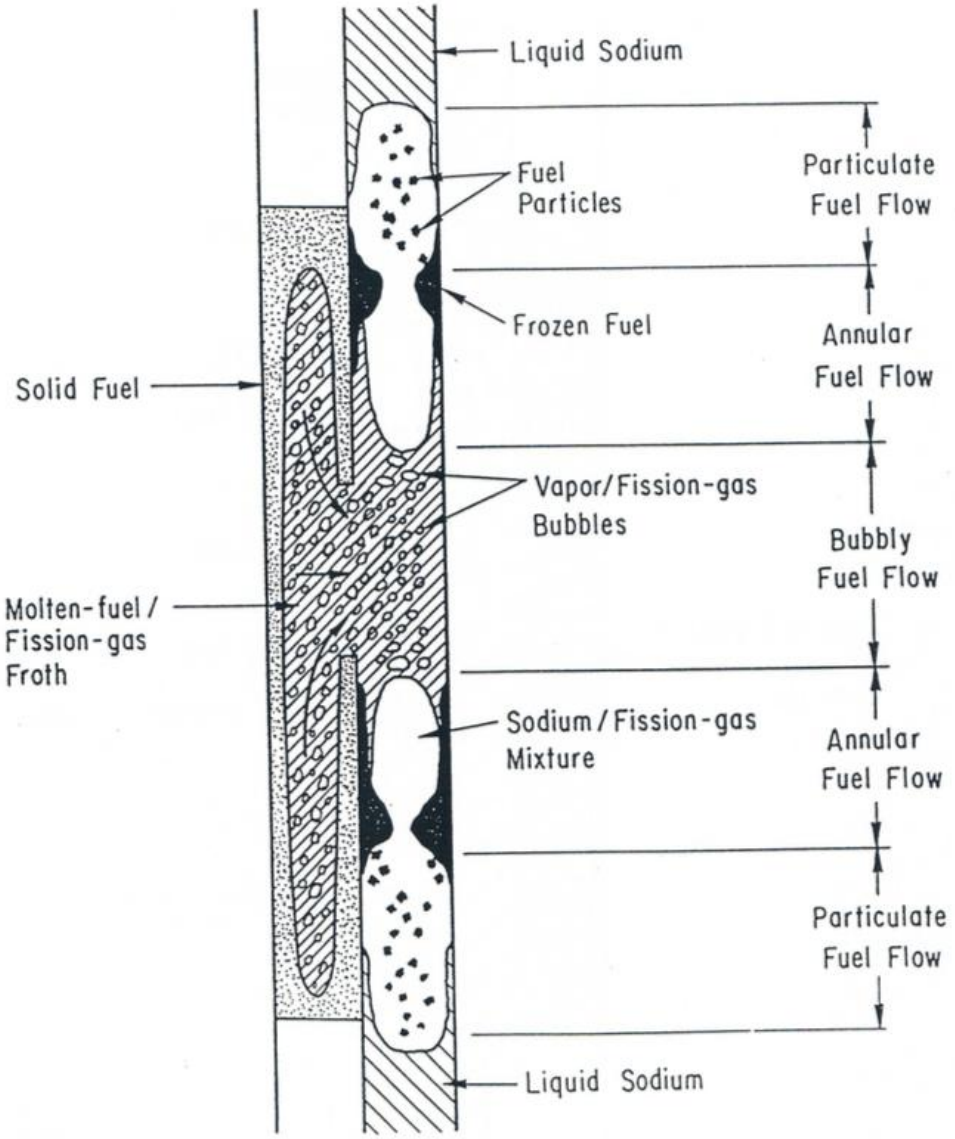

Figure. 2.4. Component behavior schematic of PLUTO2 in LOF accident[2.12]

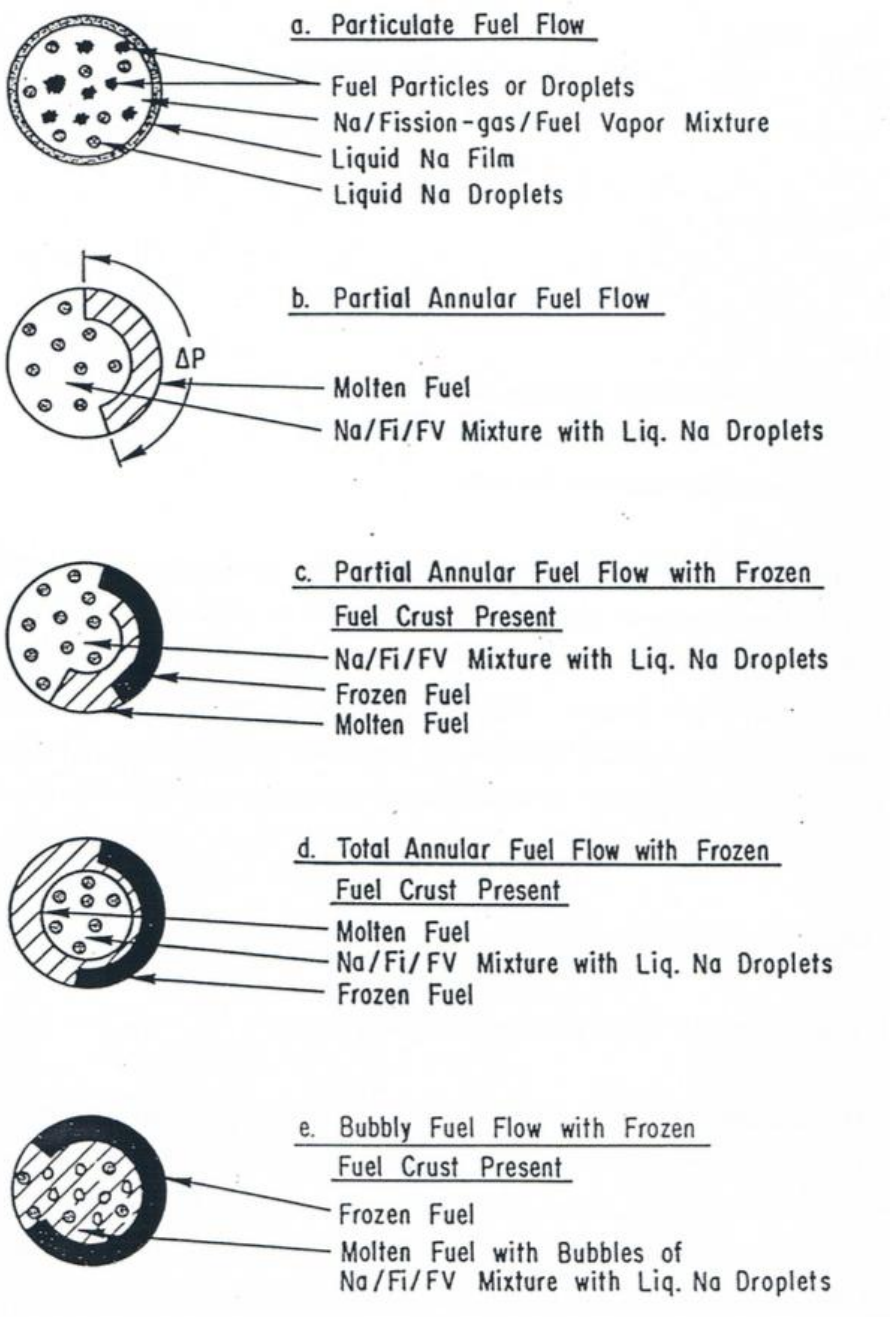

Figure. 2.5. Flow regimes in SAS4A[2.12]

2.1.2 SAS4A single/multi-assembly calculation

In previous stages of the study, accident simulations were carried out using input examples and the results were analyzed. The accident is the coolant loss accident (ULOF) caused by the power surge (UTOP) of a full liquid sodium cooling fast reactor that does not take into account the insertion of a control rod of 3,500 MW/th capacity reactor. This revealed the major phenomena in the core during the severe accident on the sodium-cooled fast reactor and the major phenomena in the release of molten fuel. In all accidents, when the molten corium was ejected, a considerable amount of pressure was created instantly, leaving the upper part out of the open air, causing a self-decreasing response. However, the actual phenomenon is judged to be different, as this interpretation has been carried out in the version of SAS4A of the oxide fuel version that has not yet taken into account the phenomenon of using metal fuel. Metallic and oxide fuels have different material properties, as well as different reactions to liquid sodium issued in severe accidents. Since a safety analysis for the construction of a domestic PGSFR using metal fuel in the future needs to simulate a response between these metals and sodium, it is necessary to analyze the main mechanism for the situation after the metal fuel has been ejected for the initial conditions for the experiment to be carried out. In particular, the current FCI simulation limits were identified for the melt release simulations by configuring single/multiple-sample of using the version of SAS4A currently in place for the reaction between metal fuel and liquid sodium coolant to be modelled in the future.

The current version of the SAS4A simulates an oxide fuel without simulating a metal fuel. This phenomenon should be simulated for the final goal of this project, in-house code. For this purpose, the results of the melt ejection from a geometry having the same dimensions as the actual PGSFR should be analyzed to identify the SAS4A limits and add additional complementary points accordingly. For this purpose, input is needed to interpret only the core, not the entire reactor, and the reactivity of the transient from these inputs is induced to cause an accident and obtain simulation results. To create these input decks, ABTR input and UTOP input, which are examples of SAS4A, could be written. ABTR input starts at the stage that makes up the core, so there is no primary heat transfer and the conditions for coolant entering the channel are designed to enter the input. These inputs were created using PRIMAR-1 without PRIMAR-4 simulating the primary or secondary side. However, the input deck used the UTOP input for this reason since there was no input to the transient melt in the core. The UTOP input is added to the ABTR input by using the option to melt the core and the LEVITATE/PLUTO module, which releases the melt into the channel from the fuel material properties fuel when molten. As a result, the inputs of the power transient giving the temperature, mass flow, and pressure to the

coolant injection on a single channel could be written. This is shown in Figure.2.6.

These inputs were used to increase a certain amount of reactivity, simulating a melt-out inside. The results of this simulation were the result of the channel's transient, the shape of the axial melting joint, the physical properties and conditions inside the melting pool, the distribution of glazing in the channel, and the cladding in DEFORM-5 results in the response. The input geometry of the input was prepared according to the geometry of the UNICORN experimental device representing PGSFR. This is shown in Figure.2.7 and Table.2.3.

As shown in Table 2.3, in cases 1 and 2, the top of the melt was ejected from the inside of the pin, but the resulting reduction in reactivity was small, resulting in the ejection outside. These results have different meanings than those for normal pin internal eruptions. Normally, a burst in the upper part of a nuclear fuel can occur after a certain period of time after melting it and pressurizing it by the temperature and the fission gases, as in this case, the core is known to be stopped due to the negative reactivity.

Figure.2.8. shows the normalized power for all cases. The output of each simulation case is determined by the total number of pins, and the output per pin is the same. As a result, in simulation cases 1 and 2, a lower negative response is generated at the time of the power surge, so that the output burst is accelerated after a certain period of time. In all the remaining cases, the power is rapidly reduced by the negative reactivity upon accident. The time of each accident was different depending on the conditions and case 5 with the largest number of pins showed the slowest response.

The following figure.2.9. shows a change in the reactivity of each case in time. It can be seen that a slight negative response will be heard when an internal eruption of pins 1 and 2. This can be seen as a result of the density changes caused by the internal eruption of the pin. However, it was not possible to stop the previous power surge because of the low response of the sound. The results of these first and second tests resulted in the release of nuclear fuel from the inside of the fuel pin into the fishbowl due to the continuous increase in power output. Nuclear fuel has been released, but the power has already increased, resulting in the entire core melting. Conversely, in the remaining cases, sufficient negative reactivity was obtained through the release of the fuel to the outside of the fuel, resulting in an accident termination. Cases 1 and 6 are simulated in the same structure, but you can see that they have different results. In both cases, exoskeleton and cases No. 4 and No. 6, only the extraneous release occurred. Table.2.4. describes the timing of the external eruption of each pin internal shunt, and the axial position in which the extraneous ejection occurred. Breakage occurred at the top of all cases except for case 1.

Figure.2.10 shows a graph of the reactivity contribution of cases 1 and 6 over time. Each graph shows the total reactivity, programmed reactivity to give transients, the Doppler reactivity, the negative reactivity by the control rod, and the reactivity of the relocated fuel. In case number 6, response to axial

expansion was added. For cases 1 they were not shown because there was no effect on the response caused by axial expansion. The horizontal axis of the graph and the vertical axis are different, so be careful. These two cases need to be considered as they simulate a core averaged in the SAS4A. Results show that the Doppler reactivity involved in fuel temperature is similar to $0.6 but is faster in case 1. One of the biggest differences between the two simulations is the contribution to the accident of negative reactivity by the control rod. For the analysis of case 1, case 1 assembly, the response by the expansion of the control rod was much less than 60 assembly. Discussions on these results are needed, but the more assembly is simulated, the more negative the response to the control rod is contributing. This negative reactivity has prevented a large power explosion of fuel by ensuring sufficient negative reactivity in case 6.

The following diagram shows the melting and spawning process of nuclear fuel from Fig. 2.11. to 2.16. The vertical axis is an axial segment and the horizontal axis represents the density for each material condition inside the fuel rod. The black line shows the density of molten fuel, and the empty space inside represents fission gas, and the area from right to bottom represents solid nuclear fuel. In cases 1 and 2, melt fuel can be seen venting to the top of the fuel pin. Unlike cases 3, 4, 5, and 6, a large proportion of the fuel was released outside after melting in cases. Table 2.5 through Table.2.6 shows data and final mass distribution for the pupil at the time of eruption for each case. Comparisons between cases 1 and 6 indicated that the accident could have ended beyond the core of the area of activity when the fuel was ejected from case 6 to the top plenum. In comparison, cases 4 and 5 showed that the total fuel mass in cases 4 and 5 was the same, but the melt fuel was released to the top of the core from case 4, but the top ejection was not made in case 5, but the accident was terminated due to sufficient negative reactivity.

In the geometry of the experimental device that used the oxide fuel version of SAS4A to represent PGSFR, simulation was performed, and the results were analyzed in different numbers of pins and assembly. In-pin phenomenon where molten corium is emitted to the outside as well as emitted to the top of the gas plenum has been observed. For In-pin phenomena, the power continued to increase as sufficient negative reactivity was not given, and most of the pins were released outside when they were melted. Nuclear fuel released externally may or may not be released at the top, resulting in reactivity reduction by molten corium stopping the core if released at the top, and a reactivity capable of stopping the core even if it was not released at the core. This identifies the limitations of interpretation on a single channel of SAS4A and also requires the addition of these models, since the reaction between metal fuel and sodium has not been taken into account when considering that it is an oxide fuel version. The two mechanisms that have been studied so far are hydrophobic and thermal dissipation

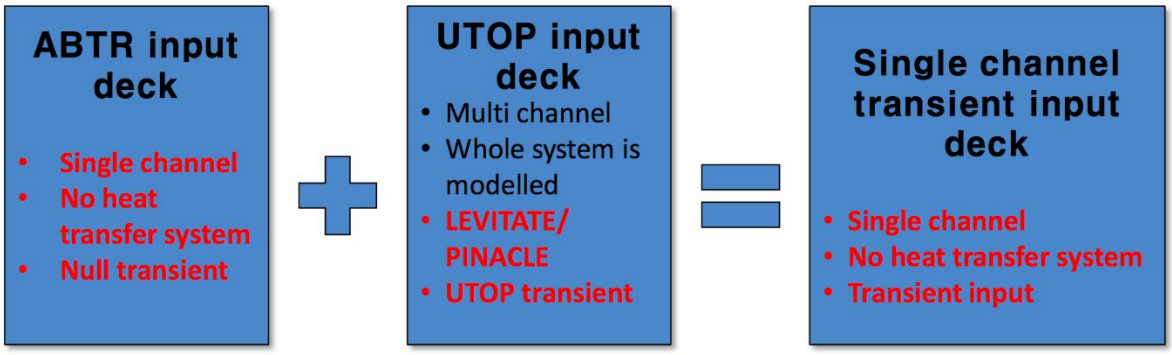

Figure. 2.6. SAS4A single assembly input deck

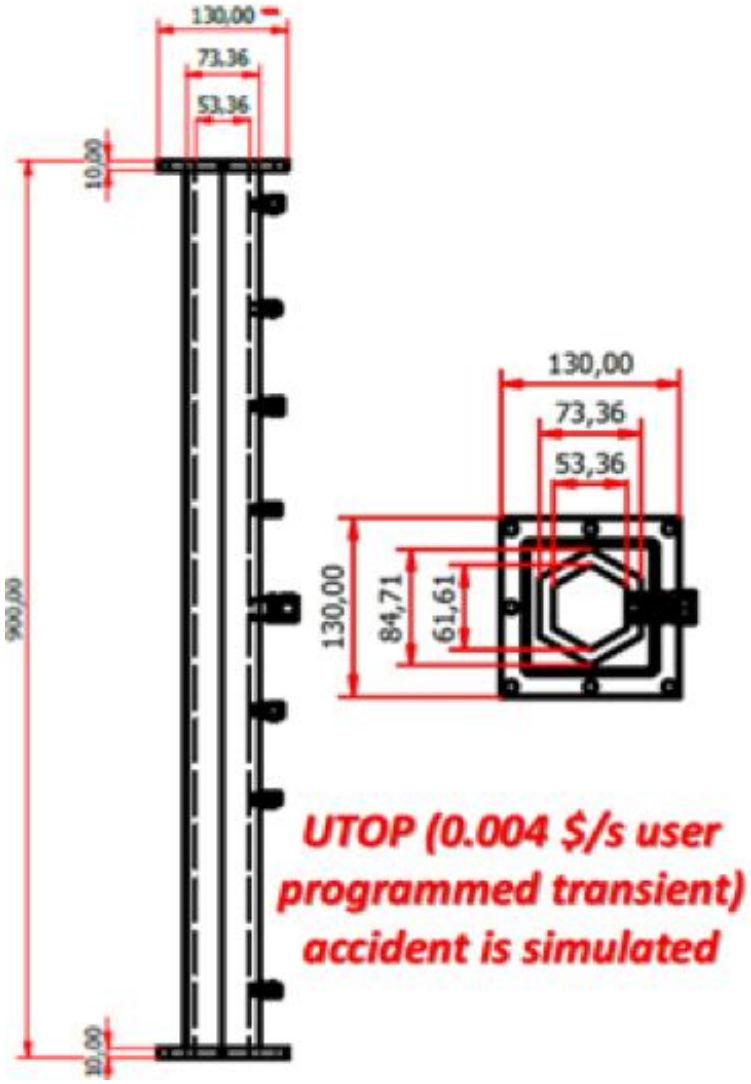

Figure. 2.7. Geometry of input deck

Table. 2.3. Geometry and its input parameter

Parameter		Input parameter
coolant channel area	0.002465825 m^2	
Pin radius	3.542565 mm	RBR
Coolant flow area per pin	2.72177e-5 m^2	ACCZ
Hydraulic diameter	2.067943 mm	DHZ
Cladding thickness	0.5 mm	RR
Cladding inner radius	3.042565 mm	RBR
Number of pins per subassemblies	37	
Number of subassemblies	1	
Length of axial segment in core and blanket		AXHI, 0.04m (total 80 cm)
Thickness of inner structure node		DSTIZ 1.727 mm
Length of fission gas plenum		PLENL 60 cm
Active fuel pin length		ZONEL 140 cm
Structure perimeter per pin		SRFSTZ 2.650 mm

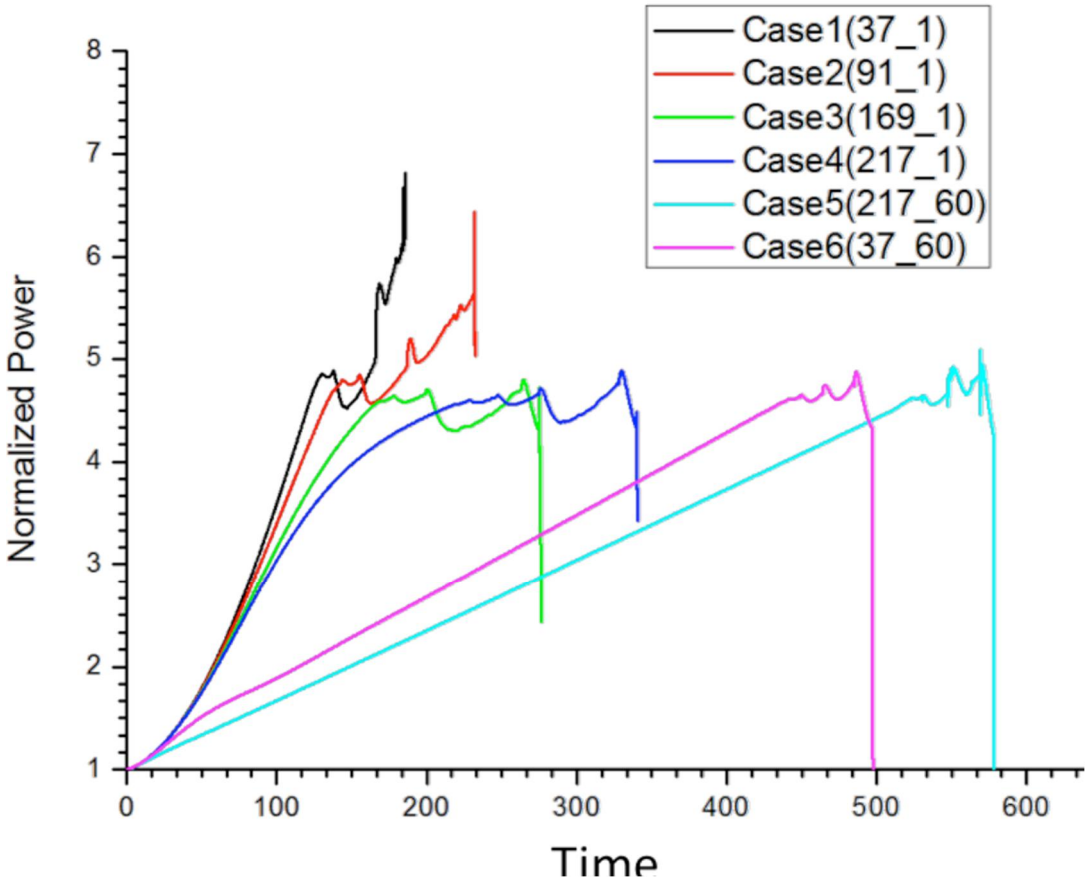

Figure. 2.8. Normalized power results

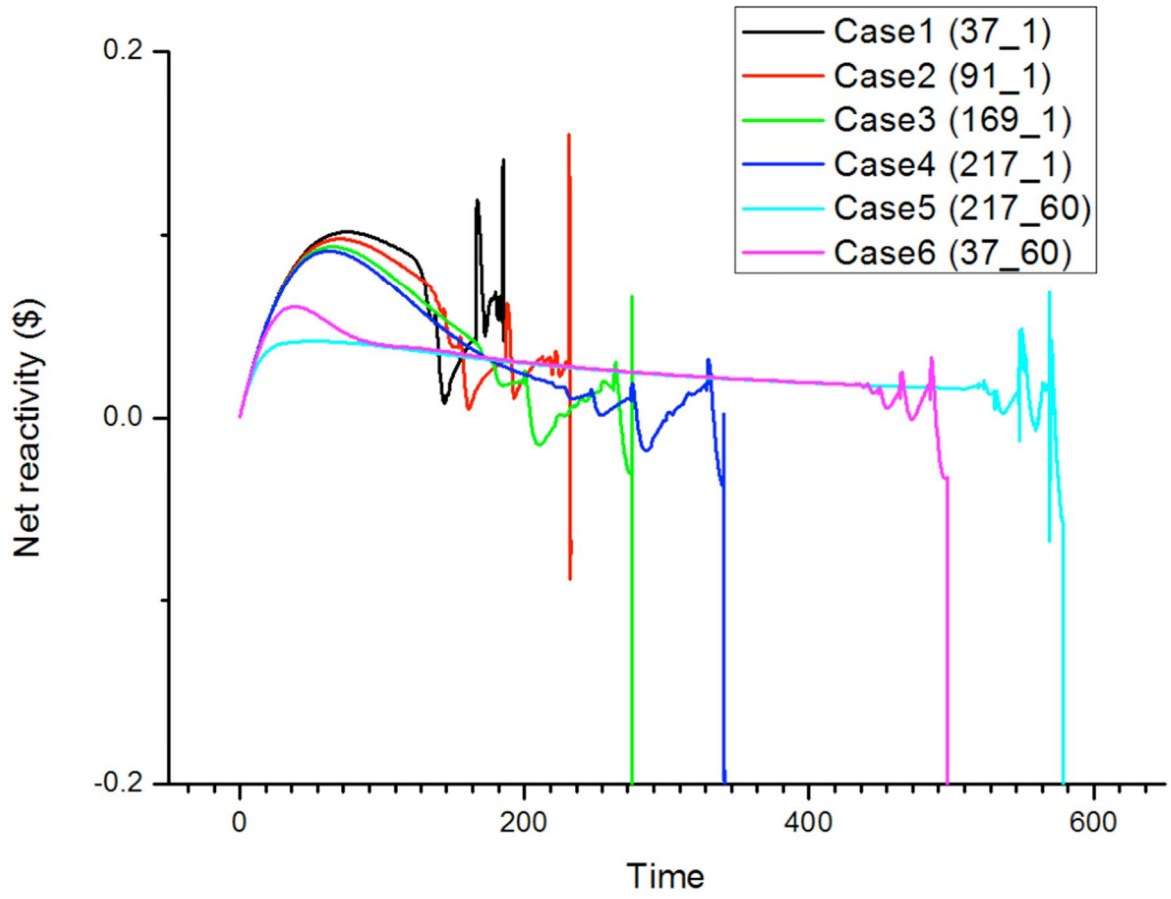

Figure. 2.9. Net reactivity results

Table. 2.4. In-pin/Ex-pin results for each case

Case	In-Pin	Ex-Pin (hoop stress)	Failure segment (total 20 segments)
Case 1.37_1	166.08 s	185.234 s	10
Case 2.91_1	187.15 s	231.265 s	18
Case 3.169_1	x	275.220 s	18
Case 4.217_1	x	340.000 s	18
Case 5.271_60	x	578.284 s	17
Case 6.37_60	x	497.180 s	18

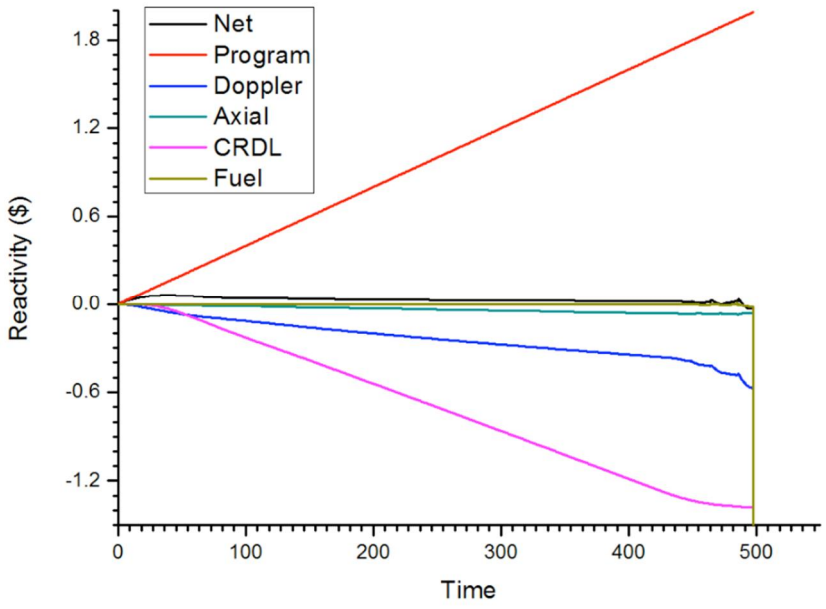

(a)

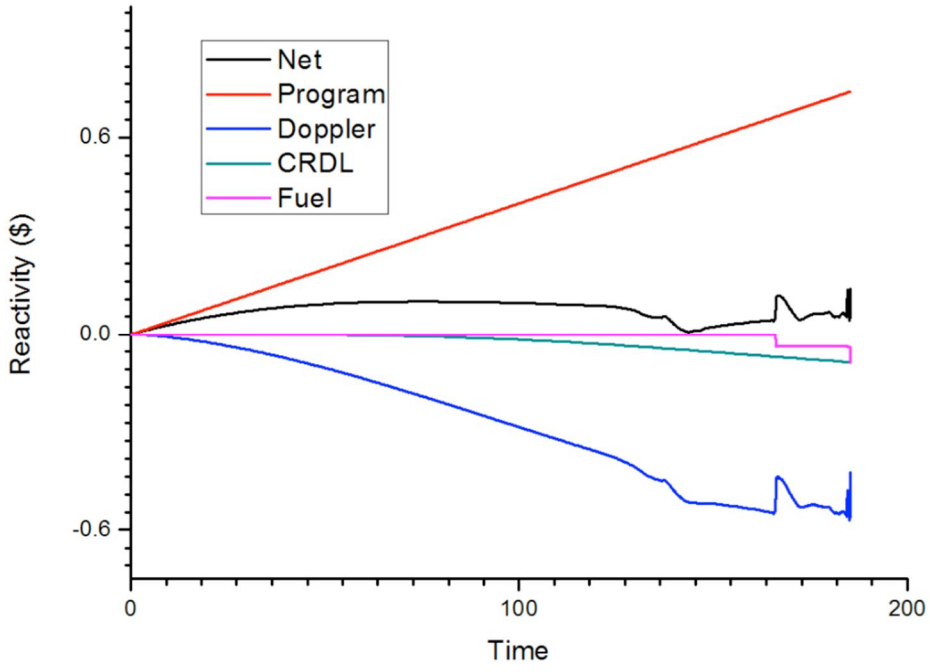

(b)

Figure. 2.10. Net reactivity results, reactivity contribution of case 1 and 6 over time

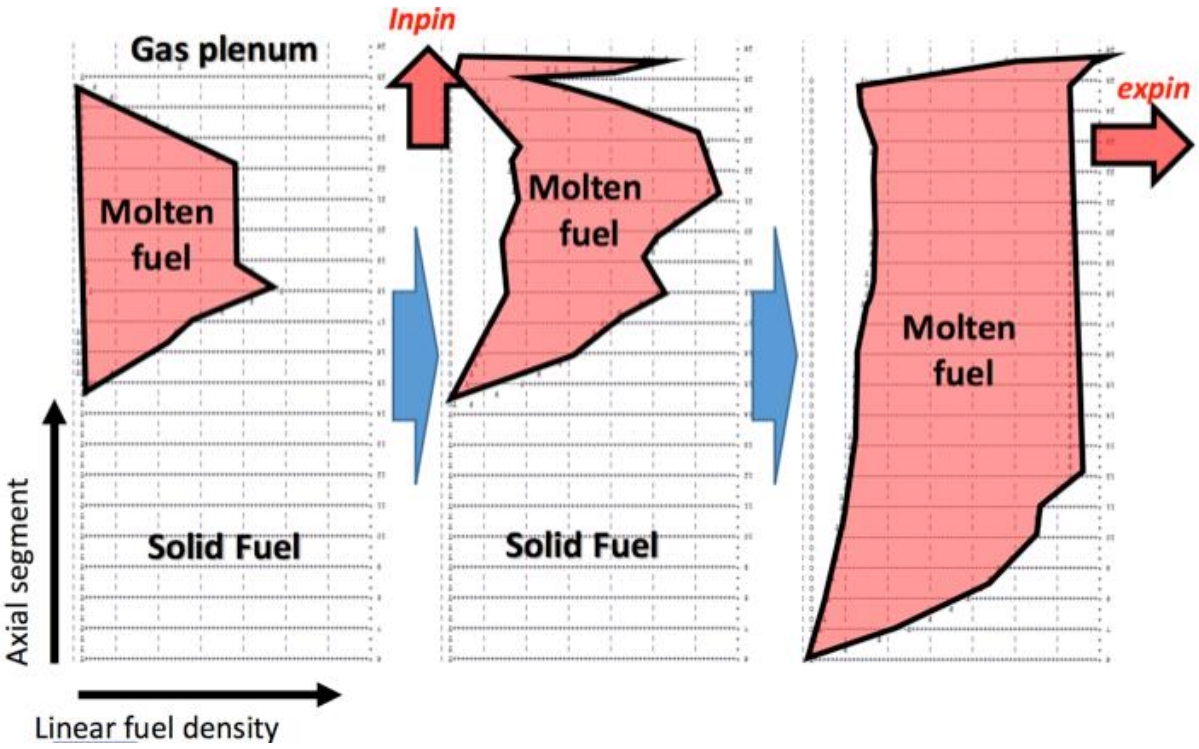

Figure. 2.11. Fuel pin prints, 37 pins, 1 assembly (case 1)

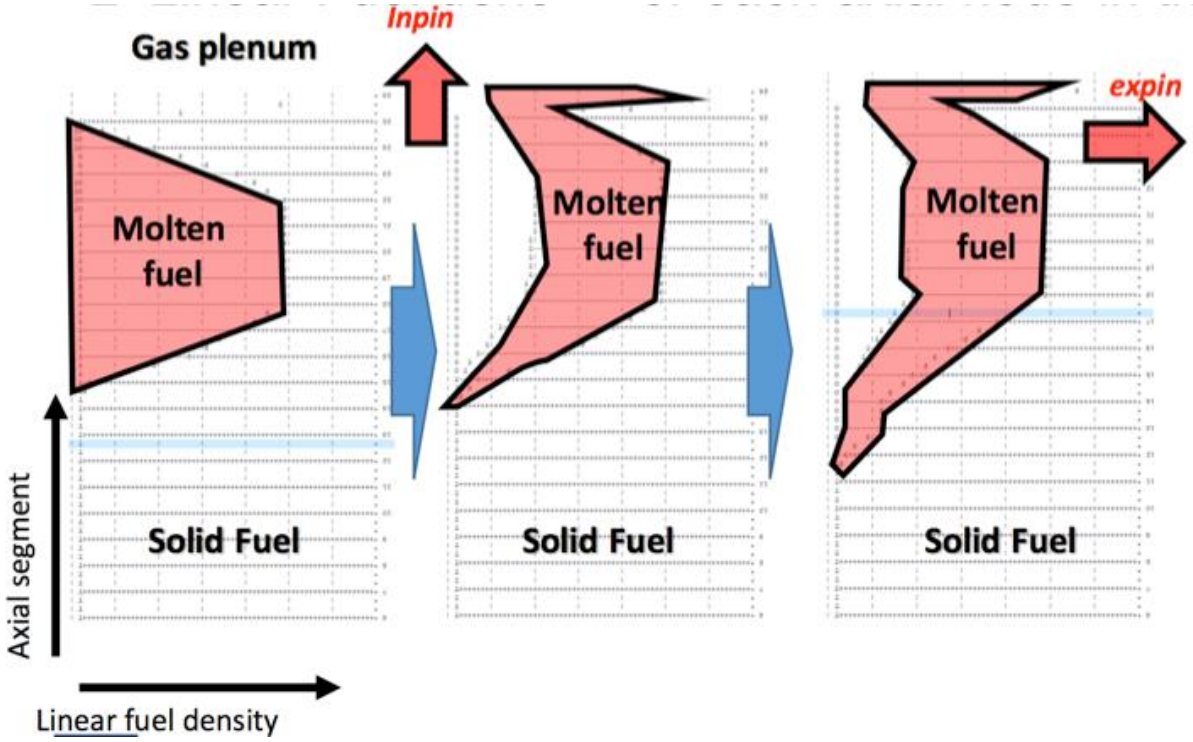

Figure. 2.12. Fuel pin prints, 91 pins, 1 assembly (Case 2)

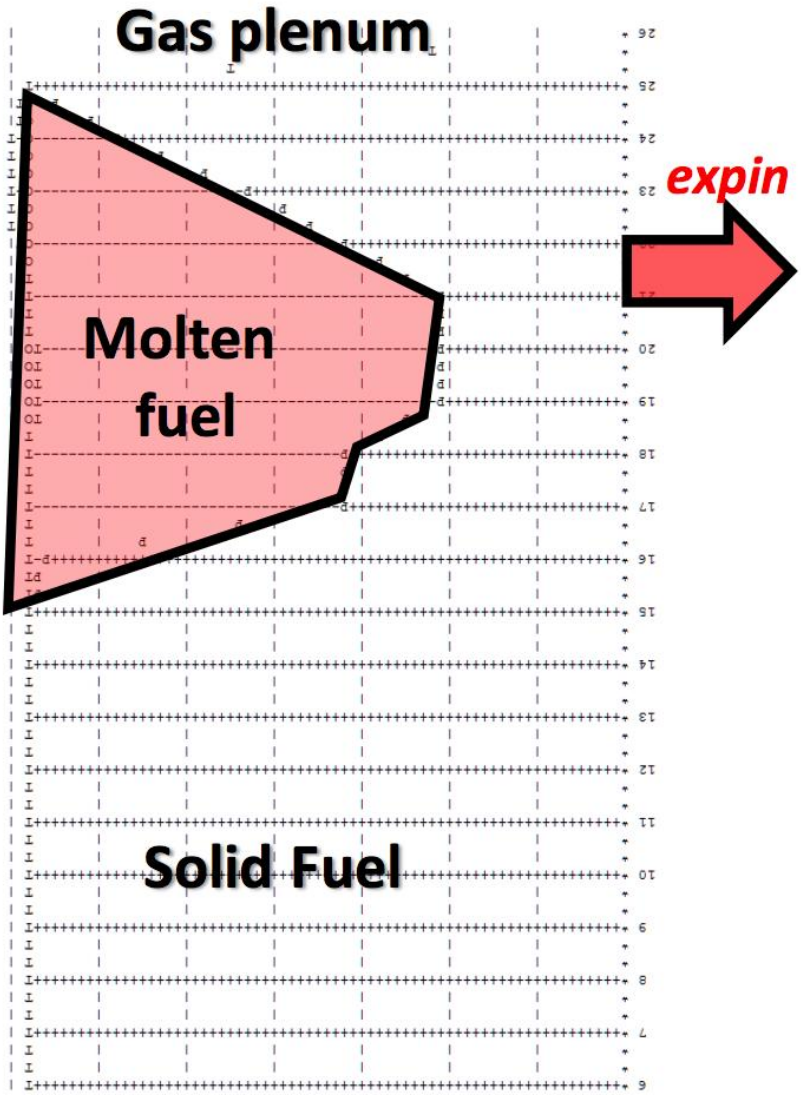

Figure. 2.13. Fuel pin prints, 169 pins, 1 assembly (case 3)

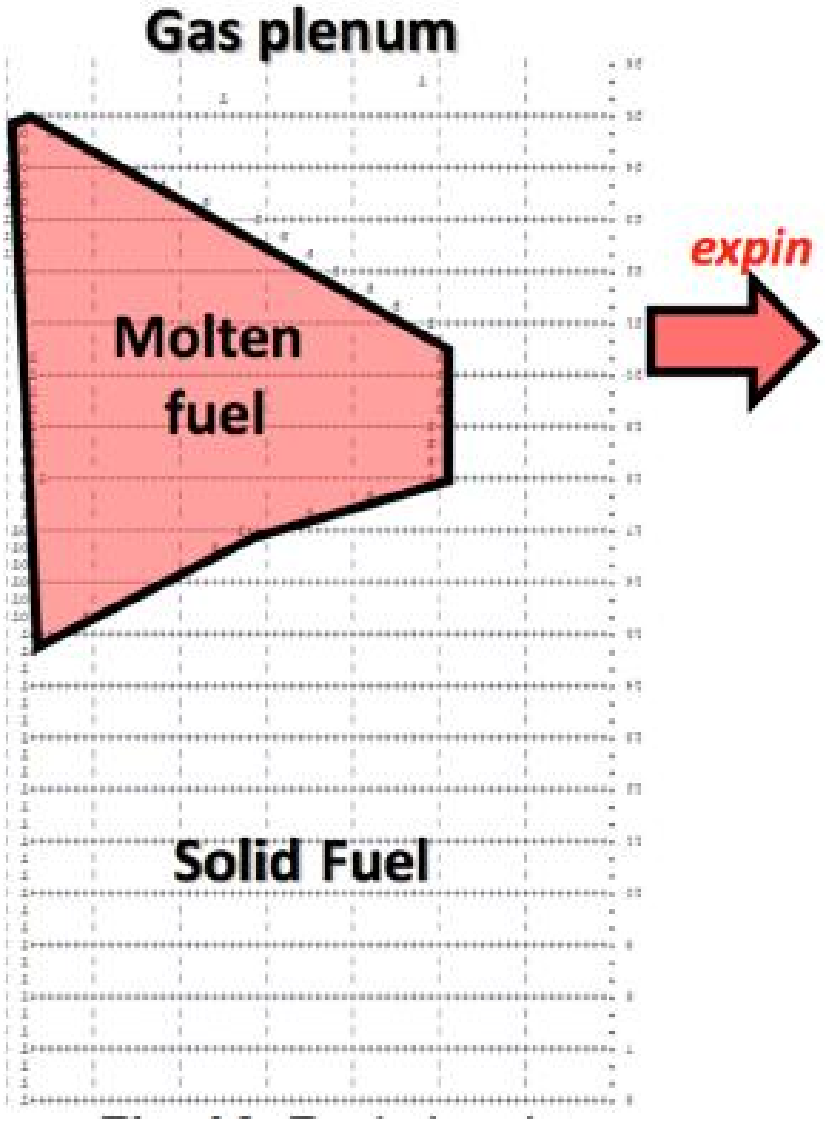

Figure. 2.14. Fuel pin prints, 217 pins, 1 assembly (case 4)

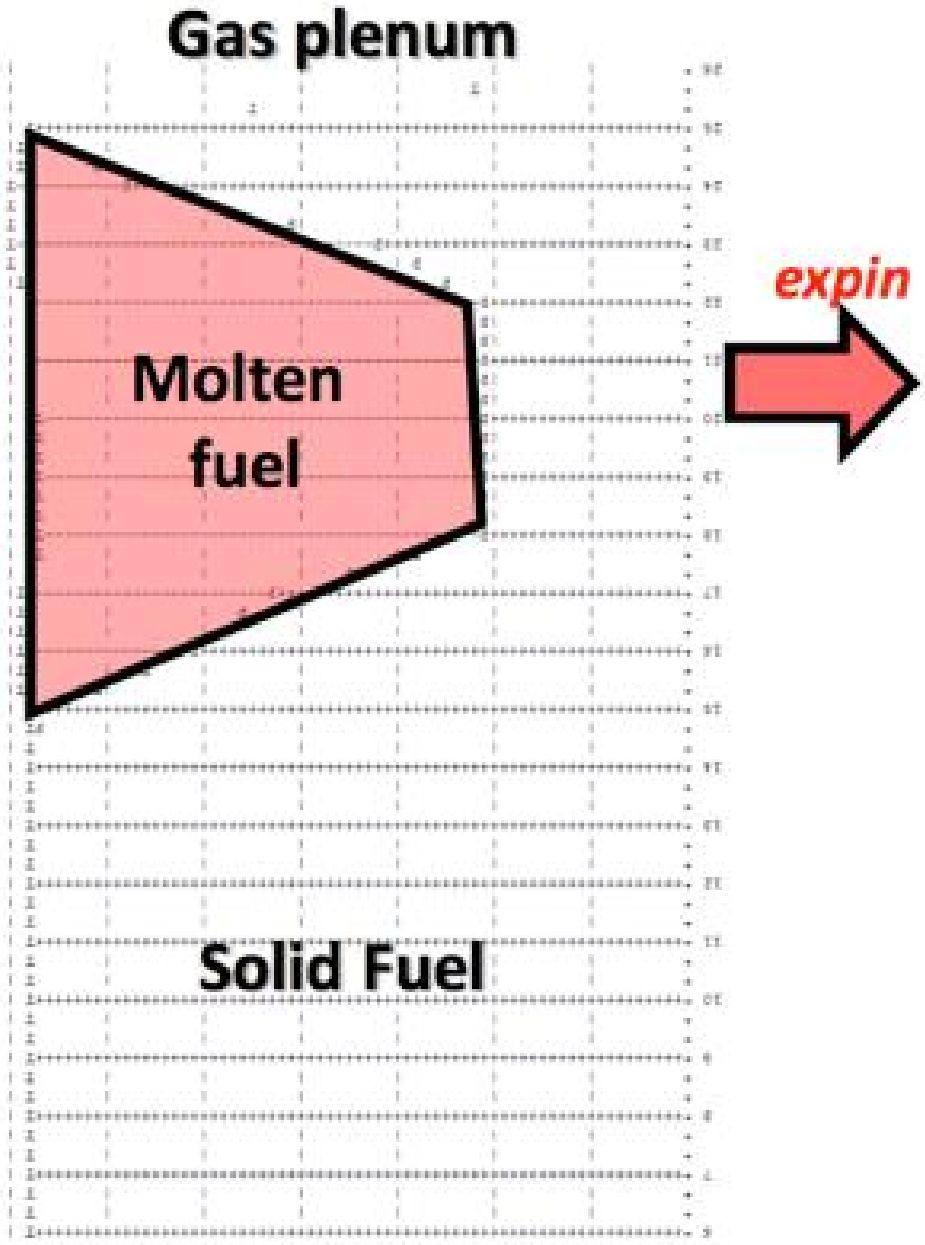

Figure. 2.15. Fuel pin prints, 217 pins, 1 assembly (case 5)

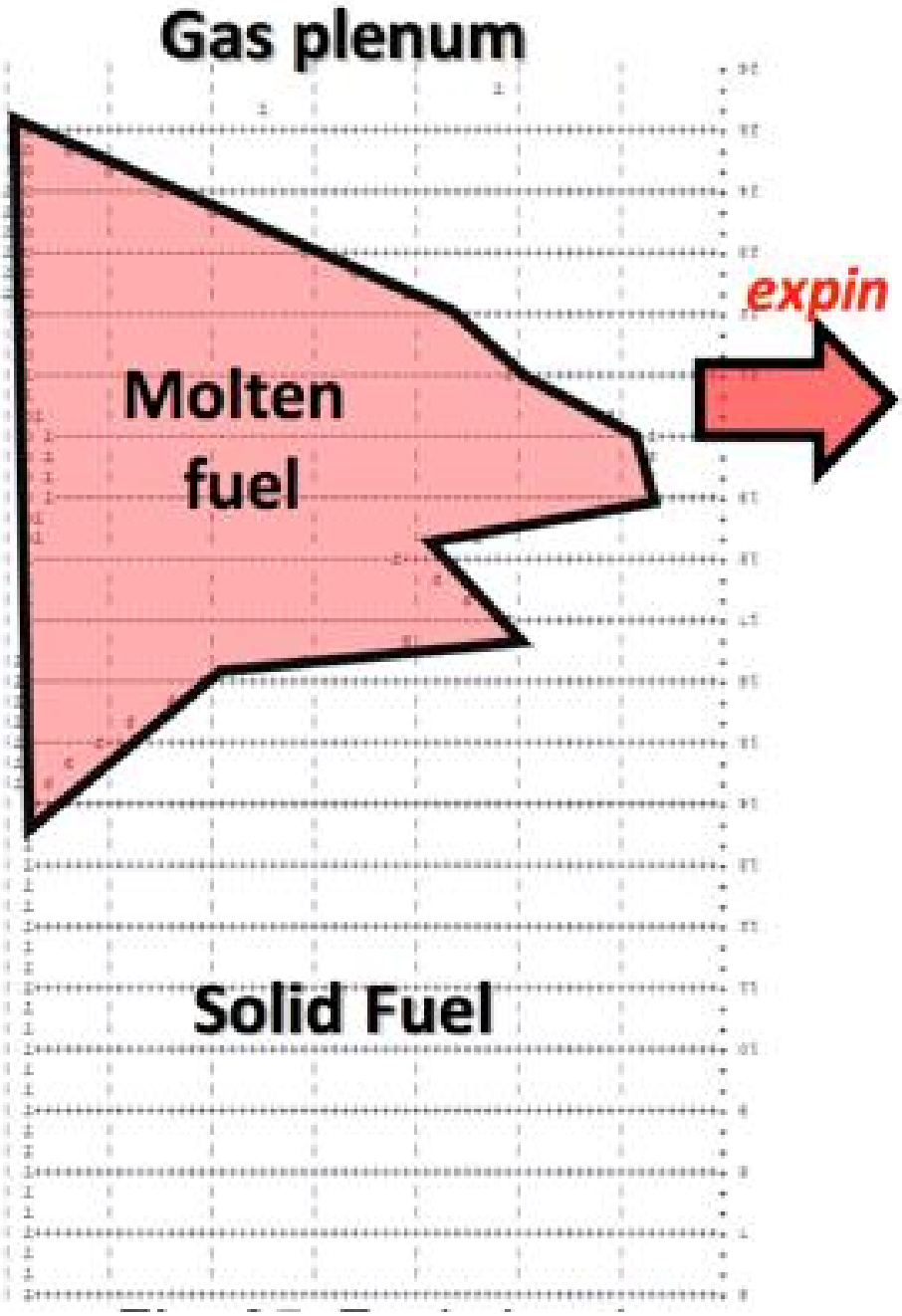

Figure. 2.16. Fuel pin prints, 217 pins, 60 assemblies (case 6)

Table. 2.5 Results of cavity property at the time of ejection (case 1)

Parameter	
Cavity Inner pressure (MAX)_In-pin	4.18 MPa
Diameter of cavity _Ex-pin	5.747 mm
Radial velocity of jet	0.0
Cavity inner pressure (max)_ex-pin	553 kPa

Table. 2.6. Results of relocated fuel in case 1

Fuel position	Mass (kg)
Solid fuel in fuel pins	0.8215
Molten fuel in pin cavities	1.5421
Molten fuel in coolant channel	6.3466
Fuel in chung/Droplets	0.0000
Frozen fuel on cladding	0.0000
Frozen fuel on structure	0.0000
Fuel vapor in coolant channel	0.0000
Fuel in Upper plenum	0.0000
Fuel in lower plenum	0.0000
Total fuel mass	8.7102

Chapter 3. MESFRAC (Metal Fueled Sodium-cooled Fast Reactor Accident analysis Code) DEVELOPMENT

3.1 Coolant channel hydrodynamics model of MESFRAC

3.1.1 Fuel-coolant interaction mechanism

It is necessary to investigate the fuel-coolant interaction (FCI) mechanism resulting from the ejection process in the severe accident of molten metal fuel lacking in the previous SAS4A, and a prior study of the models to be added to the experiments and simulations to be carried out in the future. To date, a wide range of liquid sodium falls have been carried out. Studies have been conducted, mainly in all experiments, on how dissolved solids in a pool of sodium has been caused by the fall of the melt. In most experiments, the melt drops vertically in the pool of liquid sodium. Rather than conducting a study to simulate an accident at the actual sodium cooling speed, which is directly sprayed horizontally, the behavior of the direct melting of the melt has been analyzed in the sodium pool.

Largely molten nuclear fuel undergoes hydraulically or thermo-distribution within liquid sodium, and each mechanism has a significant effect on the distribution of the final metal fuel or the size and shape of the dominant factor. These particle sizes and shapes will have a significant impact on re-criticality in the event of a severe accident on the sodium-cooled fast reactor. These phenomena cannot be simulated in SAS4A simulating oxide fuel developed so far and should be modelled in the future. Further study of dispersion in these situations is also needed, since the environment in which nuclear fuel is actually released from a narrow pool of water as it is sprayed from a narrow pool of sodium because it is different from experiments falling into a deep pool of sodium.

S. Nishimura et al[3.1] conducted an experiment in which copper and silver were dropped into liquid sodium pools instead of directly using uranium metals. These molten metal quantities were not large (approximately 300 g) and the temperature of the sodium was maintained at a maximum temperature of 500°C to 206°C. The study group focused on thermal dissipation, not hydraulics. When dissolved solids fall into sodium, they experience a small amount of sodium being trapped inside the molten corium, and this intensely boiling of sodium creates pressure inside the melt. The high pressure inside the molten corium collapses the solidified shell on the surface of the melt and causes it to disperse. They concluded that the most dominant variable in this phenomenon was the overheating temperature of the melt and the latent heat used in the melting of the melt. Especially noteworthy is that the temperature of the cooling water did not have much effect. This is illustrated in Figure. 3.1. referenced in this study. The final results of the melt are shown in Figure. 3.2.

Zhi-gang Zhang et al.[3.2, 3.3, 3.4] observed the phenomenon in detail using a smaller amount of copper melt than the aforementioned experiment. About 1 to 5 grams of copper melt were used. In this experiment, the temperature of contact was lower than the melting point of the copper, so even if the copper was solidified quickly, it was highly dispersed. At contact temperatures of more than 1050 degrees Celsius, the melting point of copper, the dispersion of a droplet of the same mass as another mass was observed to differ little, and the diameter was smaller as the overheating increased.

J. D. Gabor et al. studied the phenomena that occur when molten uranium in kilograms, uranium-zirconium alloys and uranium-ferrous alloys are poured into sodium pools of 600 degrees Celsius. The study concluded that the presence of sodium with a depth of 0.3 meters at the equator would allow hydrolysis and 25mm diameter molten stems to be solidified in an overheated state of 400 degrees Celsius. What we observed here is that these dispersed substances remained either filament or paperback. The void in these structures was calculated to reach 0.9.

Ken-ichi. Matsuba et al studied the distances required for the dispersion of molten fuel. The study also tested a situation in which molten water was spilled into sodium plenum. An experiment was conducted to emit 10 kg of aluminum oxide down a vertical direction through a sodium pool (depth 1.3 m, 0.4 m diameter, and temperature of 673 K). As a result of the experiment, the mass median diameter of the solidified particles was measured at 0.3 mm. This value was comparable to that predicted in the general hydraulically unstable theory. However, in these hydrophobic models, the larger the number of Webers, the smaller the particle size, which was not observed in the experiment. In addition, when measuring the dispersion distance of aluminium oxide, it was shown that the current typical correlation was between 60% and 70% lower. These results suggest that this is due to the predominant thermal dissipation occurring before the hydrophobic model is developed sufficiently.

J. Namiech et al. studied dispersal phenomena when molten corium, jet, enters the water. Particle or droplet detached from these jets is caused by a strong steam flow. The group has developed a statistical correlation that can predict the length of Jet break up. A brief diagram of these hydrophobic models is shown in Figure. 3.3. This is usually expressed by the Weber number. Expression 3.2.1 shows the final statistical correlation.

$$\frac{d_p}{D_j} = 33.272\left(\frac{P}{P_0}\right)^{-0.958} \times \left[1-\frac{T_s-T_L}{T_j-T_s}\right]^{0.484}\left(\frac{U_j}{U_{j0}}\right)^{-1.485}\left(\frac{U_j}{U_{M0}}\right)^{1.591} \times \left(\frac{U_{M0}D_j}{\nu_{vj}}\right)^{-0.035}\left(\frac{\sigma}{\rho_j D_j U_{M0}^2}\right)^{0.065} \tag{3.1}$$

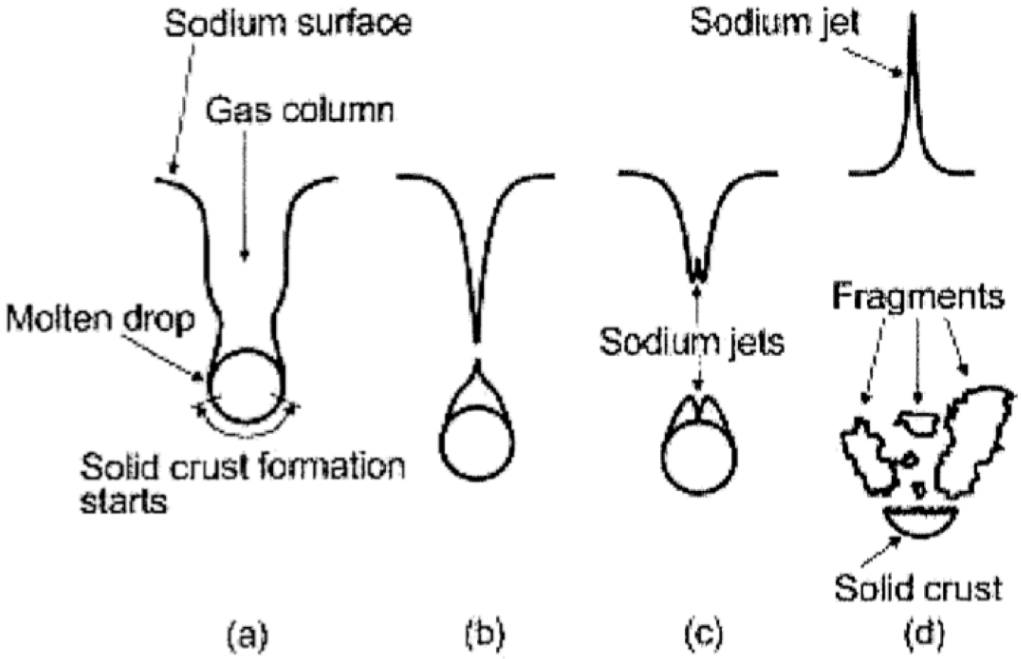

Fig. 3.1. Thermal fragmentation, boiling inside molten fuel jet[3.5]

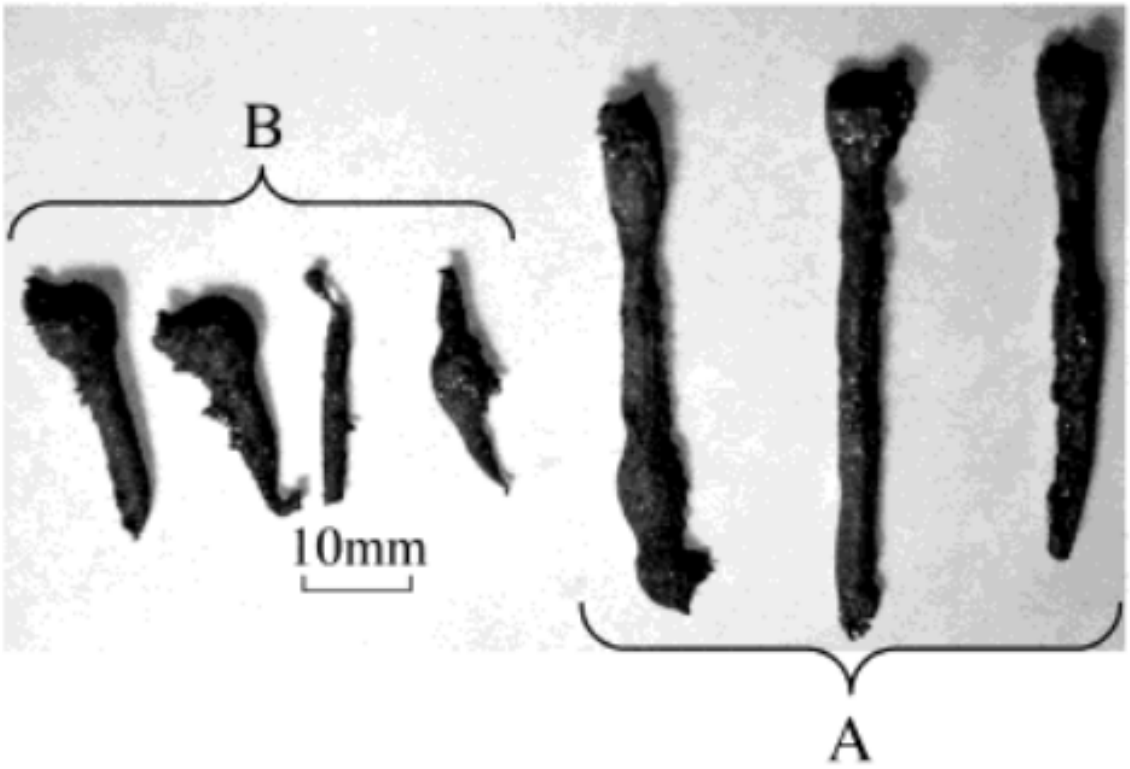

Fig. 3.2. Typical appearance of silver fragments[3,5]

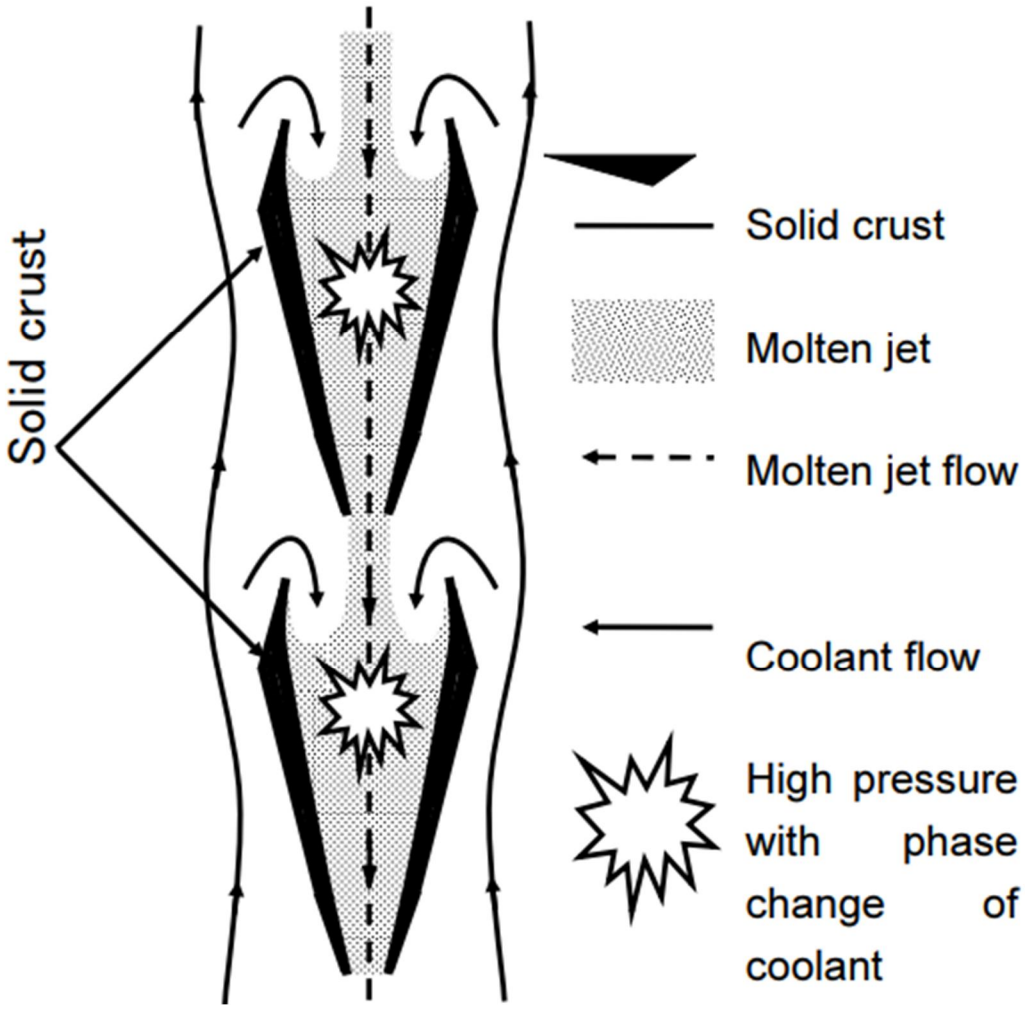

Fig. 3.3. Model description of hydro dynamic instability from velocity profile and molten fuel jet geometry

3.1.2 Limit of SAS4A and importance of FCI modelling

The SAS4A and SIMMER are the SFR accident codes. SAS4A is a code that can interpret the initializing phase during the severe accident on the SFR and a code that can calculate the overall system's response as well as the fuel behavior inside the core. The injection phase, as mentioned above, refers to the situation up to the extent that the cladding of the fuel is damaged, resulting in the release of nuclear fuel, and the ejected fuel is acting within the coolant channel. If this fuel wave goes further down to the destruction of the canal, the calculation of SAS4A will end there. The criterion that can be crossed from the Initiating phase is to ensure sufficient cooling capability when the fuel is relocated and to avoid further nuclear fission as the final reactivity does not exceed the threshold. Therefore, SFR, which is currently being developed, will design an old model to create an early end to accidents in the core if such accidents occur.

SIMMER, in the same way as SAS4A, is a code that can calculate the behavior of the core fuel as well as the overall system's response. Only differences from SAS4A will differ in the scope of accident analysis. SIMMER is a code that can calculate the damage to a buoyant canal outside the aforementioned inflating phase, additional fuel melting, pool formation of molten fuel, and thermal/mechanical impacts with the reactor vessel.

SIMMER, in the same way as SAS4A, is a code that can calculate the behavior of the core fuel as well as the overall system's response. Only differences from SAS4A will differ in the scope of accident analysis. SIMMER is a code that can calculate the damage to a buoyant canal outside the inflating phase, additional fuel melting, pool formation of molten fuel, and thermal/mechanical impacts with the reactor vessel.

For codes that can interpret these two large systems, accident interpretation simulates a phenomenon in which all phenomena, not one detail, occur in turn or in conjunction with each other, and requires a minimum of several hours of calculation for these interpretations. Moreover, as complex code is, errors on inputs and models can occur frequently. This study aims to develop analytical codes specific to a phenomenon that is specific to a phenomenon that not only allows the detailed phenomenon to be calculated quickly and the desired condition to be changed quickly, but also enables the rapid change of various models. The modelling of the behavior of the channel of fuel breaking and molten fuel that could occur in the event of a severe accident in the SFR has been performed and the associated accident analysis has been performed.

3.1.3 Preliminary development of MESFRAC; Simple_MESFRAC

The road map is shown in Figure.3.4 as well as the boundary conditions for the accident progress and the core damage progress through In-Vessel Retention at the SFR to see the importance of modelling the top eruption and re-criticality. The FCI phenomena in this study are the first of a series of accident sequences from which nuclear fuel is ejected and finally gathered to the bottom of the container. If the security is not secured in this first step, it will proceed to the next boundary. For example, if nuclear fuel injected into a channel does not escape to the top or causes re-criticality within the channel, cooling at the bottom of the aggregation should be ensured. Modeling of the behavior of these nuclear fuels can be considered the most important stage of ensuring safety in the event of an accident, since there is no reason for an accident to occur in the next phase and the safety of the SFR will be fully preserved upon the accident.

As mentioned earlier, one of the important factors in calculating the reactivity in the behavior of the projectiles in the channel is the result of dispersion of the fuel (the area according to the shape of the particles) that is initiated from the eruption. In order to model the results of these dispersion events, the first step was to model the condition of the melt when the melt was released. The reason for this modeling is to use the values modelled for fuel-discharge experiments because the initial conditions when molten corium is not measured inside the fuel located in narrow channels and confined spaces. The diagrams of these experiments are shown in the following figure.3.5. Experimental modeling essentially models an experiment in which molten nuclear fuel is injected into the cladding with a perforated outlet and injected into the channel. The main variables of the major blast melt are the temperature at which the jet is ejected, the total amount of the jet, and the velocity in the radial direction of the jet. First, the temperature of the jet is controlled by heat transfer between the jet and the cladding, and internal heat transfer of the fuel into the cladding. Second, the amount of the eruption can be calculated by considering the amount of the final eruption, which is solidified on the inside surface of the cladding by heat transfer from the process of injecting the specified nuclear fuel into the cladding. Third, the velocity of the radial direction of the emission was calculated using the pressure difference inside the cladding and outside the cladding.

Therefore, the initial conditions for the fuel escaping from the cladding described above are being specified and modelling to apply to parts not measured in the experiment. As a result, the basic heat transfer phenomena were analyzed as primary enemies and the modelling of the ejection behavior was performed. For the heat transfer analysis between molten fuel and cladding, the thermal conductivity between the fuel and cladding without phase change is calculated and the temperature results are derived

using a simple explicit numerical method.

Figure 3.6. shows the geometry of the experiment to simulate these FCI phenomena. The molten nuclear fuel is injected from the top and released through the vent at the bottom to the channel with the sodium coolant. The dissolved uranium is dispersed in response to liquid sodium. Since the solidification of the molten corium is important, heat transfer between the cladding and the molten corium was first modelled using a one-dimensional heat transfer equation in a radial direction. The algorithms for this heat transfer are shown in Figure. 3.7. Solutions for all heat transfer calculations are obtained simply through the explicit method. A node is defined in the direction of the diameter and axis, and the analysis begins by calculating the new temperature of the fuel according to the time interval dt. After calculating the temperature of the new fuel and the amount of fuel, the void fraction per cell is calculated for each cell depending on the height of the fuel in the innermost cell of each axial cell. These void environments are used to calculate conduction or convection heat transfer in an energy equation. For simple exit calculations, the linear matrix is defined, the corresponding year is obtained, and the new temperature is calculated according to dt. The control equation in the code for this series of processes is shown in Figure. 3.8. The initial conditions used the initial conditions of the experiment for the main fuel eruption and are shown in Table 3.1. To determine whether such modelling is appropriate for the heat transfer calculation, a comparison was performed with the modelling result values using the commercial numerical analysis code. The results are shown in Figure. 3.9. Both results show that the temperature balance is reaching within 0.4 seconds. In addition to these temperature gradients, subroutines are being developed to obtain an Explicit Sea for the fuel solidification according to the algorithm shown in Figure. 3.10. The process, after each node's temperature calculation, performs a solidification calculation only on cells that calculate a temperature lower than the melting point. In case of phase shift, the calculation of variation in the properties of the material and the latent heat at the melting or boiling point must be made sensitively. Therefore, the calculation should be performed only if the temperature difference is less than the defined temperature difference. If the calculation results convey too much heat, perform the calculation again by reducing the time step dt and verifying that the criteria is satisfied. If the temperature difference is appropriate, the heat used for the temperature change is absorbed by the heat used for the temperature change, divided by the heat used for the phase change, and then the amount of coagulation for the time step is calculated. Finally, a simple Bernoulli equation and an appropriate emission coefficient were used to model the rate of eruption. Since the conditions in the experiment were a drop in a simple liquid melt, we simply considered the velocity of the ejection to pressure and the rate of the ejection to the drop height difference. Reference experiments showed low-speed eruptions in low-growth and a speed of approximately 2 m/s to 3 m/s. Speed calculations also

showed reasonable values with a simple Bernoulli equation without any other assumptions. The correlation between this and this is as follows.

$$u_{ejection} = \sqrt{u_{initial}^2 + \frac{2(P_1 - P_2)}{\rho}} \tag{3.2}$$

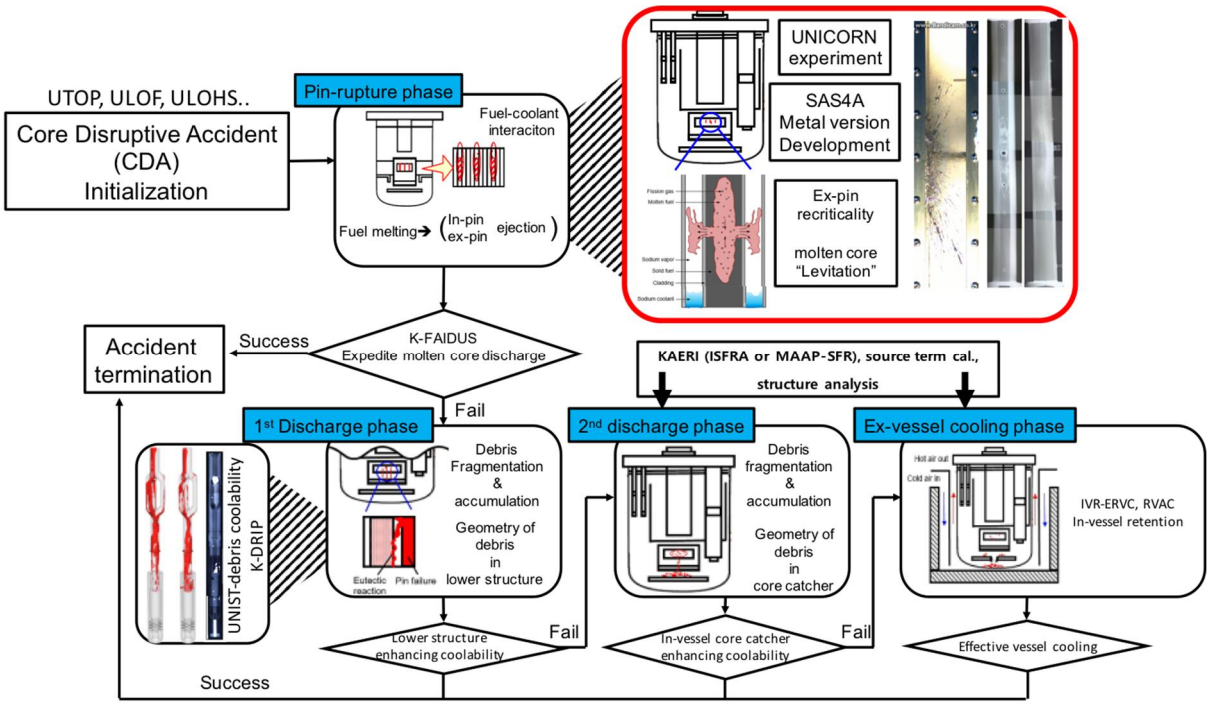

Figure. 3.4. SFR severe accident road map

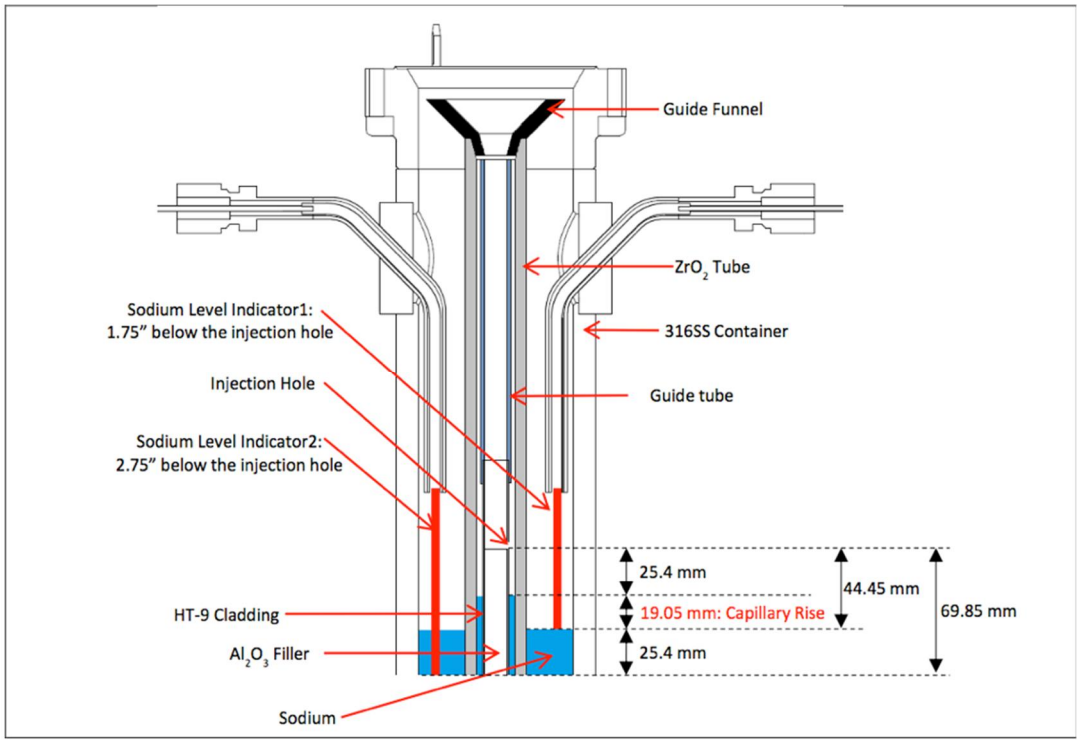

Figure. 3.5. Experimental schematic of metal fuel FCI[3.7]

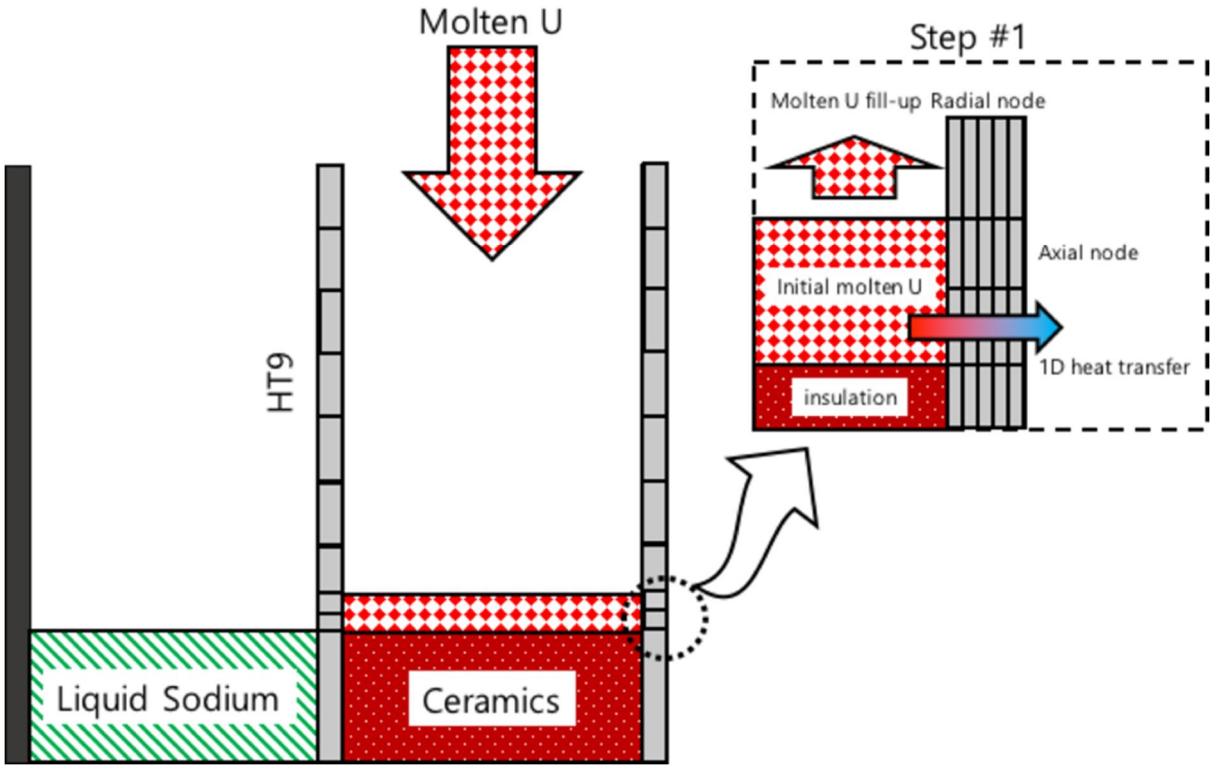

Figure. 3.6. SIMPLE_MESFRAC 1-D heat transfer schematic

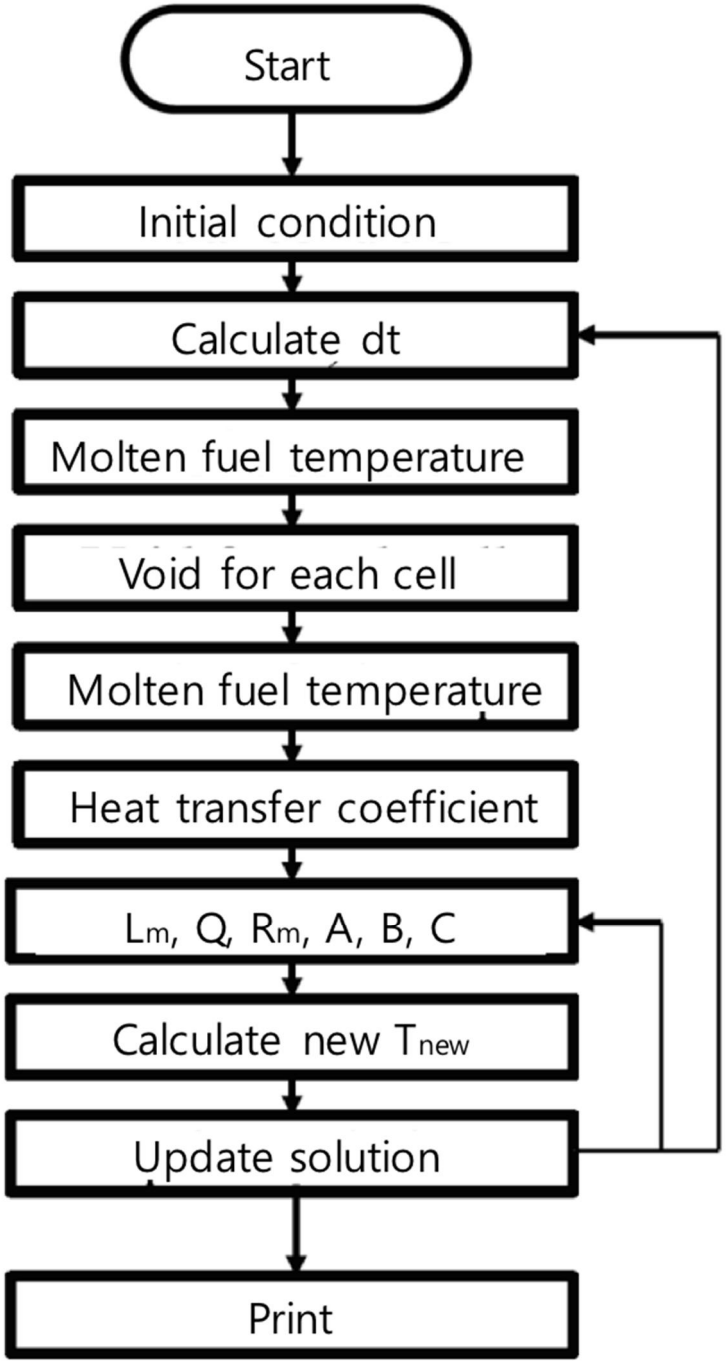

Figure. 3.7. Cylindrical geometry 1D heat transfer calculation algorithm

$$\frac{\partial u}{\partial t} = a\frac{\partial^2 u}{\partial x^2}$$

$$\frac{u_i^{n+1} - u_i^n}{\Delta t} = \frac{a}{2(\Delta x)^2}\left((u_{i+1}^{n+1} - 2u_i^{n+1} + u_{i-1}^{n+1}) + (u_{i+1}^n - 2u_i^n + u_{i-1}^n)\right)$$

$$r = \frac{a\Delta t}{2(\Delta x)^2}$$

$$-ru_{i+1}^{n+1} + (1+2r)u_i^{n+1} - ru_{i-1}^{n+1} = ru_{i+1}^n + (1-2r)u_i^n + ru_{i-1}^n$$

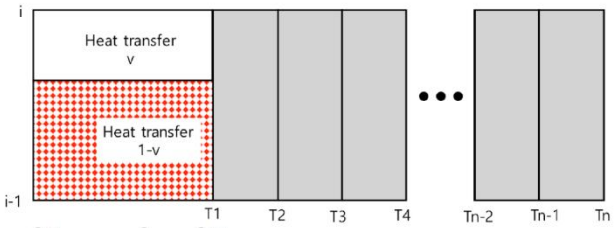

B.C: L- convection heat transfer(pool/atm)
R-steady temperature

$$\frac{\partial T}{\partial t} = \frac{\alpha}{r}\left[\frac{\partial}{\partial r}\left(r\frac{\partial T}{\partial r}\right)\right]$$

$$\frac{T_i^{l+1} - T_i^l}{dt} = \frac{\alpha}{2}\left[\frac{r_{i+\frac{1}{2}}\left(\frac{T_{i+1}^l - T_i^l}{dr}\right) - r_{i-\frac{1}{2}}\left(\frac{T_i^l - T_{i-1}^l}{dr}\right)}{r_i dr} + \frac{r_{i+\frac{1}{2}}\left(\frac{T_{i+1}^{l+1} - T_i^{l+1}}{dr}\right) - r_{i-\frac{1}{2}}\left(\frac{T_i^{l+1} - T_{i-1}^{l+1}}{dr}\right)}{r_i dr}\right]$$

$$-L_i T_{i-1}^{l+1} + (1+Q)T_i^{l+1} - R_i T_{i+1}^{l+1} = L_i T_{i-1}^l + (1-Q)T_i^l + R_i T_{i+1}^l$$

$$L_i = \frac{r_{i-\frac{1}{2}} kdt}{2r_i(dr)^2\rho C_p} \qquad Q = \frac{kdt}{(dr)^2\rho C_p} \qquad R_i = \frac{r_{i+\frac{1}{2}} kdt}{2r_i(dr)^2\rho C_p}$$

Figure. 3.8. Heat transfer governing equation in simple_MESFRAC

Table. 3.1. initial condition of basic cylindrical coordinate heat transfer

Fuel temperature	2203.15
Fuel pin length	1 m
Initial temperature of cladding	873.15 K
Ambient temperature	300 K
Boundary condition	Inner: conduction Outer: convection Some part use insulation
Velocity of molten fuel	0.1 kg/s
Mass of initial fuel	0.123 m

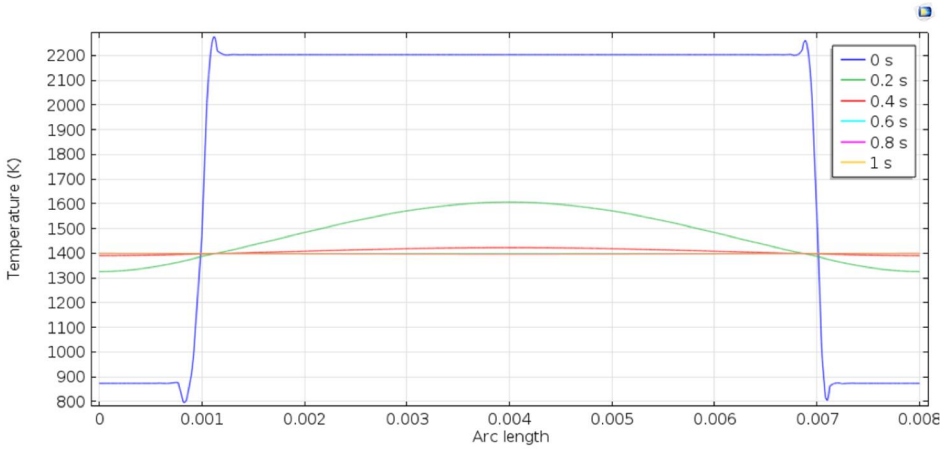

(a)

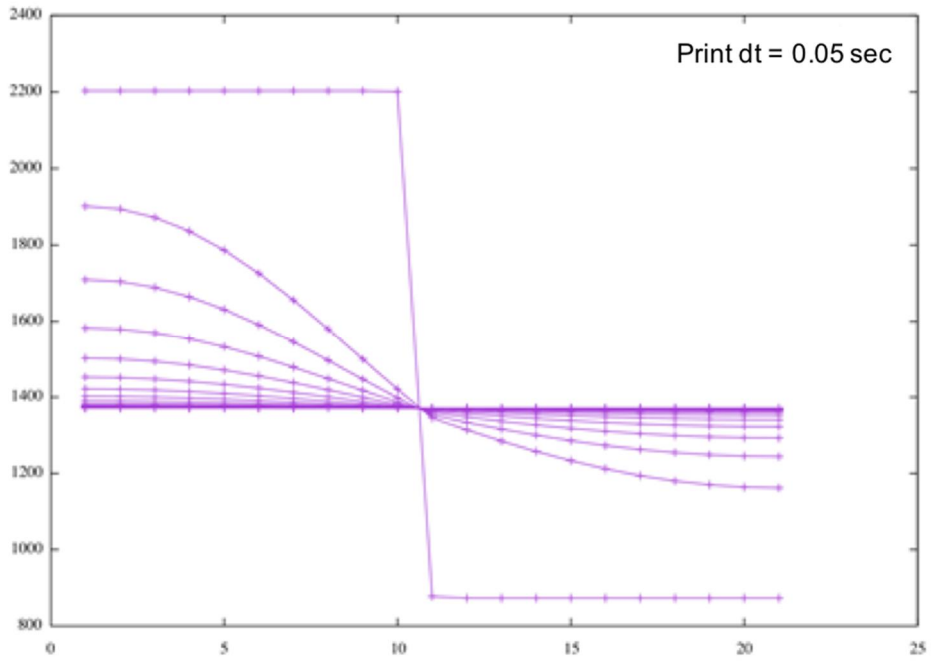

(b)

Figure. 3.9. Comparison between commercial code (a) commercial code, (b) SIMPLE_MESFRC

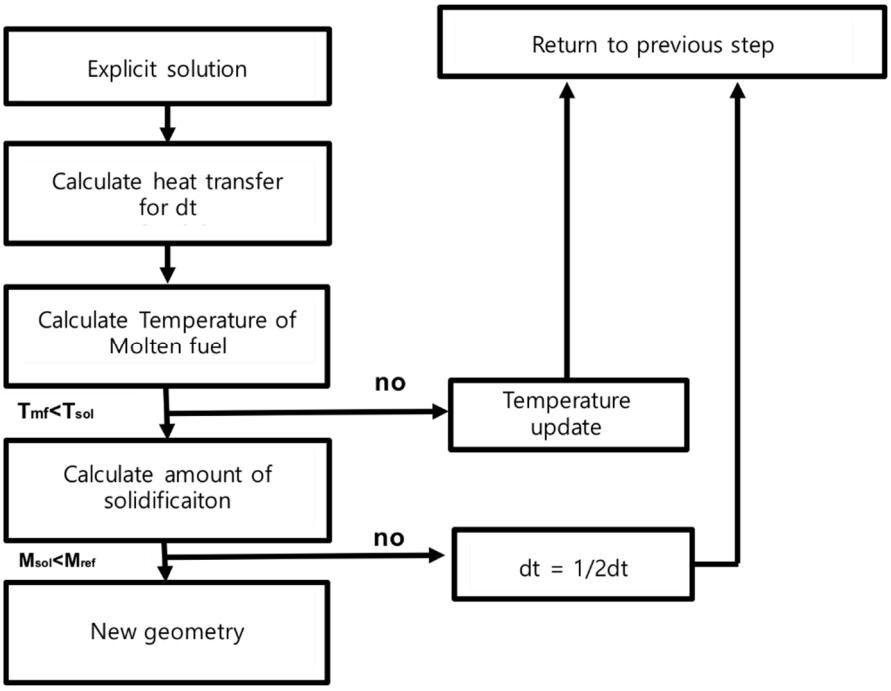

Figure. 3.10. Simple_MESFRAC solidification subroutine algorithm

3.2 List of subroutines in MESFRAC

MESFRAC is Fortran based 1-D coolant channel hydrodynamics analysis code. This section shows a list of all the subroutines that is used in the MESFRAC model. Name of subroutine and description is explained.

Table. 3.2. Subroutine list of MESFRAC

MESFRAC subroutine	**Description**
Simple_MESFRAC	Call simple_MESFRAC to calculate simple channel hydraulic which is not using MESFRAC
INPREAD	Input read, file name is fixed. “fciinp.inp” Input is fixed form.
EXPLICIT	Calculate heat transfer conduction governing equation coefficients. Temperature is calculated also in explicit way.
NODEDEF	Initialize the parameter which is used for geometry of channel and structures.
Initialroutine	Allocate every matrix that used in MESFRAC using mesh size and number information. And initialize information that is not considered in NODEDEF. Initial conditions are distributed into matrixes
MESFRAC_EX	Like EXPLICIT subroutine, calculate heat transfer conduction and convection governing equation coefficients for MESFRAC.
EJECTFUEL	Calculate ejection of molten metal fuel from inside a cavity.
MASSCONSV	Calculate Mass conservation in each axial mesh.
VOLFRAC	Calculate volume fraction of each material and determine flow regime (Yet, MESFRAC consider only annular molten fuel flow regime.)
CHANNELGEOM	Definition of local geometry update.
CHENRGCONSV	Calculate temperature of molten fuel inside channel using enthalpy. The amount of solidified fuel is calculated in this subroutine.
CHMOCONSV	Calculate velocity of molten fuel inside channel using momentum. Only molten fuel velocity is considered
PRINTOUTS	Print initial conditions and results.
STRCTTEMP	Calculate temperature of structure. This subroutine use coefficients from the results of EXPLICIT subroutine.

3.3 Fuel ejection from the pins in MESFRAC

Figure. 3.12. shows a code flow chart of the MESFRAC. The input tables of MESFRAC are shown in Table.3.3. below. First, input defining geometry and mesh for calculation in areas within the calculation range is entered. Divide mesh in axial/radius direction, and these mesh calculations inside the cladding and the temperature of the tube (hexcan wall) in the energy equation. In the case of tube, this refers to the hexagonal duct except nuclear fuel inside the channel. After input for each geometry, define the time to calculate and the time steps to start the output and the time steps to end the output. The material properties of the various substances are then entered. The substances entered are molten fuel, cladding and sodium (gaseous liquid). Next, you will enter the initial conditions for the eruption. Initial conditions for the eruption are initial melting, temperature of the molten corium, and the cavity pressure where the molten corium is present. These input conditions take advantage of the results performed in the other stages of detail before. At the end of these inputs, the resistance factor used in the kinetic equation is entered and the temperature field of the remaining initial fuel cladding and surrounding hexcan is entered as a table.

If the HYDOPT option is checked after data is entered. If HYDOPT is zero, the previous development of the simple_MESFRAC will be used to configure the geometry and perform the calculation. If the HYDOPT value is defined as 1, configure the geometry using MESFRAC and perform the calculation. Once the model is decided which model to use, the subroutine functions as mesh setting, initial condition input, etc. From then on, calculations will be performed on a time-by-hour basis by the roof gate. First of all, pressurized molten fuel in the cavity will result in the calculation in which the molten fuel is released outside the fuel. This calculation of the fuel spillage is carried out at the "EJECTFUEL" subroutine. The fuel spill has been referred to the Mechanical Model of the SAS4A. This model calculates the acceleration of a substance inside the cavity after obtaining the friction taking into account the pressure. In the SAS4A, emissions may be computed in other ways than these models. The mechanical model calculates the speed of the melt that is sprayed from the cavity as follows:

$$\Delta\rho'_{fu,k} = \rho'_{fu,k} \cdot \frac{V_{fuel\ ejected}}{V_{vuel\ cavity}} = \rho'_{fu,k} \cdot \frac{u_{fu,ca-ch,k} \cdot \Delta t}{\pi \cdot R_{ca,k}} \tag{3.3}$$

Where the speed corresponding to the speed is calculated only when the pressure inside the cavity is greater than the pressure inside the channel. If the pressure inside this cavity is less than the pressure inside the channel at any time staff, the speed is calculated by halving as shown below.

$$P_{ch,i}^{n+1} < P_{ca,k}^{n+1} \tag{3.4}$$

Velocity is calculated using previous velocity, acceleration and delta t

$$u_{fu,ca-ch,k}^{n+1} = u_{fu,ca-ch,k} + a_{fu,ca-ch,k}\Delta t \tag{3.5}$$

Acceleration is calculated the net force of molten fuel. The governing equation is below.

$$a_{fu,ca-ch,k} = \frac{\sum \text{Forces}}{\text{Mass}} = \frac{R_{ca,k} \cdot \Delta z_k}{0.9 \cdot R_{ca,k}^{z} \cdot \Delta z_k \cdot \rho_{fu,k}} \left\{ \Delta P_{ca-ch,k} - 0.5 \cdot \rho_{fu,k} \cdot u_{fu,ca-ch,k} \cdot \left| u_{fu,ca-ch,k} \right| \cdot C_{ORIFICE} - C_{SHEAR} \cdot \eta_{fu,k} \cdot \frac{u_{fu,ca-ch,k}}{R_{ca,k}} \right\} \tag{3.6}$$

Figure.3.12. below shows the diagram for applying these mechanical models in the SAS4A. The C_{orfice} coefficient is the orifice coefficient and is the coefficient for calculating the pressure drop for the flow between the vents, which is defined as 0 in the SAS4A and not considered in the MESFRAC. The C_{shear} represents the friction between the unaccelerated and the non-accelerated fuel compared to the accelerated molten fuel.

The next subroutine is MASSCONSV, which calculates the mass retention equation inside the channel. The calculation is carried out with the mesh shown in Figure. 3.13. except for the calculation of momentum. In MESFRAC, the mass/motor/energy conservation equation is not calculated from all mesh of the chain but is calculated for the specified domain. The variables defining these domains are HYDTOP and HYDBOT, respectively, which are responsible for the top/bottom of the computed domain. In order to prevent the spread of the actual molten corium faster than the speed of the actual molten corium by a relatively large mesh size, the movement distance of the molten corium according to the speed is calculated within each bouncer and the size of mesh compared to the calculated travel distance determines the expansion or reduction of the computed domain. The interactive term is then calculated to calculate the mass retention within the domain. mass probable term is determined based on the speed at the boundary of mesh and the mass at which the velocity at these boundaries is positive and negative is calculated differently. Calculate the change in mass at each mesh using the probable terminals of this calculated mass retention equation. After calculating the mass change, the variable "CCMO" is calculated, which stores the mass ratio between each mesh and uses that ratio to calculate the velocity at the boundary.

VOLFRAC is a subroutine that calculates volume fraction inside the channel. Volume fraction is an important step in determining flow time flow within a channel. In MESFRAC, it was modelled to consider only the annular flow time. Determining this flow time is necessary to define the heat transfer area.

CHANNELGEOM is a subroutine for updating the Local geometry. The flow time defines the period that defines the interface between the molten fuel and the structure. A variable called JETFRAC is used, which means the area fraction that affects the surrounding structure when molten water is sprayed. Then, the aggregated area, characteristic length, and area concentration are calculated. The allocated area is calculated by multiplying the area by the period, and the cyclical length is calculated by dividing the area by the meter.

After these calculations are completed, energy and kinetic calculations are carried out inside the channel. The calculations will be performed by CHANNAELGEOM and CHENRGCONNSV respectively. First, the energy calculation will be carried out. The modified heat transfer coefficient is calculated using the area coefficient and the periodic calculated in the previous step, and the heat transfer in each component is calculated. Using the calculated enthalpy, the temperature of the fuel is calculated. If the temperature of the fuel is calculated below the melting point, re-calculate the mesh. Then, the corresponding area ratio inside the channel is calculated and the pressure value is calculated. The calculation module of the Simple_MESFRAC is called for the 2-dimensional temperature calculation of the cladding and the tube to perform the calculation. These subroutines are specified by STRCTTEMP.

Subroutines of CHMOCONSV are then called to calculate the amount of motion inside the channel. As shown in Figure. 3.14, the calculation is carried out by considering the material at the top half of the boundary and at the bottom half of the boundary. These calculations are also performed only in mesh between HYDBOT and HYDTOP. The mass, temperature, and speed of each of these final calculated cells are printed and then moved on to the next step.

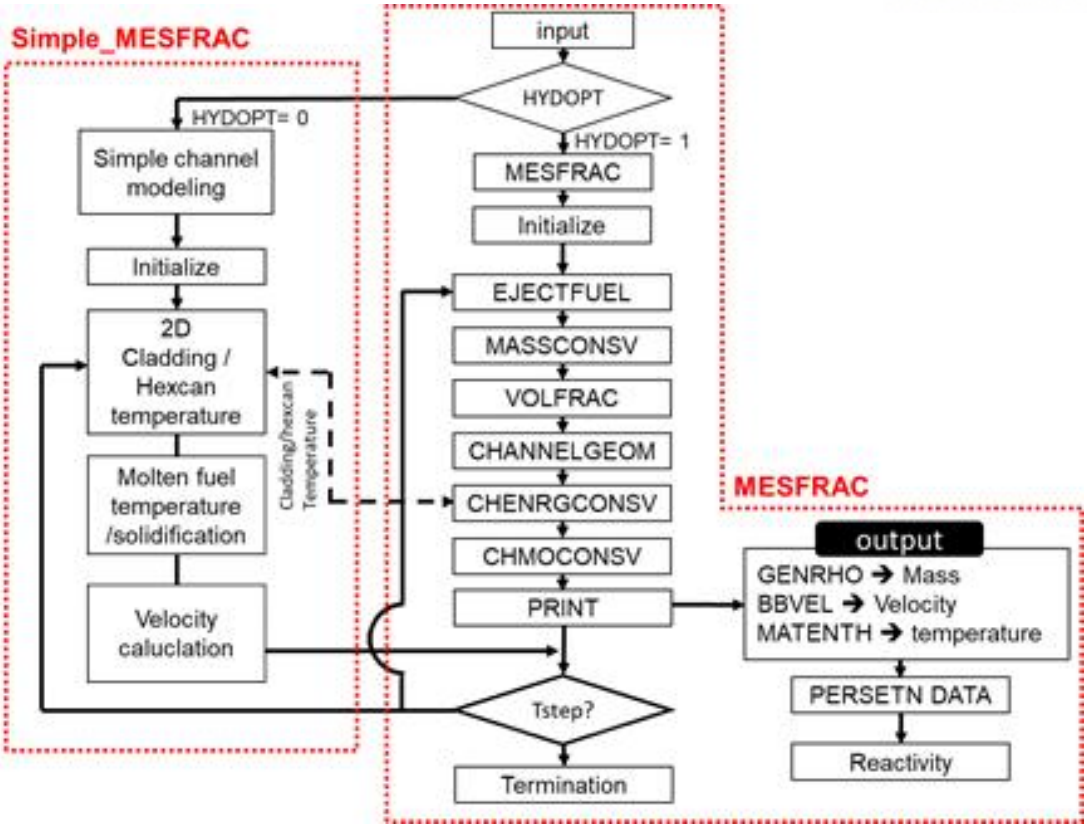

Figure. 3.11. MESFRAC flow chart

Table. 3.3 MESFRAC input deck parameter

Parameter		Parameter	
KZ, NR,	Mesh, axial/radial,	mfNR, tbNR	Radial mesh
NPIN	Number of pin	pinlngth	Length of fuel pin
DHY	Hydraulic diameter	AFLWPIN	Area of open flow
DISTP	Breach axial position	arearef	Reference area
finz, fin_OD, fin_w	fuel geometry,	tube_w	tube(hexacan) geometry
D_open	Breach diameter	ttot, dt, printdt	Time input
printfrm, printto	Output option	k_cld, rho_cld, cp_cld	Cladding property
k_tb, rho_tb, cp_tb	tube (hexcan)	cp_mf, rho_mf, mu_mf, k_mf	Fuel property
UMP	Uranium melting point	ULTHF	Latent heat of fusion
MFST	Molten fuel surface tention	cp_atm, rho_atm, mu_atm, k_atm, beta_atm	Air property
mu_Na	Sodium surface tension	T_atm	Vapor sodium temperature
CAViniP	cavity initial pressure	Tinjtot	Initial molten fuel temperautre
avgmfv	Initial velocity of fuel (not used)	injmass	Mass of molten fuel
wallfric	Resistance coefficient	dragcoef	Drag coefficient

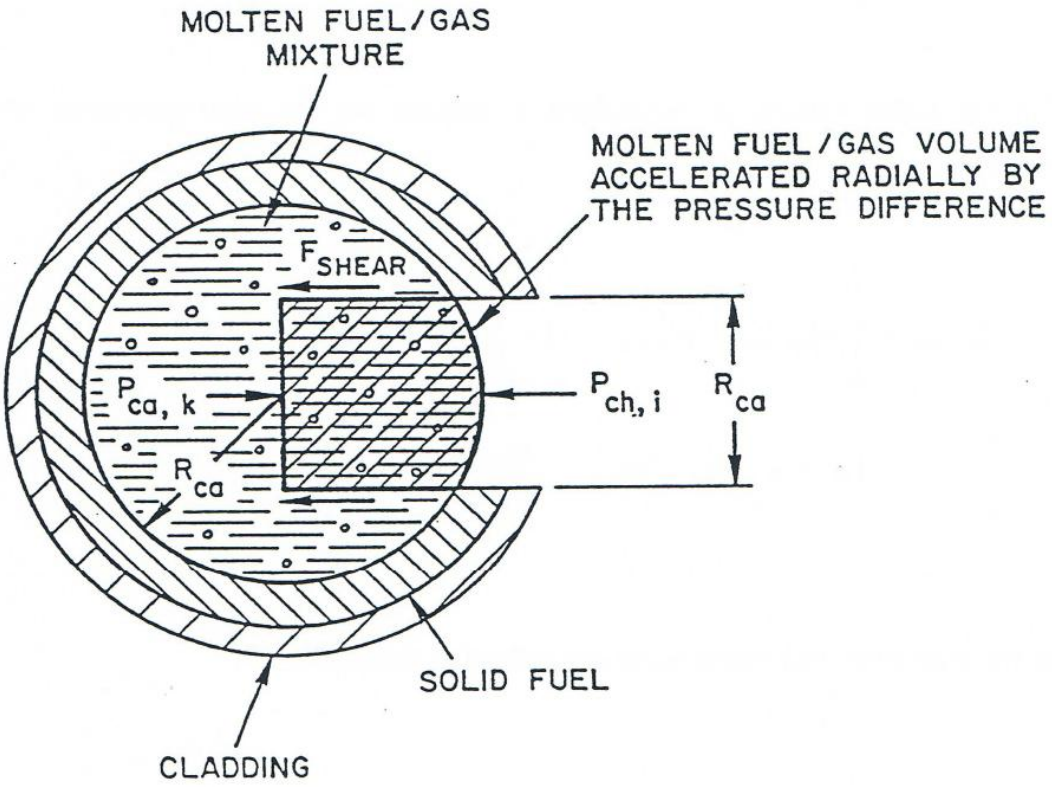

Figure. 3.12. SAS4A mechanistic molten fuel ejection model

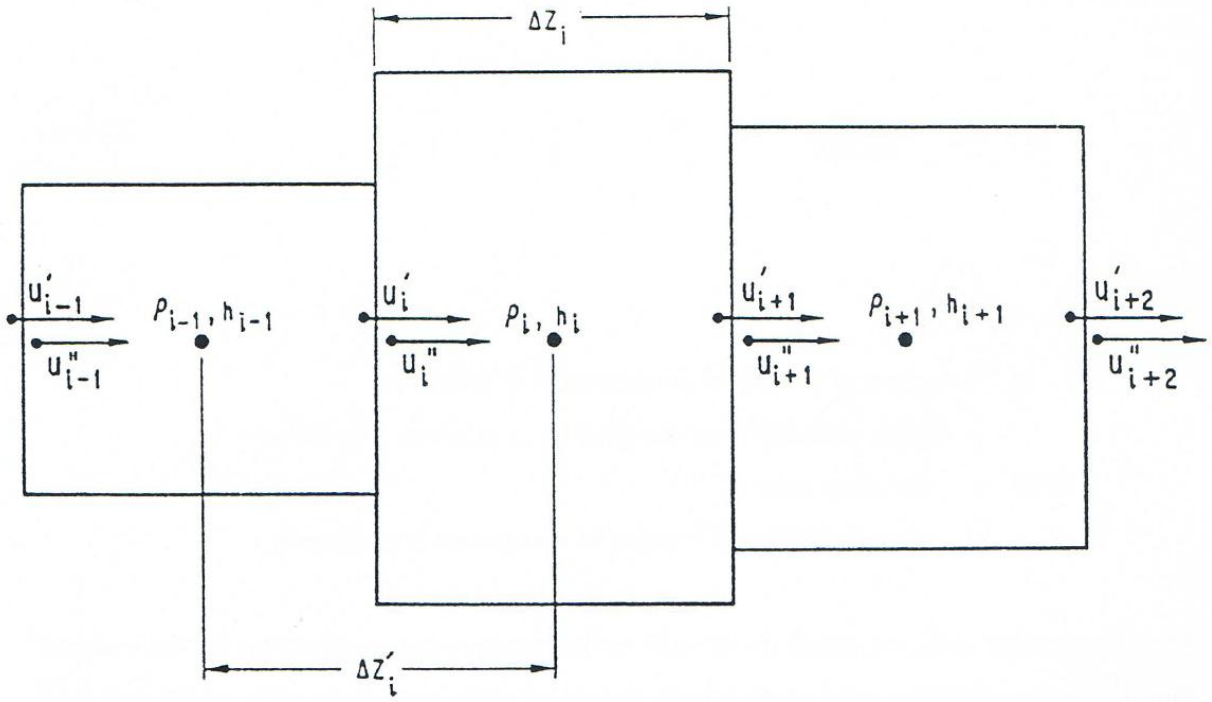

Figure. 3.13. Mesh grid used in the channel hydrodynamic model

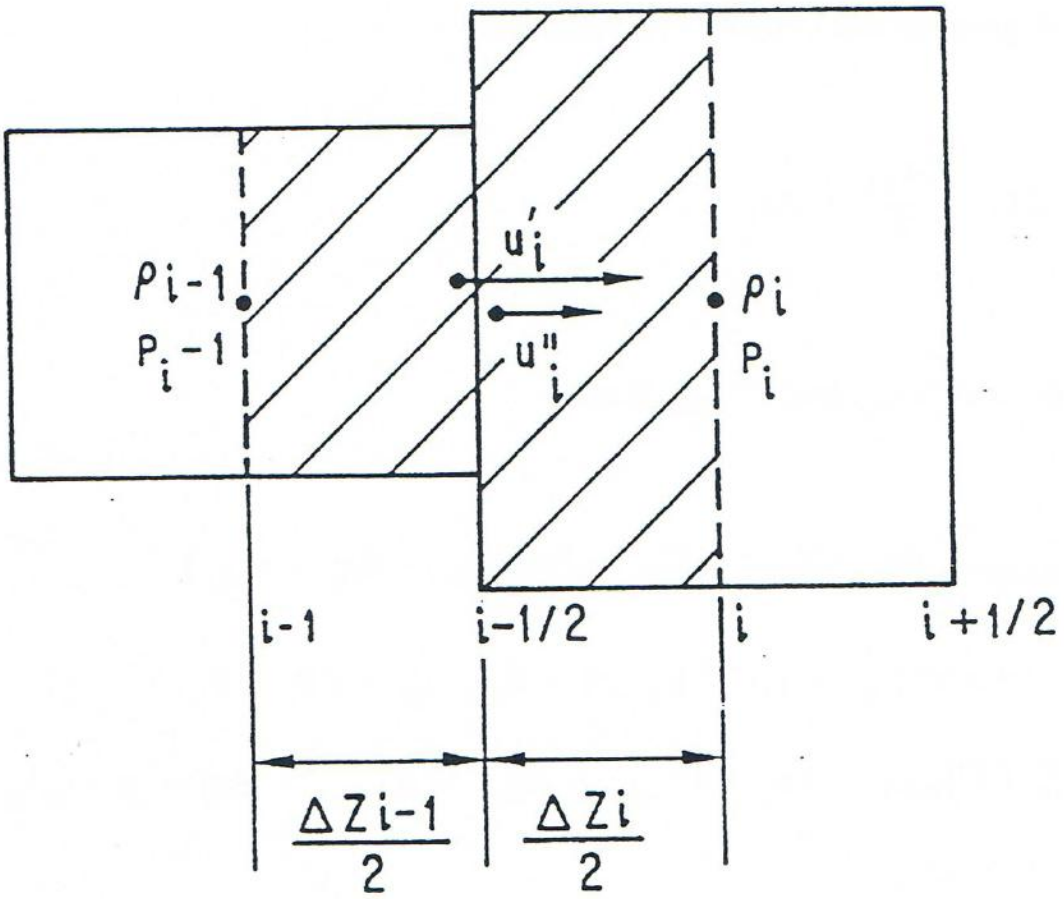

Figure. 3.14 SAS4A Control volumes used for the solution of the momentum equation

3.4 Main conservation equations in MESFRAC

MESFRAC is using 3 conservation equations; Mass, Energy and momentum. The solution of equation is solved by finite difference explicit time integral. Most of property is defined in the middle of meshes except velocity related values. In the boundary, dual velocities are used to deal with continuity equation between two meshes.

The original mass conservation is written as:

$$\frac{\partial}{\partial t}\left(\rho_{k,i}A_{k,i}\Delta z_i\right) + \left[(\rho Au)_{k,i+1/2} - (\rho Au)_{k,i-1/2}\right] = 0 \tag{3.7}$$

This conservation equation is integrated over a time step Δt. Equation below is obtained.

$$\rho'^{n+1}_{k,i} = \rho'^{n}_{k,i} - \left[(\rho' u)_{k,i+1/2} - (\rho' u)_{k,i-1/2}\right] \cdot \frac{\Delta t}{\Delta z_i} \tag{3.8}$$

This is the solution of mass conservation equation. In this calculation, original density is not used in the solution of mass conservation equation. This ρ' means generalized density that equals density divided by total open channel area. The mass convective term is calculated by the velocity and the mass which is determined by the direction of velocity at the boundary. If velocity is greater than zero, the generalized density below boundary will be used and If velocity is less than zero, generalized density over the boundary will be used.

Liquid fuel energy equation is written as:

$$\begin{aligned}\frac{\partial}{\partial t}\left(\rho_{fu,i}h_{fu,i}A_{fu,i}\Delta z_i\right) + \left[(\rho Ahu)_{k,i+\frac{1}{2}} - (\rho Ahu)_{k,i-\frac{1}{2}}\right] \\ = Q_{fu,i}\rho_{fu,i}A_{fu,i}\Delta z_i - \textstyle\sum_j H_{fu,j,i}A_{fu,j,i}\Delta T_{fu,j,i}\end{aligned} \tag{3.9}$$

This equation is also divided by open channel area to deal with generalized density. Heat generation from nuclear fuel is not considered. This heat generation parameter equals zero. In the energy equation, the heat transfer coefficient will be changed into corrected heat transfer coefficient. This heat transfer coefficient is calculated using area in channel and axial node length. This calculation is below:

$$H'_{fu,j,i} = H_{fu,j,i}\frac{A_{fu,j,i}}{A_{open\ channel}\Delta z_i} \tag{3.10}$$

Using this parameter, after integral with Δt, this energy conservation equation is turn into this:

$$\Delta h_{fu,i} = \{ - \left[(\rho' hu)_{fu,i+\frac{1}{2}} - (\rho' hu)_{fu,i-\frac{1}{2}} \right] \cdot \frac{1}{\Delta z_i} + h^n_{fu,i} \left[(\rho' u)_{fu,i+\frac{1}{2}} - (\rho' u)_{fu,i-\frac{1}{2}} \right] \cdot \frac{1}{\Delta z_I} - \sum_j H'_{fu,j,i} \cdot \Delta T_{fu,j,i} \} \cdot \frac{\Delta t}{\rho'^{n+1}_{fu,i}} \quad (3.11)$$

Enthalpy in each mesh is defined in the center of each mesh. Energy convective terms are also using velocity in each boundary of meshes. The method is same with the case of mass convective in mass conservation equation. In this MESFRAC, only molten fuel is considered, heat transfer coefficient in the last line is very simplified. If enthalpy change is calculated, this enthalpy is used to calculate the temperature of uranium.

Finally, the momentum conservation equation is presented below:

$$\frac{\partial}{\partial t}\left[\rho_{i-1}\frac{\Delta z_{i-1}}{2}A_{i-1}u'_i + \rho_i \frac{\Delta z_i}{2} A_i u''_i\right] + [(\rho A u^2)_i - (\rho A u^2)_{i-1}] = -A_{i-\frac{1}{2}}(P_i - P_{i-1}) + \sum_l \left(\Gamma^l_{i-1}\frac{\Delta z_{i-1}}{2} + \Gamma^l_i \frac{\Delta z_i}{2}\right) - \rho_{i-1}\frac{\Delta z_{i-1}}{2}A_{i-1}g - \rho_i \frac{\Delta z_i}{2} A_i g \quad (3.12)$$

$\sum_l \left(\Gamma^l_{i-1}\right)$ means the momentum sink or source term between two or more component interaction. In this MESFRAC, momentum sink term will consider wall friction and drag between gas and molten fuel. Only annular molten fuel flow regime is considered. Using a same integration procedure, this equation is obtained and the velocity change is calculated:

$$\Delta u_{fu,i}\left[\rho'^{n+1}_{fu,i-1} \cdot C^{n+1}_{Mo,fu,i} \cdot \Delta z + \rho'^{n+1}_{k,i} \cdot \Delta z\right] \cdot \frac{1}{\Delta t} = -\left[(\rho' u^2)_{fu,i} - (\rho' u^2)_{fu,i-1}\right] - \theta_{fu,i-\frac{1}{2}} \cdot (P_i - P_{i-1}) - u_{fu,i} \cdot C_{Mo,fu,,i} \cdot \Delta z_i \cdot \frac{\Delta \rho'_{fu,i-1}}{\Delta t} - u_{fu,i} \cdot \Delta z_i \cdot \frac{\Delta \rho'_{fu,i}}{\Delta t} - \rho'^{n+1}_{fu,i-1} \cdot u_{fu,i} \cdot \Delta z_i \cdot \frac{\Delta C_{Mo,fu,i}}{\Delta t} - \sum_m \left(\Gamma'_{Mo,fu,i-1} \cdot \Delta z_i + \Gamma'_{Mo,fu,i} \cdot \Delta z_i\right) - \rho'_{fu,i-1} \cdot \Delta z_i \cdot g - \rho'_{fu,i} \cdot \Delta z_i \cdot g \quad (3.13)$$

3.5 Timestep consideration of MESFRAC

MESFRAC is using explicit method to calculate the behavior of molten fuel in coolant channel and temperature of cladding and other structures. This explicit method uses the former timestep results of as an initial condition of the next time step. This explicit numerical scheme can increase the low-accuracy results if appropriate timestep is not chosen. Courant condition which is used for the numerical analysis of explicit time integration schemes is used for timestep size in MESFRAC. Courant condition (which is also known as Courant-Friedrichs-Lewy; CFL condition) is for the numerical stability of methods which is not stable. If the mesh size is getting smaller, the timestep size which will be used for transition should be smaller for stability of solution. Default timestep size is 1.0 x 10^{-6} sec which is much smaller than calculated or expected minimum size of timestep in MESFAC. Because MESFRAC calculates the behavior of molten fuel inside channel with 1-D scheme, CFL condition for one-dimensional case is used. For one-dimensional case, The Courant condition shows below.

$$C = \frac{u\Delta t}{\Delta x} \leq C_{max} \tag{3.14}$$

The number C is named as Courant number. u is the absolute value of velocity. Δt is timestep and Δx is mesh length. This C_{max} changes for different numerical scheme. If solution is explicit, the value of C_{max} = 1 and implicit solver is usually less sensitive, and this makes bigger value of C_{max} can be used. The speed of sound is widely used as velocity u. To give better solution, the value C_{max} is fixed as value of 0.4. Finally, the recommended timestep is presented below.

$$\Delta t = 0.4 \cdot \min\left[\frac{\Delta z}{u_{sonic}+|u_{gas\ mixture}|}\right] \tag{3.15}$$

The domain of this calculation is considered in all meshes that calculate velocity of molten fuel. In this MESFRAC, this timestep consideration is simplified because of two condition of molten fuel ejection. First, this timestep consideration domain should consider all of meshes. But in MESFRAC, the biggest pressure difference and the shortest mesh length condition is between cavity and coolant channel. So, time step will use calculated between cavity and coolant channel (disrupted position). Second is that MESFAC is not considering the velocity of gas mixture. So just speed of sound is used.

3.6 Ex-pin molten metal fuel relocation and bond sodium effect

Using the MESFRAC described above, the results from other details were set to their initial values to perform the calculation. Table.3.4 through Table.3.6 shows the conditions of eruption for each severe accident. Each accident represents the BOEC and EOEC conditions for CRWM + SBO, PPA and PPC. Overall, the temperature of the molten corium may be almost similar, but the difference in the discharge pressure remains significant. This difference is due to a large difference in the amount of fission gases produced by the industry. In the event of a CRWM+SBO accident, the fuel was crushed at a location equivalent to 88.1 % from the bottom of the fuel, with a total mass of 57.5 g, 53.4 g, and a pressure of 0.51 MPa for BOEC and 5.56 MPa for EOEC. In the case of PPA, it was confirmed that the upper part was higher than the previous accident at a location of 94.5 % from the lower part, and the molten corium was found to be 21.8 g and 45.0 g respectively. The PPA accident also showed a difference in the amount of molten corium. In the case of pressure, 0.61 MPa and 5.55 MPa were shown, respectively, similar to previous accidents. In case of PPC accident, injection occurred at a location corresponding to approximately 88.6 % at the lower part. In the case of EOEC, the eruption occurred at a height slightly higher than 90.8%. At 54.4g and 49.9 g, the melting rate was slightly smaller at the BOEC and at the pressure, the pressurized phenomenon was 0.60 MPa and 5.52 MPa. As a result, the pressure between BOEC and EOEC was 10 times different, and this pressure difference is expected to have a significant effect on the behavior of the eruption.

In addition, considering the second sodium to increase heat transfer between the fuel and the cladding inside the fuel, the pressurization phenomenon will change. First, all sodium inside the fuel has evaporated. The pressure of sodium when evaporated was calculated in the following manner.

$$P_{Na,Partial} = \frac{m\tilde{R}_{Na}T_{Na}}{V_{void}} \tag{3.16}$$

The resultant values for pressurization are shown in Table. 3.7 below when all have evaporated and only sodium in the comfort has evaporated. It indicates that all sodium inside the fuel can be pressurized up to 100 MPa if evaporated. Considering that the pressure at the time of the accident is at least 0.5 MPa, it is quite high. Of course, this inflation cannot be caused by fuel temperature conditions. Next, if all the sodium in the cavity evaporates, it was calculated. The magnitude of this pressurized phenomenon was pressurized in proportion to the melting capacity of the fuel. In the first case it was shown that it was pressurized to approximately 50.17 and 46.53 MPa, 39.07, 18.99 MPa in the second case, and 47.49, 43.33 MPa in the last case. This can be seen that the pressurization of the bond sodium vaporization is not affected at all by the burn up of the fuel. In addition, the size of this inflation is much higher than the inflation of the EOEC (less than about 6 MPa) with large burn-up and is seen at up to

50 MPa to 19 MPa. As mentioned earlier, it can be expected that the cavity pressure inside the fuel will not vary, regardless of the burn up of the molten fuel, since the pressurization of the bond is most affected by the temperature of the fuel. However, since this calculation requires us to see the difference in molten fuel behavior due to the difference in pressure, the calculation was performed using pressure that did not consider the effect of the bond sodium in the calculation.

Figure. 3.15. through Figure. 3.20. illustrates the eruption of molten fuel under each condition and the behavior in the channel. In each case, the height of the vent is different, so the ejection is initiated from the height of the vent defined at each input. In most cases, where the pressurization is large (in the case of the EOEC where there are many nuclear heat gases), large quantities of molten water can be rapidly ejected from the vent and rapidly escape to the top. This shows that the fuel initially pressurized behaves dimly by driving force under pressure. In each accident, the temperature of the fuel is not significantly different, so the behavior is not significantly different under the same BOEC or EOEC conditions.

Table. 3.8 shows the increase in the upper and lower emissions of molten corium and the upper and lower emissions of EOEC relative to BOEC. In case of a UTOP+SBO accident, the lower part was not discharged at the BOEC with a top discharge of 2.83 % and a bottom discharge of 0.0%. This was shown by the injection speed of low fuel, which was shown in previous graphs, at a slow rate. When large quantities of fission gases were considered for this accident, approximately 58% of nuclear fuel was discharged to the upper part, indicating a 1951.6% increase over the previous 2.83%. In addition, the fuel discharged to the lower part also increased, resulting in more volume escaping outside the core. This means that the accident can be safely terminated by fuel beyond the active core in the event of a severe accident. For the other two accidents as well as this one, EOEC was shown to be pressurized by these fission gases to release more nuclear fuel into the upper/lower section.

Based on these upper/lower emissions, the possibility of accident termination was determined in the six previous analyses. Related studies include a re-sector generation assessment of the top emissions of fuel-use by FAIDUS in Japan's JSFR. A diagram of the FAIDUS is shown in Figure. 3.21[3.7]. In this study, the factors that insert the greatest amount of reactivity in the event of a severe accident where the fuel at the high speed of sodium is dissolved and released into the channel were specified as sodium Voiding, and the safety core design was performed for when the fuel fell outside through the fuel core release structure called the FAIDUS. Figure. 3.22[3.7] shows a contrast graph of the reaction of Fuel disposals to the FCI void response in the event of a severe accident in the US. The most important variables for this conflicting response are the response value, the FCI onset enthalpy value of the core mean, when the channel is void as a whole, and the Axial gradient of fueled forward. The maximum void reactivity of the 1m core was set to $6 and the response was compared using SAS4A. As such, the

results of the melt behavior inside the channel of MESFRAC can be used to determine the contribution of negative reactivity by comparing the positive sodium void reactivity values as a tool to assess safety in the event of an accident. [cavity pressure (discharge rate) for key factors to assess safety of the six accident data carried out previously. Figure. 3.23. shows the upper emission. Consequently, high joint pressurization of EOEC by fission gases, together with rapid discharge of molten corium, resulted in a much greater amount of upward movement than BOEC, and the density inside the core was reduced due to the mass of the fuel emitted outside the core, resulting in a safer end to the accident.

Table. 3.4 Initial condition of cavity results of CRWM +SBO BOEC and EOEC

Parameter	Value	
	BOEC	EOEC
Melt Temperature	1412 K	1410 K
Failure site	88.1 %	94.7 %
Melting volume	5421 mm^3	5035 mm^3
Melting mass	57.5 g	53.4 g
Pressure at failure	0.51 MPa	5.56 MPa

Table. 3.5 Results of PPA BOEC and EOEC

Parameter	Value	
	BOEC	EOEC
Melt Temperature	1412 K	1404 K
Failure site	94.5 %	96.6 %
Melting volume	2059 mm^3	4246 mm^3
Melting mass	21.8 g	45.0 g
Pressure at failure	0.61 MPa	5.55 MPa

Table. 3.6 Initial condition of cavity results of PPC BOEC and EOEC

Parameter	Value	
	BOEC	EOEC
Melt Temperature	1412 K	1432 K
Failure site	88.6 %	90.8 %
Melting volume	5131 mm^3	4616 mm^3
Melting mass	54.4 g	49.0 g
Pressure at failure	0.60 MPa	5.52 MPa

Table. 3.7 Cavity pressurize results of PPC BOEC and EOEC

Cases		Fully vapor / Cavity vapor Bond sodium partial pressure
UTOP+SBO	BOEC	101.23 MPa / 50.17 MPa
	EOEC	101.08 MPa / 46.53 MPa
UTOP	BOEC	100.65 MPa / 39.07 MPa
	EOEC	100.87 MPa / 18.99 MPa
ULOF	BOEC	101.23 MPa / 47.49 MPa
	EOEC	102.66 MPa / 43.33 MPa

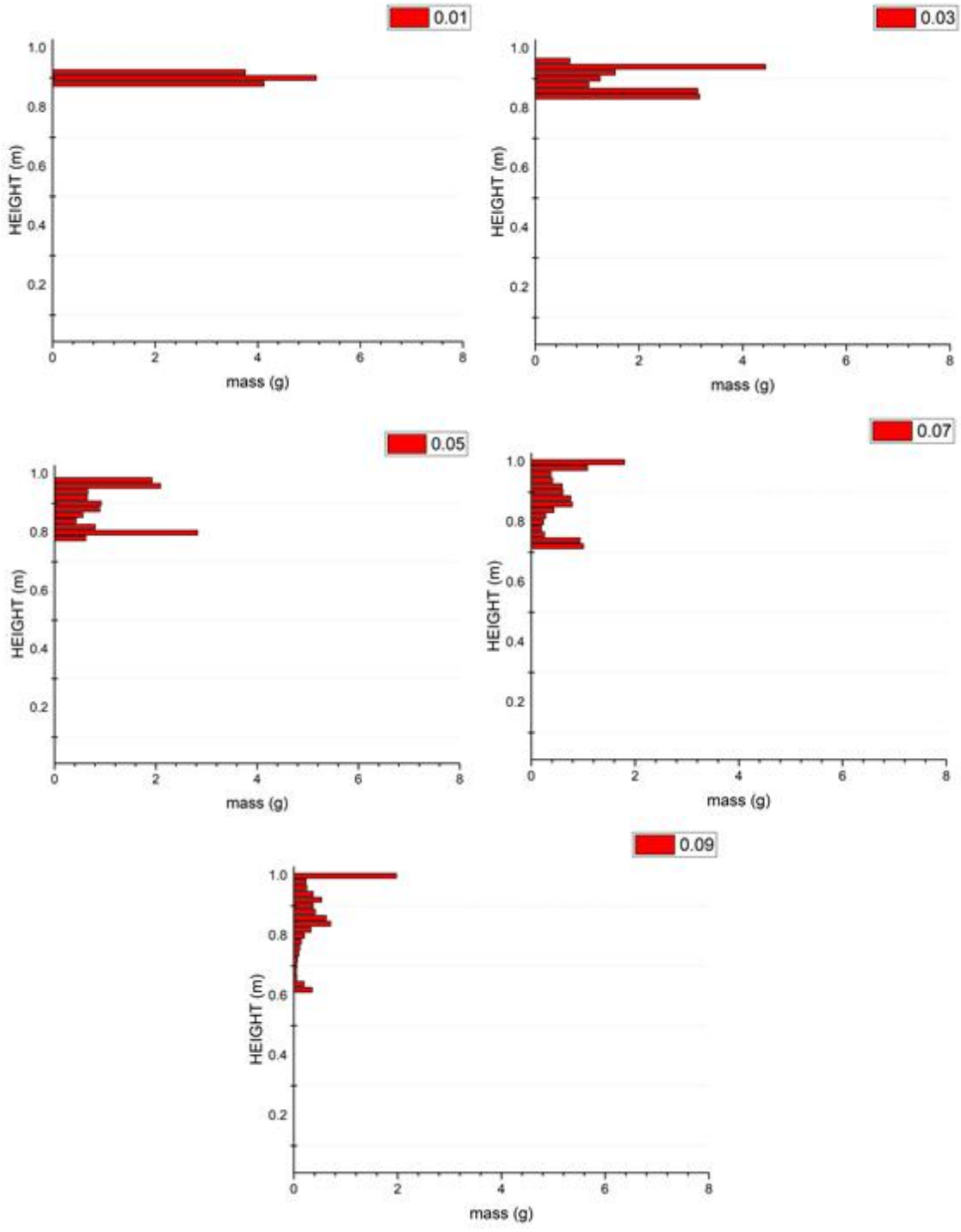

Figure. 3.15 CRWM +SBO(BOEC) MESFRAC results

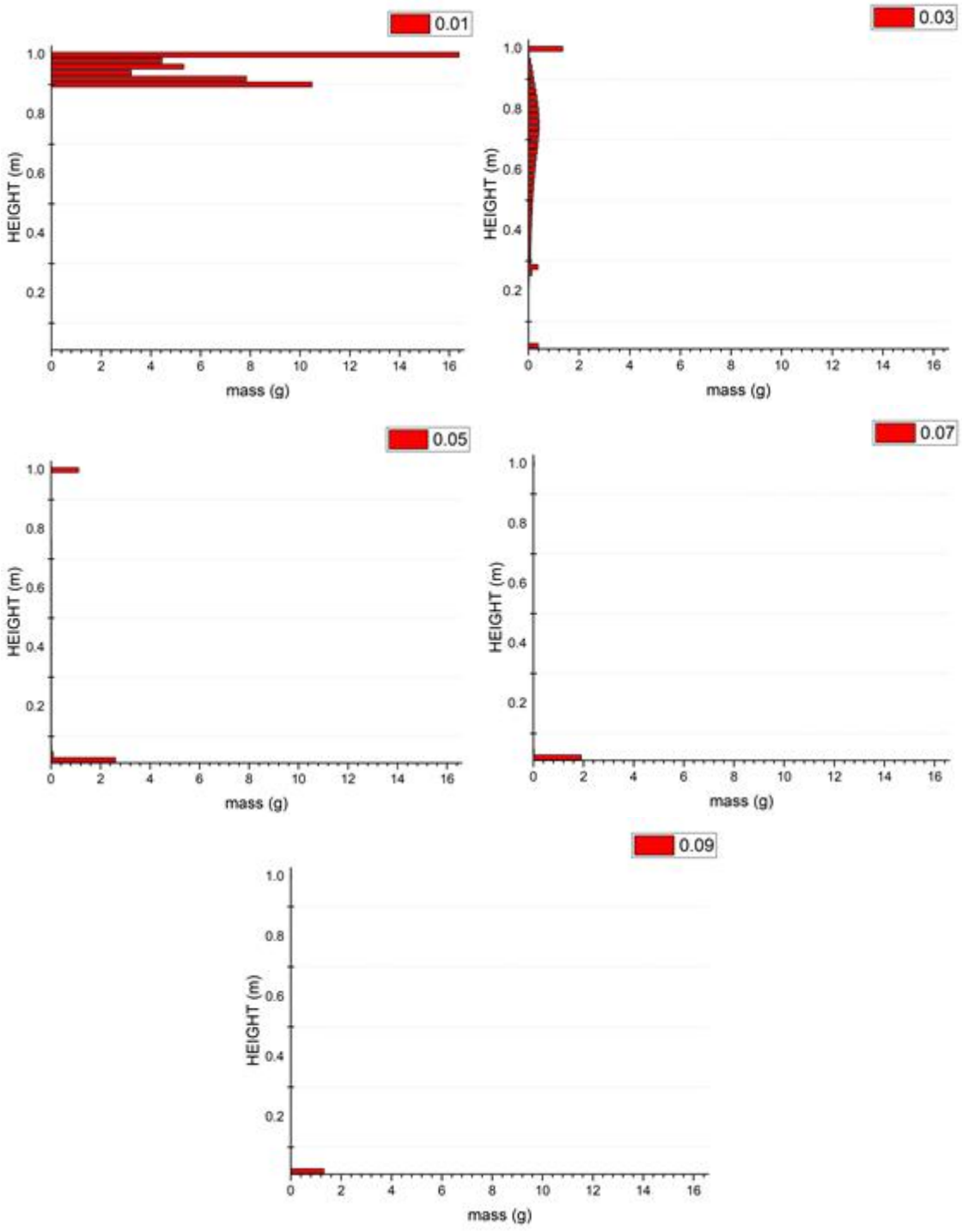

Figure. 3.16 CRWM +SBO(EOEC) MESFRAC results

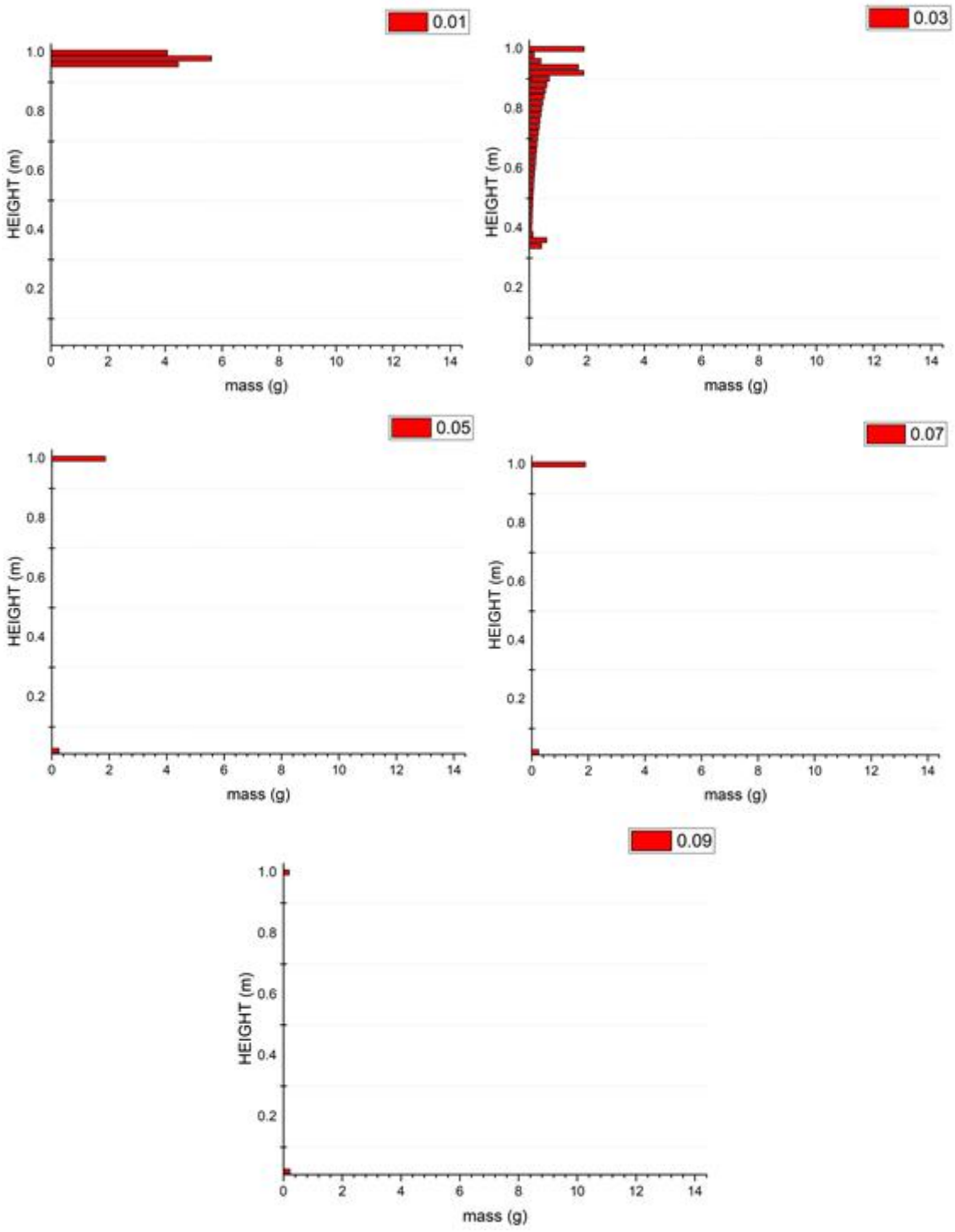

Figure. 3.17 PPA +SBO(BOEC) MESFRAC results

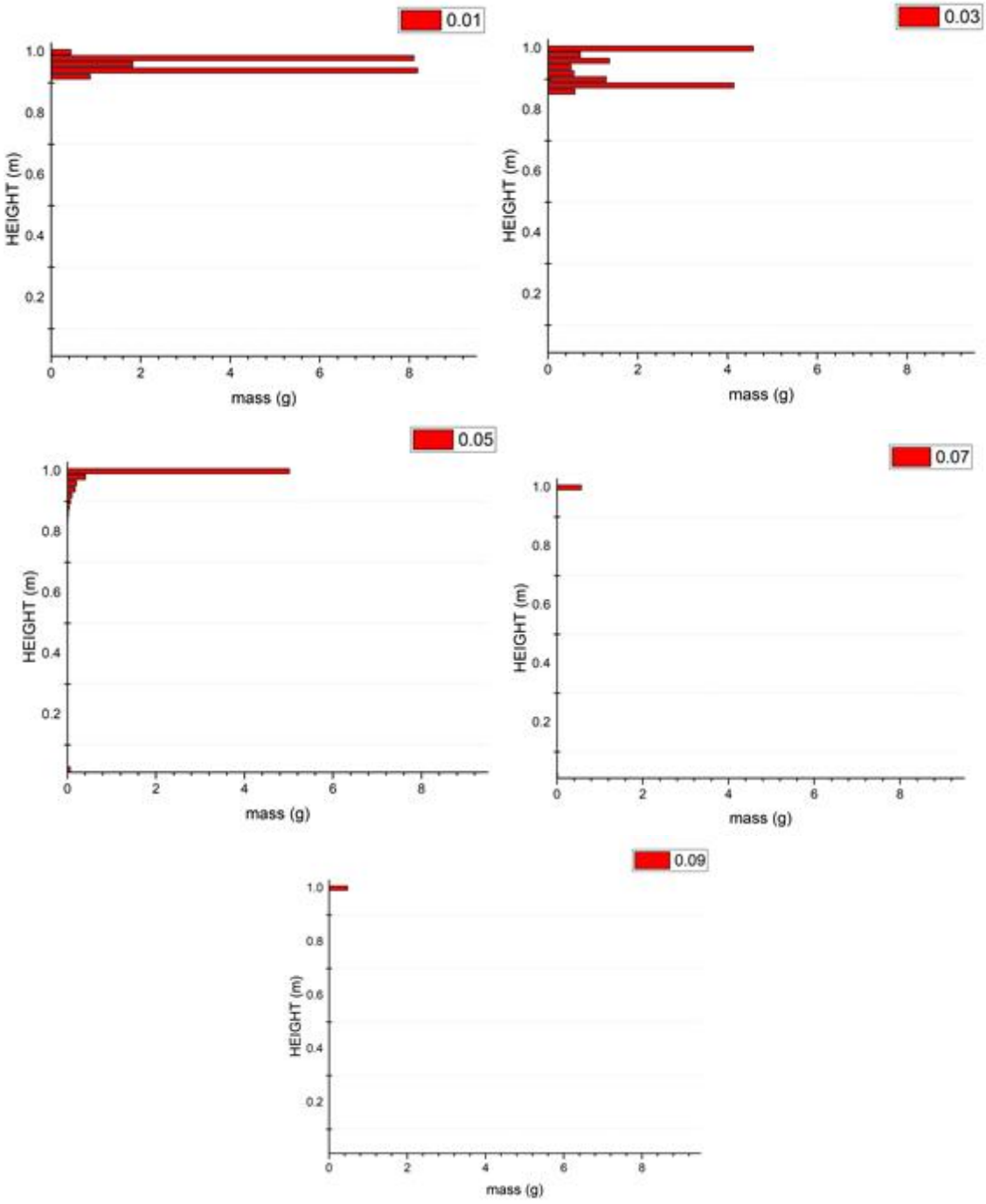

Figure. 3.18 PPA +SBO(EOEC) MESFRAC results

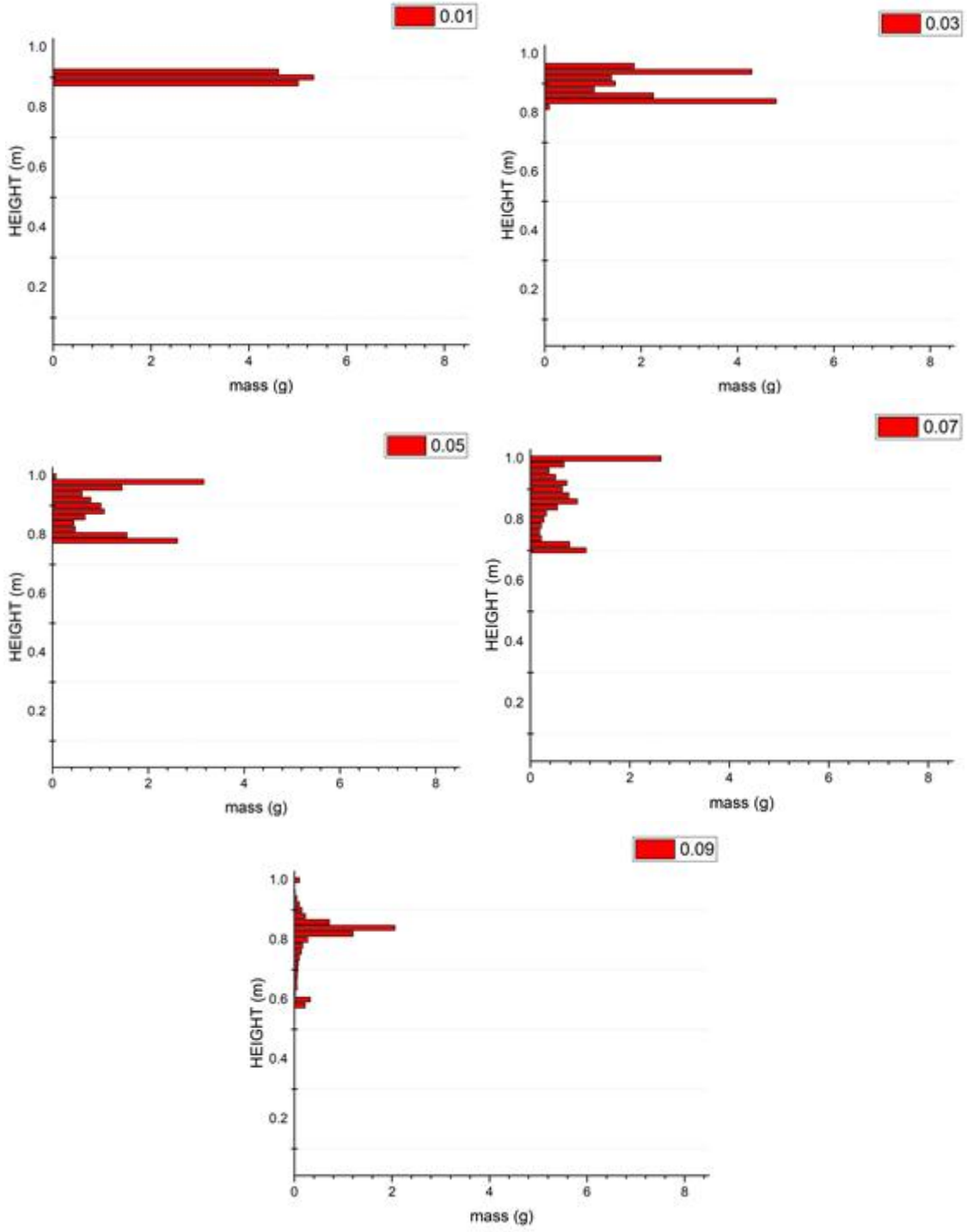

Figure. 3.19 PPC +SBO(BOEC) MESFRAC results

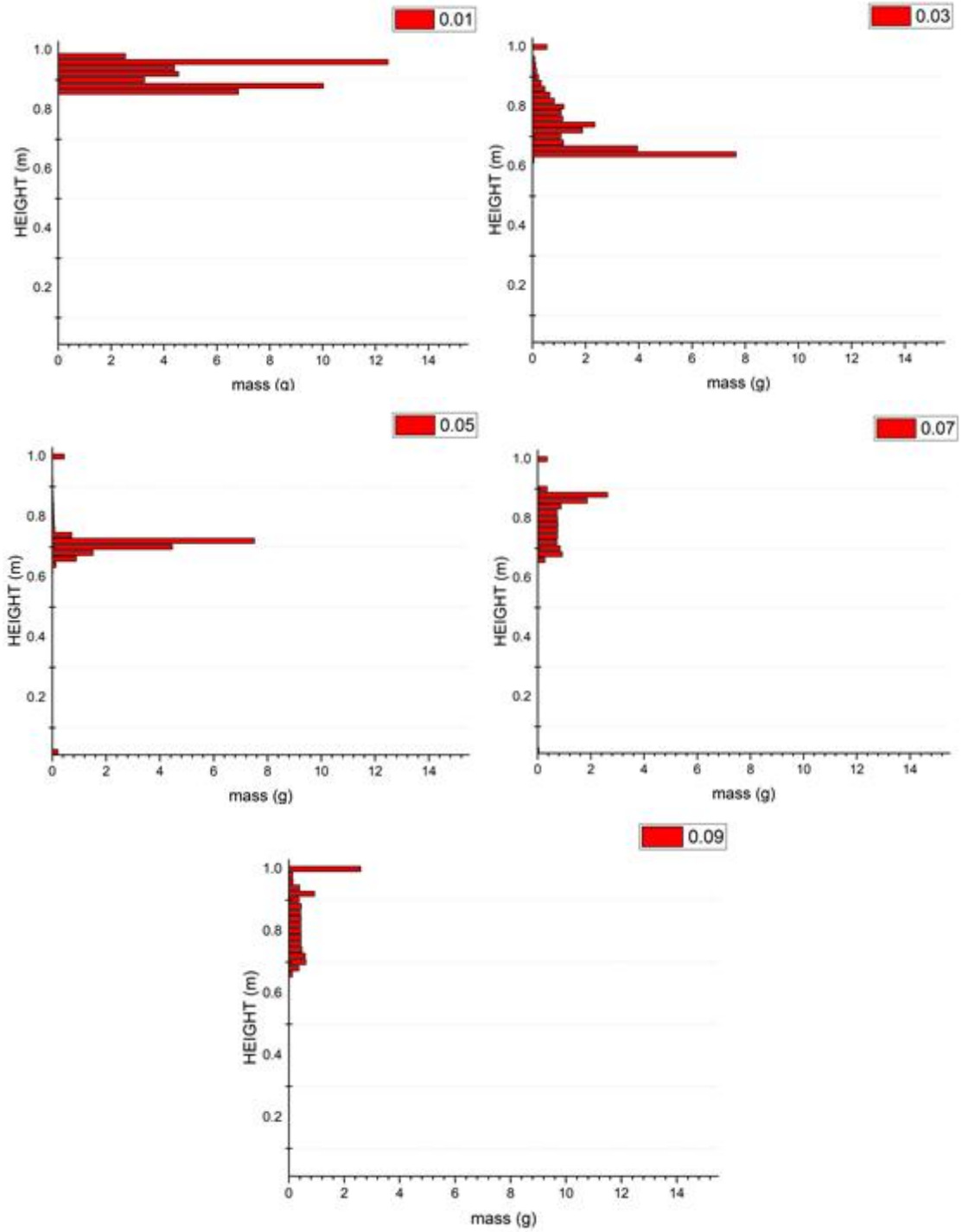

Figure. 3.20. PPC+SBO(EOEC) MESFRAC results

Table. 3.8 Upper disposal amount results

Cases		BOEC	EOEC	(A-B)/B*100
UTOP+SBO	Upper plenum Disposal(A) [%]	2.83	58.06	1951.59 %
	Lower plenum Disposal(B) [%]	0.0	1.92	-
UTOP	Upper plenum Disposal(A) [%]	2.89	45.22	1464.71 %
	Lower plenum Disposal(B) [%]	0.1	0.18	80 %
ULOF	Upper plenum Disposal(A) [%]	3.936	21.764	452.95 %
	Lower plenum Disposal(B) [%]	0.017	0.225	1223.53 %

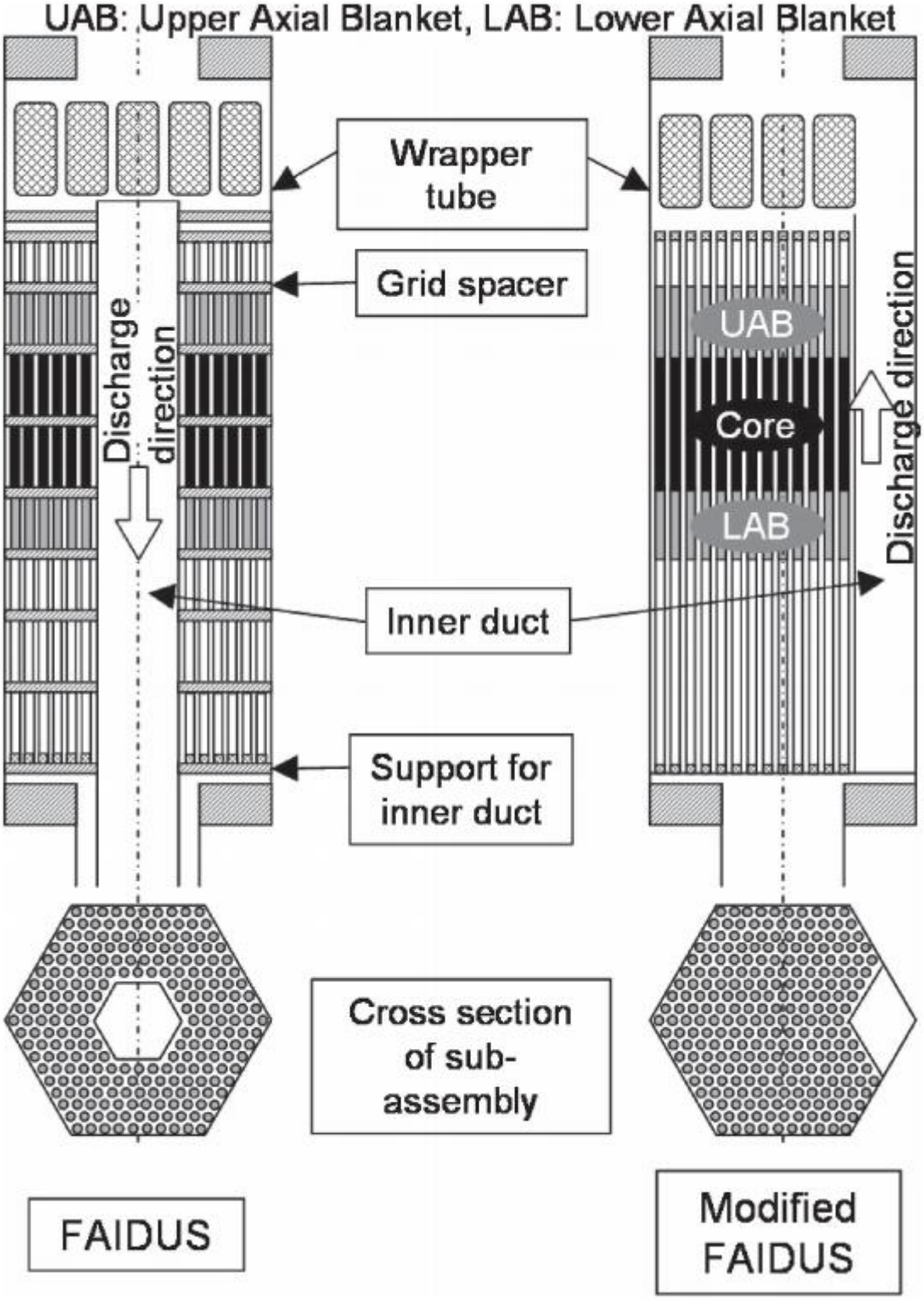

Figure. 3.21. JSFR, FAIDUS, molten fuel discharge apparatus[3.8]

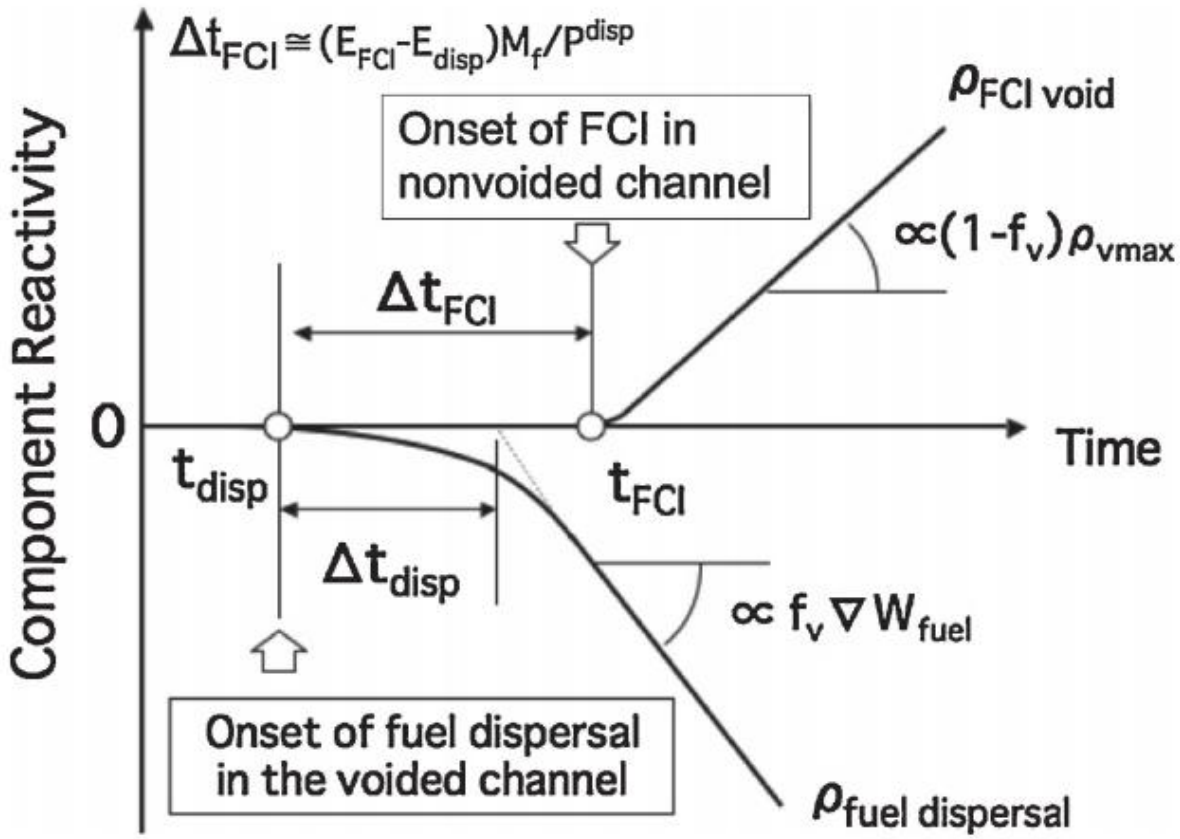

Figure 3.22. Reactivity comparison between fuel disposal and FCI void in FAIDUS severe accident[3.8]

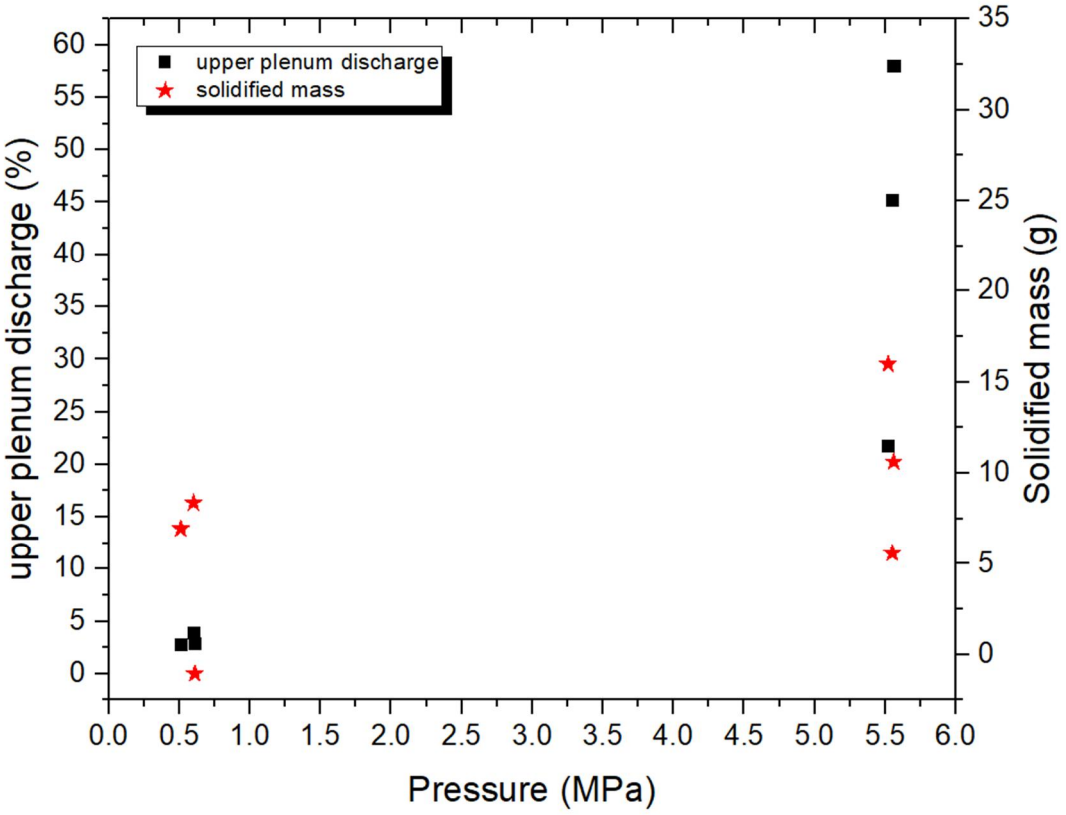

Figure. 3.23 Discharge mass and solidification mass inside channel with different pressure

Chapter 4. Conclusion and Recommendations

4.1. Conclusion

In this research, beginning with SAS4A analysis, sodium-cooled fast reactor core disruptive accident analysis code is developed to calculate the behavior of molten fuel inside coolant channel. The base of this code is FORTRAN and 1-D coolant channel hydrodynamics. Also, the heat transfer between molten fuel and structure like cladding and hexcan is considered. The model of SAS4A channel hydrodynamic simulation module LEVITATE is referred to model MESFRAC. In this research, the new finding model of this code is the effect of bond sodium pressurization. If the temperature of molten fuel increases up to its melting point, the sodium would boil because the boiling temperature of sodium is less then the temperature of molten fuel. The pressure of bond sodium cannot be higher than the pressure of EOEC burnup condition, but if break of cladding can make continuous pressure inside cavity which means the driving force of upward movement of molten fuel. This discharged fuel out of active core will make significant negative reactivity which means accident termination. In the case of BOEC condition, this sodium bonding pressurization will increase pressure inside cavity up to about 10 times bigger. This would be also safe for the accident.

This MESFRAC has strong points and weak points. The strong point is, first, MESFRAC can calculate initial phase of SFR severe accident only. Other severe accident codes like SAS4A or SIMMER shows the total situation of severe accident of SFR. While they show the total phenomena of severe accident, MESFRAC can show the detailed phenomena of severe accident especially on the initial phase of CDA. The second strong point comes from this first point. The second strong point is that it is easy to develop, modify and validate because of its flexibility. This code can be used for easy validation of some experimental or numerical data. Model is easy to be changed using 1-D explicit solution of main conservation equations. The third strongpoint is that it has less computing time and computing load compared to other CFD codes or severe accident codes. In the table. 4.1. shows the computation time comparison between commercial codes and SAS4A. In the case of commercial code, COMSOL is used for comparison as commercial CFD code. They use similar situation like ejection of molten fuel into coolant channel. Commercial code can use 2-D and 3-D schematic and can produce good looking post-processed image or movie. This is most powerful advantage of using commercial code. But, the time during computation is much larger than that of MESFRAC and SAS4A because they use much complicated calculation with implicit scheme. In the case of SAS4A, calculation time is much smaller than commercial code but longer than MESFRAC. To use this code, whole plant input is needed to calculate severe accident. This can be advantage for results of total nuclear power plant phenomenon but it is too much for results of just CDA phenomena. The reason of this is that MESFRAC use 1-D explicit scheme for solution of problems and just calculate the phenomena inside coolant channel. Other CFD codes use 3-D calculation with implicit scheme. And other accident codes use much data that

covers from core to other secondary systems (and also implicit method). Those big difference can reduce the computing time and load for the user who needs fast calculation results. Not only those advantages, there are weakness of MESFAC. First, 1-D explicit scheme can reduce the quality of results. This calculation scheme has advantage of flexibility, but it has disadvantage of its calculation result accuracy. This low-dimension code needs many assumptions to enhance calculate results. Because of this disadvantage, MESFRAC needs validation with broad data of initial condition.

Table. 4.1. Computing load comparison with other codes (Similar simulation using COMSOL and SAS4A)

	MESFRAC (1-D)	COMSOL (2-D)	SAS4A (1-D)
Mesh size [m]	0.02	5.0e-5	0.01
Number of mesh (core channel)	50	1.0e6	100
Time of computing	Few seconds (-10 sec)	Number of hours (-2 hrs)	Number of minutes (-15 min)
Calculation results	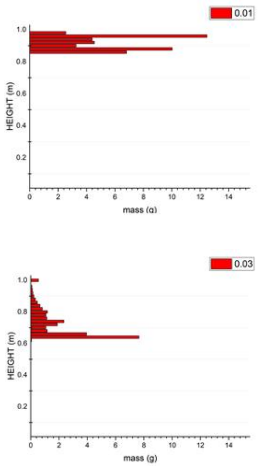 Mass distribution in each time step	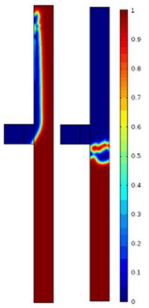 Easy post-process available Two phase flow without phase change	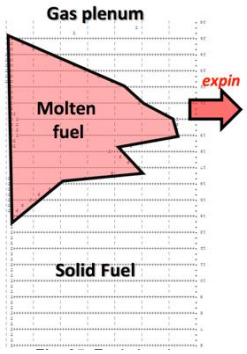 Text based output Mass distribution with multiphase, phase change

4.2 Recommendations

This MESFRAC is able to calculate the behavior of molten fuel inside coolant channel and outside of the active core. Because the modeling is not fully conducted and lots of assumptions are implemented, for the future, more model should be updated in, especially, momentum and energy equation. Most of ignorable coefficient is assumed to be zero and the heat generation of metal fuel form reactor power is not considered. Those models can be updated for the correct answer (but some condition, MESFRAC is agreed with experimental results). Not only the amount of discharge of molten fuel out of active core, the amount of molten metal fuel inside coolant channel can be used for real-time reactivity tracking. Point kinetics is available if reactivity worth of fuel inside channel is provided. This real-time tracking can calculate power of ejected molten fuel which can enhance the heat transfer source term and accuracy of calculation. And If this reactivity is smaller than that of criteria, it can be determine the end of accident without amount of discharge.

References

1.1. Hideki Kamide. Sodium cooled fast reactor, International workshop on advanced reactor systems and future energy market needs, 2017, OECD conference centre, paris, France. https://www.oecd-nea.org/ndd/workshops/arsfem2017/presentations/16_KAMIDE_Session4b.pdf

1.2. Richard Stainsby.Generation IV Fast Reactors, AMEC https://www.google.com/url?sa=t&rct=j&q=&esrc=s&source=web&cd=7&ved=2ahUKEwjW8PGg04ffAhULNrwKHZdnDWcQFjAGegQIAxAC&url=https%3A%2F%2Fwww-diva.eng.cam.ac.uk%2Fmphil-in-nuclear-energy%2Fexternal-lectures%2F2011-12-lectures%2Fgeneration-iv-fast-reactors.pdf%2Fat_download%2Ffile&usg=AOvVaw3g1J2l1f9u2bRPKp0bwA7t

1.3. INSAG-12. Basic safety principles for nuclear power plants 75-INSAG-3 Rev.1, A report by the International Nuclear Safety Advisor Group, 1999 https://www-pub.iaea.org/MTCD/Publications/PDF/P082_scr.pdf

1.4. George Flanagan, Tom Fanning, tanju Sofu. Sodium-cooled Fast Reactor (SFR) Technology and Safety Overview, Office of Nuclear Eenrgy, U.S. Department of Energy, 2015

1.5. J.E cahalan and T.H. Fanning. The SAS4A/SASSYS-1 Safety Analsysis code system, Chapter 1: Introduction, ANL/NE-12/4, Nuclear Engineering Divisoin, ANL, 2012

1.6. Y.Tobita, Sa. Kondo, h. Yamano, K. Morita, W. Maschek, P. Coste and T. cadiou. The development of SIMMER-III, an advanced computer program for LMFR safety analysis, and its application to sodium experiments, *Nuclear Technology.* 2017; Vol. 153, 245-255. DOI:10.13182/NT06-2

1.7. Tanju Sofu. A review of inherent sfaety characteristics of metal alloy sodium-cooled foast ractor fuel agianst postulated accidents, *Nucl Eng Technol.* 2014;47(3):227-239. DOI:10.1016/j.net.2015.03.004

1.8. Tohru Suzuki, Kenji Kamiyama, Hidemasa Yamano, Shigennobu Kubo, Yoshiharu Tobita, Ryodai Nakai and Kazuya Koyama. A scenario of core disrutpive accident for Japan sodium-cooled fast reactor to achieve in-vessel retention. *Journal of Nuclear Science and Technolgoy*. 2014; 51(4):493-513. DOI: 10.1080/00223131.2013.877405

1.9. W. Maschek, A. Rineiski, T. Suzuki, X. Chen, Mg. MORI, S. Wang. The SIMMER-III and SIMMER-IV code family: 2-D and 3-D Mechanistic simulation tools for reactor transients and accidents. Technical meeting on procress in development and usse of coupled code sfor accident anlaysis, Vienna, Aurtria, 2003, Nov,26-28.

2.1 S. Nishimura et. al. “Thermal interaction between molten metal jet and sodium pool: effect of principal factors governing fragmentation of the jet”, *Nuclear technology* 249, 2005, pp. 189-199.

2.2 Zji-Gang Zhang and Ken-Ichiro Sugiyama. “Fragmenation of a single molten metal droplet penetrating into sodium pool. IV thermal and hydrodynamic effects on fragmenation in copper”. *Journal of nuclear science and technology* 49, 2012, pp. 602-609.

2.3 Zji-Gang Zhang and Ken-Ichiro Sugiyama. “Fragmentation of a single molten metal droplet penetrating sodium pool in coper droplet and the relationship with copper jet”. *Journal of nuclear science and technology* 46, 2009. pp453-459.

2.4 Zji-Gang Zhang and Sugiyama. “Fragmentation of a single molten metal droplet penetrating into sodium pool: thermal and hydrodynamic effects on fragmentation in stainless steel”. *Nuclear Technology* 175, 2011, pp. 619-627.

2.5 J. Namiech et. al. “Fragmentation of a molten corium jet falling into water”. *Nuclear Engineering and design* 229, 2004, pp. 265-287.8.

2.6 E.S. Sowa, J.D. Babor, J.R. Pavik, J.C. Cassulo, C.J. Cook and L.Baker Jr, Molten core debris-sodium interactions: M-serise experiments, 1979.

2.7 J. D. Gabor. “Break and quench of molten metal fuel in sodium”, In: American nuclear society safety of next generation power reactors meeting. 1988.

2.8 J.D. Gabor, R.T. purviance, R.W. Aeschlimann, and B.W. Spencer, characterization of IFR metal fuel fragmentaion, 1987.

2.9 Sachin Thakre et. al. “A numerical simulation of jet breakup in melt coolant interaction

2.10 T. Ginsberg. “Liquid jet breakup characterization with application to melt-water mixing”, in: thermal reactor safety meeting, 1986.

2.11 A. W. Cronenberg and M. A. Grolmes, “A review of fragmentation models relative to molten UO2 Breakup when quenched in sodium coolant”, in: Nuclear energy agency of the OECD 1976.

2.12 AM.Tentner, The SAS4A/SASSYS-1 Safety Anlaysis code system, ANL/NE-12/4, 2012.

3.1 S. Nishimura et. al. “Thermal interaction between molten metal jet and sodium pool: effect of principal factors governing fragmentation of the jet”, *Nuclear technology* 249, 2005, pp. 189-199.

3.2 Zji-Gang Zhang and Ken-Ichiro Sugiyama. “Fragmenation of a single molten metal droplet penetrating into sodium pool. IV thermal and hydrodynamic effects on fragmenation in copper”. *Journal of nuclear science and technology* 49, 2012, pp. 602-609.

3.3 Zji-Gang Zhang and Ken-Ichiro Sugiyama. “Fragmentation of a single molten metal droplet penetrating sodium pool in coper droplet and the relationship with copper jet”. *Journal of nuclear science and technology* 46, 2009. pp453-459.

3.4 Zji-Gang Zhang and Sugiyama. “Fragmentation of a single molten metal droplet penetrating into sodium pool: thermal and hydrodynamic effects on fragmentation in stainless steel”. *Nuclear Technology* 175, 2011, pp. 619-627

3.5 S. Nishimura, I. Kinoshita, K.I. Sugiyama and N. Ueda, “Thermal fragmentation of a molten metal jet dropped into a sodium pool at interface temperature below its freezing point”, *Journal of Nuclear Science and Technology*, 2012, pp. 1881-1248

3.6 Ken-ichiro Sugiyama and Zhigang Zhang, Thermal and hydrodynamic fragmentation of a single molten stainless steel droplet penetrating sodium pool, 2009, Fr09, Kyoto , Japan, December 7-11, FR09P1277.

3.7 T. Kim, C. Gerardi, D. Harbaruk, S.G. Wiedmeyer, D.J. Kilsdonk, N. Bremer, T.A. Waches, M.T. Farmer, Y.I. Chang, “Quaterly progress report No. 4: for the period ending October 31”, Argonne National Labratory, 2016.

3.8 Tohru Suzuki, Kenji Kamiyama, Hidemasa Yamano, Shigenobu Kubo, Yoshiharu Tobita, Ryodai Nakai, Kazuya Kiyama, “A scenario of core disruptive accident for Japan sodium-cooled fast reactor to achieve in-vessel retention”*, Journal of Nuclear Science and Technology 51*, 2014, pp. 493-513.

Acknowledgement (감사의 글)

2013년 3월 울산과학기술원에서 4년의 학부과정을 마치고 대학원생으로 다시 입학한 뒤 6년차가 되는 해에 많은 분들께서 주신 조언과 보살핌, 그리고 가르침 덕분에 석박통합과정을 마치고 학위를 받게 되었습니다. 그 동안 많은 도움을 주신 많은 분들께 이렇게 감사의 글을 쓰고자 합니다.

먼저 6년동안 많이 부족했던 저에게 많은 지도와 격려, 그리고 많은 기회들을 만들고 관심을 쏟아 주신 지도교수님 방인철 교수님께 감사의 말씀을 전합니다. 대학원 입학 초, 비록 연구 주제가 실험에서 모델링으로 바뀌었지만, 실험실의 핵심이었던 비등실험을 바탕으로 연구지도를 해주시고 많은 기회를 주셨습니다. 여러가지 현상에 대하여 물리적 의미를 찾는 것, 이를 분석하고 새로운 아이디어를 찾는 것에 대한 많은 조언들을 주셨습니다. 뿐만 아니라 6개월간에 아르곤 국립연구소에서 연구경험을 쌓을 수 있도록 신경 써 주시고 도와 주신 덕분에 다양한 경험을 할 수 있도록 도와주셨으며, 결과적으로 이렇게 학위논문을 쓸 수 있게 되었습니다. 지도해주신 지난 6년간 작고 큰 부분에서 연구 주제 뿐만 아니라 제가 앞으로 사회인으로써 지녀야할 소양에 대해서 많은 말씀들을 해 주셨고, 저는 앞으로 항상 이것들을 마음속에 간직하고 실천할 수 있도록 노력하도록 하겠습니다. 지도교수님 뿐만 아니라 학위논문 지도를 해 주신 교내의 이승준 교수님, 윤의성 교수님 그리고 교외의 정동욱 교수님, 김윤재 교수님, 저를 위해 해 주신 말씀 감사히 듣고 잘 따르도록 하겠습니다. 감사드립니다.

그리고 6년간 연구실 생활을 같이 한 선배, 동기 그리고 후배들에게 감사의 말씀을 전합니다. 먼저 저보다 일찍 연구실에 들어오셔서 노력하시고 훌륭하게 졸업하신 선배님들, 이승원 박사님, 박성대 박사님, 김성만 석사님, 강사라 석사님, 서한 박사님께 감사의 말씀을 전합니다. 특히 비등실험 및 MELCOR 해석 관련 연구 사수이셨던 박성대 박사님께 큰 감사의 말씀을 드립니다. 항상 상대방을 존중해주시는 태도를 많이 배울 수 있었습니다. 거의 비슷하게 연구실에 들어온 김경모, 서석빈, 김인국 동기들에게도 감사의 말씀을 전합니다. 먼저 연구실에 들어와서 가장 오랫동안 연

구에 매진하고 멋진 연구결과를 낸, 연구실의 구심점인 경모에게, 항상 연구실에 대한 무한 애정을 가지고 책임감 있었던 너의 모습에서 가장 배울 점이 많았던 것 같다. 가장 많이 대화를 하기도 해서 앞으로 네가 떠나게 되면 많이 허전할 것 같아. 앞으로 더 승승장구하길 빈다. 여러모로 같이 지내면서 잘하는 게 많다고 느꼈던 석빈에게, 경모와 마찬가지로 자기가 맡은 연구주제에 대해 고뇌하는 모습이 멋지다 생각했어. 앞으로 더 멋진 연구결과를 내길 기대할 게. 학부생 때부터 인연이 있었던 인국에게, 같이 미국에서 랩투어를 다닐 때가 기억나고 우리가 이렇게 학위를 따게 될 시간까지 온 것이 감개무량하다. 앞으로 바쁘겠지만 자주 볼 수 있었음 좋겠어. 모든 동기들에게 이전에 내가 술을 살 기회가 많이 없었는데 앞으로 기회를 꼭 만들 수 있었으면 한다고 전합니다. 연구실 후배들, 효, 영신이, 민호, 한얼, 유경, 규민, 수민이 모두 부족한 선배를 두고 연구적 심적 도움을 많이 주어서 고맙다. 특히 6개월간 같이 미국에 파견을 나갈 수 있었던 효에게, 다사다난했지만 같이 미국생활을 지낼 수 있어서 정말 좋았다. 내가 판 자전거 조심히 출퇴근 때 잘 타고 비가 올 때 타지 말고.

이렇게 연구실 내부에서 도움을 주신 분들뿐만 아니라 연구실 외부에서 격려와 사랑을 주신 분들께도 감사를 전합니다. 우리 연구실뿐만 아니라 노심랩의 현석이 형과 원경이 그리고 여러 후배들, 재료 연구실 친구와 형들에게 감사의 말씀을 전합니다. 학부생 때부터 친하게 지낸 기계과 친구들, NEST, UNICH, Unplugged 늙은이, 후배들 그리고 고등학교 친구들 모두 외로울 수 있었던 길에서 서로 뿔뿔히 흩어져서 물리적 거리가 멀어졌지만 묵묵히 자기 자리를 지키는 와중에도 심적으로 많은 도움을 줘서 고맙다고 전한다. 계속해서 모임에 못나가고 해서 미안하게 생각하고, 다음엔 꼭 참석할 수 있도록 할 게. 그리고 연구 코옵을 수행한 서울대, 고려대 친구들에게도 감사의 말씀을 전하고자 합니다. 전부 연구참여기간동안 고생 많았어요. 그리고 실험할 때 실험장치를 만들어주신 네오시스 이종수 사장님께도 감사합니다.

마지막으로 저를 키워주신 아버지 어머니께 감사의 말씀을 드립니다. 앞으로 항상 건강하시고 효도할 수 있는 아들이 되도록 하겠습니다. 여동생에게도 못난 오빠로 잘 대해주지 못해 미안하기도 하고 고맙기도 하다는 말을 전합니다. 친가와 외가 친척 모든 분들에게도 감사의 말씀을 전합니다.